THÈSE

En vue de l'obtention du

DOCTORAT DE L'UNIVERSITÉ DE TOULOUSE

Délivré par *L'UNIVERSITE DE TOULOUSE III- PAUL SABATIER*
Discipline ou spécialité : *Chimie-Biologie-Santé*

Présentée et soutenue par *VU Thi Thu*
Le *24 Février 2014*

Titre : *Study of nano-engineered solid/liquid interfaces based on polymer brushes and biomimetic multifunctional glue*

JURY
Jean Pierre SOUCHARD, Professeur, Université Paul Sabatier, Toulouse
Patrick ABGRALL, Chercheur, Formulaction, Toulouse
Catherine PERRIN, Professeur, Université de Montpellier 1, Montpellier
Xavier COQUERET, Professeur, ICMR, Reims
Anne-Marie GUE, Directrice de Recherche, LAAS, Toulouse
Jan SUDOR, Maître de Conférences, Université Paul Sabatier, Toulouse

---

Ecole doctorale : *Sciences de la Matière*
Unité de recherche : *Pharmacochimie et pharmacologie pour le développement, PHARMA-DEV, UMR 152 IRD-UPS*
Directeur(s) de Thèse : *Jan SUDOR*
Rapporteurs : *Catherine PERRIN/ Xavier COQUERET*

Remerciements

Le travail présenté dans ce manuscrit a été réalisé au Laboratoire «Pharmacochimie et Pharmacologie pour le Développement » (*PHARMA-DEV, UMR 152-IRD*), Toulouse, France.

Je remercie très sincèrement Monsieur le docteur Jan SUDOR, mon directeur de thèse, pour m'avoir encadré et suivi mes travaux avec rigueur et efficacité pendant ces trois années, dans une ambiance toujours conviviale.

Je souhaite également remercier Madame le Professeur Françoise NEPVEU, chef de l'équipe RED-STRESS, pour m'avoir accueillie dans son équipe de recherche.

Je désire remercier Madame la Directrice de Recherche Marie-Anne GUE du Laboratoire d'Analyse et d'Architecture des Systèmes (LAAS) de Toulouse d'avoir soutenue à travailler dans son équipe.

Je tiens également à remercier le docteur Ennaji NAJAHI d'avoir partagé ses connaissances en synthèse des polymères avec moi.

Je remercie Marc FOUET pour m'avoir aidé à fabriquer des dispositifs micro-fluidiques en PDMS au LAAS.

Je remercie sincèrement les chercheurs Benjamin REIG et Jean Baptise DOUCET, Thi Ty Mai DINH au LAAS pour m'avoir aidé à travailler dans la salle blanche.

Un grand merci également aux personnels administratifs du laboratoire. Je pense tout particulièrement à Eliane PELISSOU, Marie Agnes BELLIERES et Franck MARIE-SAINTE pour leur sympathie et leur gentillesse.

Bien entendu, je remercie tous les membres, passés ou présents, du laboratoire qui m'ont permis de travailler dans une ambiance toujours sympathique: Fabrice COLLIN, Karine REYBIER, NGUYEN Thi Hoang Yen, Pierre PERIO, Laure-Estelle CASSAGNES,

Clémence CHEIGNON, Nambinina RAKOTOARIVELO, Armelle MONTROSE, LE Hong Luyen, Béatrice MOUKARZE, Aida CHAKER, Hany IBRAHIM, Rémi MANCZAK, Nehal IBRAHIM, Cynthia GIRARDI.

Enfin un grand merci à mes parents et mon frère, ainsi que toute ma famille et mes amis, pour leur soutiens et les encouragements qu'ils m'ont apportés.

Acknowledgements

I would like to express my sincere gratitude to my supervisor, Dr. Jan SUDOR, for his support and guidance. I truly appreciated his leadership, inspiration and encouragement in every step during my PhD study, giving me the trust and freedom to carry out the research.

I am truly grateful that Professor Françoise NEPVEU, head of RED-STRESS group, did welcome me in her research group.

I would also like to express my sincere gratitude to Dr. Anne-Marie GUE, who has graciously offered permission to use the lab and provided so many helpful and detailed comments on micro-fluidic devices as well as on surface characterization.

Deep thanks must to be given to Dr. Ennaji NAJAHI for his kind assistance with numerous experiments and his helpful discussions and suggestions on synthesis of polymer.

I also want to thank Marc FOUET for his kind help and assistance in fabrication of PDMS based micro-fluidic devices.

I need to thank Benjamin REIG, Jean Baptise DOUCET, Thi Ty Mai DINH at LAAS for help and training in clean room.

I would like to express my gratitude to the business office personnel, Eliane PELISSOU, Marie Agnes BELLIERES and Franck MARIE-SAINTE for all their help through all these years.

I would also like to extend my appreciation to other past and current members of PHARMA-DEV for being a friendly laboratory and providing helpful insight, including Fabrice COLLIN, Karine REYBIER, NGUYEN Thi Hoang Yen, Pierre PERIO, Laure-Estelle CASSAGNES, Clémence CHEIGNON, Nambinina RAKOTOARIVELO, Armelle MONTROSE, LE Hong Luyen, Béatrice MOUKARZE, Aida CHAKER, Hany IBRAHIM, Rémi MANCZAK, Nehal IBRAHIM, Cynthia GIRARDI and many others.

Lastly, I would like to thank my family, my parents and my brother for your unconditional love, support, courage, dedication and selflessness. I would like to dedicate this thesis to you, who I love the most.

DEDICATION

This thesis is dedicated to my entire loving and supportive family.

Table of contents

List of abbreviations

List of figures

List of schemes

List of tables

Introduction

Motivation and aims

Thesis outline

Chapter 1: Literature review

1.1. Solid / liquid interfaces and microfluidic devices

1.1.1. Introduction 13

1.1.2. Omnipresence of solid / liquid interfaces (SLIs) 14

1.1.3. Control of properties of SLIs 17

1.1.3.1. Self-assembled monolayers (SAMs) 17

1.1.3.2. End-tethered polymers at SLIs 19

1.1.3.3. Adsorbed polymer layers 20

1.1.4. A microchannel - scaling laws (importance of Surface to Volume ratio) 23

1.1.4.1. Scaling laws in down-scaling: the predominance of surface forces on volume forces 23

1.1.4.2. Dimensionless numbers in microfluidics 24

1.1.4.3. Adsorption phenomena 25

1.1.5. Microfluidic devices (lab-on-chips) 26

1.1.5.1. Commercerlization of microfluidic devices 26

1.1.5.2. Advantages of miniaturization and integration 26

1.1.5.3. Microfabrication of microfluidic devices 27

1.1.6. Conclusions 34

1.2. Mussel inspired surface chemistry

1.2.1.Introduction....40

1.2.2. Principles of mussel inspired surface chemistry 41

1.2.2.1. Mussel adhesion 41

1.2.2.2. Oxidation of dopamine....41

1.2.2.3. Deposition regime of DOPA-type films 44

1.2.3. Properties of DOPA....45

1.2.4. Effect of oxidation conditions on formation of DOPA-type films....46

1.2.5. Applications of mussel inspired surface chemistry 47

1.2.6. Conclusions 50

Chapter 2: Amine terminated polymers

2.1. Introduction 55

2.2. Materials....56

2.3. Experiments....57

2.3.1. Mechanism of chain transfer radical polymerization....57

2.3.2. Procedure 58

2.4. Results and discussions 59

2.4.1. Fourier transform infrared spectroscopy (FTIR) 59

2.4.2. Nuclear magnetic resonance (NMR) 59

2.4.3. Matrix-assisted laser desorption/ionization – Time of flight (MALDI-TOF) 63

2.4.4. Size exclusion chromatography (SEC)....64

2.4.5. Fluorescence labelling 66

2.4.6. DCC/HOBT mediated amidation....68

2.5. Conclusions 70

Chapter 3: Optimization of oxidation of dopamine

3.1. Introduction 73

3.2. Materials....74

3.3. Experiments....75

3.4. Characterization 76

3.4.1. UV-Vis absorption....76

3.4.2. Water contact angle (WCA)....76

3.4.3. Atomic force microscopy (AFM) 76
3.4.4. Nano analyser 77
3.5. Results and discussions 78
3.5.1. Intrinsic huge aggregates and high roughness of DOPA films 78
3.5.2. Effect of oxidation conditions on oxidation kinetics, deposition kinetics and surface morphology 79
3.5.2.1. Effect of oxidation conditions on oxidation kinetics 80
3.5.2.2. Effect of oxidation conditions on deposition kinetics 81
3.5.2.3. Effect of oxidation conditions on surface morphology 83
3.5.3. Versatility of DOPA film 84
3.6. Conclusions 86

Chapter 4: Monitoring wettability of heterogeneous material surfaces in fluidic devices

Introduction 89
A new and easy surface functionalization technology for monitoring wettability in heterogeneous nano- and micro-fluidic devices *(Published article)* 90
Supporting information 103

Conclusions

Future outlook

Résumé (en français)

List of abbreviations

AAO	Anodic Aluminum Oxide
AFM	Atomic Force Microscopy
AM	Acrylamide
AmPAM	Amine terminated PolyAcrylamide
AmPNIPAM	Amine terminated Poly(N-Isopropylacrylamide)
CE	Capillary Electrophoresis
CTA	Chain Transfer Atom
CTRP	Chain Transfer Radical Polymerization
CV	Cyclic Voltammetry
DCC	N,N'-DicyclohexylCarbodiimide
DHI	5,6-DiHydroxylIndole
DOP	Dopamine
DOPA	Polydopamine/pseudo-dopamine/dopamine-melanin
FITC	Fluorescein isothiocyanate
EOF	Electro-Osmotic Flow
FTIR	Fourier Transform Infrared Spectroscopy
HOBT	1-Hydroxy-benzotriazol
iCMBAs	injectable Citrate based Mussel inspired BioAdhesives
KPS	Potassium Persulfate
LOCs	Lab-on-chips
MALDI-TOF	*Matrix-assisted laser desorption/ionization – Time of Flight*
MiSC	Mussel inspired Surface Chemistry
MW	Molecular Weight
NIPAM	N-IsoPropyl-Acrylamide
NMR	Nuclear Magnetic Resonance
PAM	PolyAcrylAmide
PC	PolyCarbonate
PDMS	Poly(DiMethylSiloxane)
PEG	Poly(EthyleneGlycol*)*
PEO (=PEG)	PolyEthylene Oxide
pI	Isoelectric point
PL	Poly(Lactide)

PMMA	Poly(MethylMethacrylate)
PNIPAM	Poly(N-IsoPropylAcrylamide)
pSBMA	Poly(SulfoBetaine MethAcrylate)
PU	PolyUrethane
SAMs	Self-Assembled Monolayers
SEC	Size Exclusion Chromatography
TEMED	N,N,N',N'-TetraMethylEthyleneDiamine
WCA	Water Contact Angle
μ TAS	micro total analysis system

List of figures

Figure 1.1. Illustration of a cell-membrane 15
Figure 1.2. Animation of scaling laws at nano- / micro-scale 16
Figure 1.3. Illustration of self-assembled monolayers 18
Figure 1.4. Adaptable approaches to grafting polymer brushes on a wide range of materials. 19
Figure 1.5. Adsorption and Depletion of polymer chains on surface 21
Figure 1.6. Example of adsorption of polyelectrolytes on surfaces 23
Figure 1.7. Scaling laws in a microchannel 24
Figure 1.1. Illustration of Wet etching of glass 30
Figure 1.2. Illustration of Molding process of PDMS microchannels 32
Figure 1.3. Illustration of Casting process 32

Figure 2.1. ^{1}H NMR spectra of PNIPAMc and PAMc 60
Figure 2.2. ^{1}H NMR spectra of PAM synthesized at different monomer concentrations and different initiator concentrations 61
Figure 2.3. ^{1}H NMR spectra of PNIPAM synthesized at different monomer concentrations and different initiator concentrations 61
Figure 2.4. ^{13}C NMR spectra of PAM synthesized at different monomer concentrations and different initiator concentrations 62
Figure 2.5. ^{13}C NMR spectra of PNIPAM synthesized at different monomer concentrations and different initiator concentrations 62
Figure 2.6. MALDI-TOF of amine terminated PNIPAM 63
Figure 2.7. FITC conjugated polyacrylamide 67
Figure 2.8. ^{13}C NMR spectra of unmodified PNIPAM and PNIPAM modified with acrylic acid 69

Figure 3.1. AFM measurements of DOPA film deposited in sealed reactor 79
Figure 3.2. Evolution of DOPA film on silicon oxide wafer in various oxidation conditions. 81
Figure 3.3. Deposition kinetics analysis of DOPA films in various oxidation conditions 82
Figure 3.4. AFM topography of DOPA on silicon oxide wafer in various oxidation conditions 83
Figure 3.5. Wettability of DOPA film on various substrates 84

List of schemes

Scheme 1.1. Oxidation mechanism of dopamine 42
Scheme 1.2. Strong non-covalent bond in DOPA from hydrogen bond 43
Scheme 1.3. Mix of non-covalent bond and covalent bonding in DOPA 43
Scheme 1.4. Attachment of DOPA to surface by chemical affinity 44
Scheme 1 5. Attachment of DOPA to surface by adsorption of catechol radicals 45
Scheme 2.1. Mechanism of chain transfer telomerization mechanism 57
Scheme 2.2. Conjugation of amine terminated polymer with FITC 67
Scheme 2.3. DCC/HOBt mediated amidation between amino terminated PNIPAM and acrylic acid 69

List of tables

Table 2.1. List of synthesized polymers 58
Table 2.2. Molecular weights (determined from SEC) of synthesized polymers 65

Introduction

Motivation and aims

The objective of the thesis was to develop a surface nonspecific technology for modifying solid/liquid interfaces of virtually any material used in the fabrication of multicomponent nano- and micro- fluidic devices. Our objective was accomplished by using and optimizing **mussel inspired surface chemistry** based on sticky DOPA films. This new technology offered an opportunity for the homogenization of surface energy of all studied materials.

Lab-on-chips (LOCs), also called "micro total analysis systems (μTAS)", is a newly emerging field that represents a breakthrough in biomedical analysis and diagnosis. The aim of this field is to develop miniaturized and integrated fluidic devices that permit to decrease the time and cost of an analysis and that operate in an automated manner. From historical point of view, LOCs emerged from efforts to control liquid flow at subnanoliter scale in the early 1990s. Over the last twenty-five years, hundreds of microfluidic research groups and tens of microfluidic related companies have been established. At present, we can find some commercial products based on LOCs, such as iSTAT blood analyzer from Abbott Point-of-Care, glucose meter from Bayer Healthcare, DNA and peptide analyzer from Agilent.

To fabricate complex microfluidic devices, various solid materials, spanning from silicon, glass and plastics can be employed. The material of choice is often governed by the specific requirements of a given application while the price of the device can also play a crucial role. It was demonstrated that the cost of a microfluidic device can be dramatically reduced by applying hybrid technology in which silicon-based actuators are incorporated into non-expensive polymeric materials. On the other hand, it is well known that decreasing the size of any fluidic device leads invariably into increase of the surface-to- volume ratio. This often imposes the necessity to perform laborious, chemical or physical tailoring of the surfaces, especially in the micro- and nano-fluidic devices dedicated to biological applications. In general, surface modification approaches are developed case-by-case. They depend only on the properties of the modified materials and

tethering molecules. The methods most commonly employed for the functional modification of solid surfaces include the formation of self-assembled monolayers (SAMs) on metals, silane-based chemistry on silicon and glass substrates and polyelectrolyte layer-by-layer assembly on charged surfaces. It is clear that with these state-of-the-art surface modification approaches, it would be impossible to homogenize the surface properties in multicomponent or hybrid fluidic devices, integrating silicon, glass, metals, photoresists (e.g., SU8) and elastomers (e.g., polydimethoxysilane, PDMS) together.

The mussel adhesion to any solid surface in wet condition has now become the inspiration for the development of a universal surface functionalization approach, namely *mussel inspired surface chemistry (MiSC)*. To cling to rocks during high tide, mussel secretes adhesive proteins that harden into solid, water-resistant glue. These biomimetic glues allow us to tailor the physic-chemical properties of almost any solid / liquid interface in a desired way.

In this study, we present a substrate-independent route for grafting end-functionalized polyacrylamide chains onto any solid surfaces through mussel inspired chemistry. Dopamine spontaneously oxidizes, under alkaline conditions, and forms highly reactive products that further polymerize and self-organize. This leads to a formation of thin-layer coating (DOPA films) that can be additionally modified with various molecules of interest. It has been shown in the literature that amines, thiols and carboxyl groups react with DOPA films. We have synthesized a variety of amino-terminated polyacrylamide and polyacrylamide derivative chains of different molecular weights. The polyacrylamide chains were end-tethered on different materials via a *one-pot* approach and the modified surfaces were thoroughly characterized.

The specific objectives of this study are:

- To synthesize amino-terminated polyacrylamide-based chains (PAM, PNIPAM) with variable molecular weights
- To characterize structural properties of synthesized polymers and to determine their molecular weights
- To optimize oxidation conditions of dopamine in order to achieve low-roughness DOPA-type thin films

- To graft synthesized polymers to flat surfaces made of different materials using *one-pot* mussel inspired surface chemistry at optimized conditions
- To demonstrate the possibility to obtain non-fouling surfaces inside microfluidic devices

Thesis outline

This thesis is organized into four chapters and a general conclusion.

In the **first chapter**, the literature overview on the solid / liquid interfaces (SLIs) and the mussel inspired surface chemistry (MiSC) is depicted. First we describe the omnipresence of solid / liquid interfaces and their growing importance in downscaling, i.e., in micro- and nano- fluidic devices. The state-of-the-art of the modification of SLIs is described here as well and it is shown that the surface chemistry is highly substrate-dependent. Consequently, we give a general overview on the mussel inspired surface chemistry and we describe the mechanism of this approach. It is shown that the MiSC is substrate-independent and that it can be utilized as a universal method for the homogenization of surface energy in microfluidic channels built from various materials.

The **second chapter** of the thesis describes the synthesis of the amine terminated polyacrylamide and poly(N-Isopropylacrylamide) by the chain transfer radical polymerization. The experimental conditions of synthesis and detailed characterization of the synthesized polymers by Fourier Transform Infrared Spectroscopy (FTIR), Nuclear Magnetic Resonance (NMR), Size Exclusion Chromatography (SEC), Matrix-assisted laser desorption/ionization Time-of-Flight (MALDI-TOF) mass spectroscopy are given here. The qualitative verification of the presence of amine end-group in the synthesized polymers, by fluorescent FITC labeling and HOBT/DCC mediated amidation, is also described in this chapter.

In the **third chapter**, wetting and homogeneity of surfaces modified by MiSC are investigated by water contact angle measurement and atomic force microscopy. The effects of oxidation kinetics on deposition kinetics and surface morphology are thoroughly examined here by the two techniques. The results of this study are utilized to design optimized experimental condition, with the help of employing an oxidant, for obtaining faster deposition kinetics and surfaces with an ultralow roughness and much less

aggregation. Finally, we suggest applying these experimental conditions for an easy modification of surfaces in nano- and micro-fluidic channels.

The **last chapter** presents our paper that was published in Sensors and Actuators B: Chemical (http://dx.doi.org/10.1016/j.snb.2014.01.085). The goal of this manuscript is to demonstrate the versatility and the generality of our substrate-independent surface modification strategy. We show that we can end-graft amino-terminated polyacrylamide chains onto virtually any solid surface. Moreover this strategy is easily applicable to the modification of wetting properties of heterogeneous materials in nano- and micro-fluidic devices by a simple manner. The modified surfaces under optimized condition are characterized by analytical surface techniques, including water contact angle measurements, atomic force microscopy, cyclic voltammetry, and by studying a protein adsorption by fluorescence microscopy. In conclusion, we point out four major advantages of our approach: *(i)* substrate independency, *(ii)* compatibility with grafting of biologically active molecules, such as enzymes, because it is accomplished in aqueous solutions *(iii)* possibility to regenerate a modified surface when necessary and, *(iv)* possibility to apply this approach for functionalization of sub-micrometer sized channels because it works in a low-viscosity regime.

At the end of this manuscript, we give a general conclusions and an outlook for a future work.

Chapter 1: Literature overview

1.1. Solid / liquid interfaces and microfluidic devices

1.1.1. Introduction

In this section, a necessary background of the solid / liquid interfaces (SLIs) and the microfluidic devices are presented. We describe the omnipresence of solid / liquid interfaces and their growing importance in downscaling, i.e., in micro- and nano-fluidic devices. The state-of-the-art of the modification of SLIs is described here as well and it is shown that the surface chemistry is highly substrate-dependent. The state-of-the-art of the microfabrication of microfluidic devices is also presented here and, finally, it is suggested that there is a need to develop a universal technology for functionalizing of surfaces of such devices.

1.1.2. Omnipresence of solid / liquid interfaces (SLIs)

Solid / liquid interfaces play vial roles in governing a number of phenomena encountered in many fields including biology, chemistry, material science and nano- / micro-fluidics. The interfacial properties determine behaviors of not only the solid substrates but also the liquid itself. Let's consider some examples of solid / liquid interfaces.

In biology, the most important solid / liquid interfaces are cell-membrane / water interfaces. The plasma membrane encloses the cell and defines the boundary between the cytoplasm and the extracellular environment. Albert et al., (2008) has given a comprehensive study about the structure of cell-membrane and its roles in cellular processes [1]. Despite their differing function, all biological membranes have a common general structure: a mosaic liquid membrane that consist lipid molecules (mostly, phospholipids) and membrane proteins [2]. The lipid molecules are arranged in a lipid bilayer to which proteins are embedded (see figure 1.1). Those parts within cell membrane serve different functions in extracellular processes. The **lipid bilayer** provides fluid structure of the membrane and also acts as a relatively impermeable barrier to the passage of most water soluble molecules. Although lipid is the major component of cell membrane (about 50% of the mass of most cell membrane), the **membrane proteins** are responsible for most membrane functions. They act as transport proteins, enzymes, specific receptors, and so on. For example, the **peripheral proteins** that span from one side to the other side of lipid bilayer act as membrane *transport proteins* to selectively transport substances (oxygen, nutrients, and wastes) in and out of the cell [3, 4]. There are two classes of membrane transport proteins: *transporters* and *channels*. Whereas transmembrane movement mediated by transporters can be either active or passive, solute flow through channel proteins is always passive [1]. Differing from peripheral proteins, the **integral proteins** stay on one side of membrane and can slide around the membrane. These proteins (e.g., actin) are involved in maintaining the *shape and mobility* of cell [5, 6]. Certain peripheral proteins (e.g., hydrolase, phospholipase, cholesterol oxidase, and etc) can also act as an *enzyme* to catalyze reactions in the cytoplasm [7, 8]. The **glycoproteins** (e.g., immunoglobins, histocompatibility antigens, and etc) that contain proteins and carbohydrates are usually involved in cell recognition which is part of immune system [9,

10]. Certain glycoproteins (e.g., Human chorionic gonadotropin (HCG), thyroid-stimulating hormone (TSH)) can also act as *receptors* in cell signaling [11, 12].

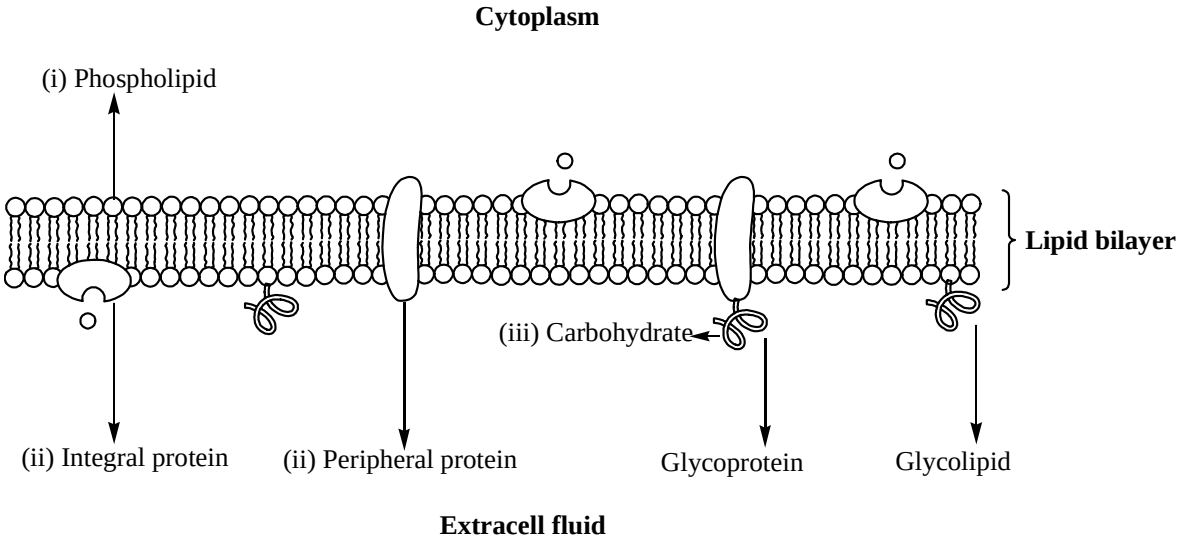

Figure 1.4. *Illustration of a cell-membrane:* (i) The phospholipids are arranged in a *bilayer* with hydrophilic polar phosphate heads facing outwards and hydrophobic non-polar fatty acid tails facing each other in the middle of the bilayer; (ii) The proteins can span from one side of the phospholipid bilayer to the other (*integral proteins*), or stay on one of the surfaces (*peripheral proteins*); (iii) Carbohydrate chains are often bound to the proteins (*Glycoprotein*), or to the membrane phospholipids (*Glycolipid*).

In chemistry, the properties of solid / liquid interfaces that determine the surface area available for contact between reactants are critical factors to control reaction rate. For example, electrochemical reactions are strongly dependent on the quality of metal surfaces on which they take place. A polymeric coating that is deposited on oxidizable metal surfaces (e.g., iron, copper, and aluminum) is available to protect them from the corrosion [13]. In electrochemical analysis, the properties of electrodes (e.g., cleanness and conductivity) are critical factors that determine the accuracy and reproducibility of obtained results [14]. And in heterogeneous catalysis where the phase of catalyst (e.g., metals) differs from that of reactants, the rate of catalytic reactions is strongly affected by the properties of catalyst / solvent interfaces [15, 16].

In material science, properties of hybrid materials (e.g., implants) is controlled by their facial behaviors. Hybrid materials consist of inorganic moieties with high physical strength and organic moieties that have to be biocompatible. Only a thin layer of organic coating is sufficient to change completely behaviors of underlying materials as well as to allow the control of its interaction with surrounding environment. For example, the coatings of biodegradable synthetic polymers (mostly PL, PGA and their derivatives) are ideally suited for *orthopedic* applications where a permanent implant is not desired [17, 18].

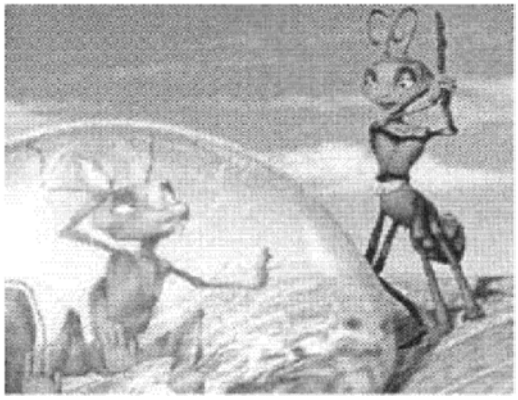

Figure 1.5. *Animation of scaling laws at nano- / micro-scale:* The surface forces are dominant at nano- / micro-scale. It would take a significant effort for an ant to free a comrade imprisoned in a bubble. At the scale of an ant, capillary forces are very significant with respect to the muscular forces the insect can exert [19].

And *in nano- / micro-fluidics*, the importance of solid / liquid interfaces in governing phenomena that happens on surfaces increases dramatically. Figure 1.2 is a famous animation about the predominance of surface phenomena on bulk phenomena in nano- / micro- systems. When reducing the size of a system, the scaling laws that describe the variation of physical quantities with the typical length change completely [19]. Consequently, the control of properties of surface of microchannels becomes extremely important in order to regulate all phenomena that happen in a microchannel, such as biomolecular interactions, separation process in chromatography, Electro-Osmosis Flow (*abbreviated EOF*) and molecular adsorption on surfaces [20, 21]. For example, the EOF that comes from the interaction between and the charged walls (e.g., silica or plasma treated PDMS) starts to be observable when their typical size of a microchannel falls to

about several hundred micrometers [19]. When these surfaces are in contact with aqueous solution at pH>2, a negatively charged layer is formed from its silanol groups (Si-OH). The ions that are close to surface can bind firmly or loosely to it. When applying a voltage, the ions that loosely attach to surface starts to move then drag the liquid with it. This liquid motion is known as EOF. Another common problem encountered in microfluidics is the adsorption of organic molecules on inner walls of microchannels. The non-specific adsorption of moieties may lead to significant loss of sample. In effort to eliminate the surface adsorption, the microchannels can be modified with a polymer coating that is bound non-covalently or covalently to surface [22].

1.1.3. Control of properties of SLIs

In many decades, a vast amount of methods have been developed to coat polymer films on surfaces. The methods in which strong non-covalent bonding or covalent anchoring were constructed are the preferred choices to fabricate polymer films since they meet almost fundamental requirements of thin film deposition, for instance, controllable thickness, adjustable functionality, high homogeneity and long-term stability. In general, all current methods to control polymeric SLIs show certainly serious drawbacks in spite of their advantages, especially the *surface specificity for a given modification chemistry*. This fact requires the innovations of universal techniques which are independent of the nature of surfaces. Here we point out the necessity for surface specificity in some common approaches: self assembled mono-layers (SAMs), grafted polymer brushes and adsorbed polymers layers.

1.1.3.1. Self-assembled monolayers (SAMs)

Self-assembled monolayers (SAMs) are ordered molecular assemblies formed by the adsorption of a functional active surfactant from solution onto a solid surface [23]. Since its introduction in 1980s, SAM has attracted significant attention as the best candidate to tailor thin polymer films. This method allows us to easily decorate interfaces with limitation of surface defects and structure control at nanoscale. We can flexibly utilize this method for modifying surfaces made of a wide range of materials. Adapting to the surface chemistry of substrates, different anchoring chemistries can be applied. Here we consider the two most popular SAMs: thiolization and silanization (see figure 1.3).

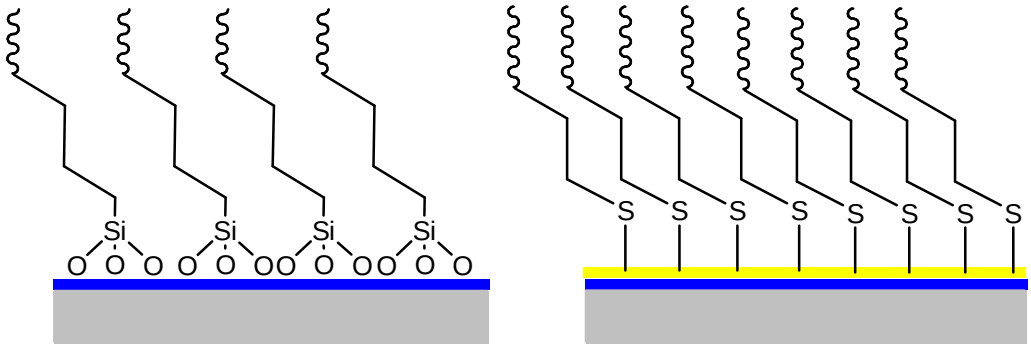

Figure 1. 6. *Illustration of Self-assembled monolayers:* Silanization (left) and Thiolization (right).

Thiolization is the adsorption of organosulfure on noble metal surfaces. The thiols (e.g., alkyl thiol) assemblies can be spontaneously adsorbed by immersing freshly clean metal substrate (e.g., gold) into dilute thiol solutions in an organic solvent. This is based on the high affinity between organosulfures and metal surfaces [24]. The interest in alkanethiol SAMs stems from their stability and ease of preparation [25]. In addition, the organic monolayers that adsorb onto surfaces are usually well-organized even at nano-scale [26]. The metal surfaces modified by this method show potential applications in biosensors, biomimetics, and anti-corrosion [27]. Despite of its advantages, thiols, in general, show low physical and chemical stability due to their facile oxidation. And above all, *this method works only on metal substrates with gold being the best candidate for this chemistry*.

Silanization is the assembly of organosilicon derivatives onto silicon oxide, quartz, glass, mica, etc. A simple immersion of the mentioned substrates into dilute solution of silanes (e.g., OTS, APTES) can spontaneously form these organic assemblies on surfaces [28, 29]. This results from the chemical reactions between compounds containing *silane* groups and surfaces containing *silicon oxides* [29]. In this method, the molecules that anchor to surfaces can self-assembly into highly ordered monolayers [30]. The surfaces modified by this method have received considerable attention in biology and microfluidics [31]. However, the high moisture-sensitivity of silane molecules (particularly in case of chlorosilanes) requires us to handle carefully these chemicals during the assembly steps.

1.1.3.2. End-tethered polymers at SLIs

To graft polymer chains onto surfaces, the covalent bonding is the preferred choice in most cases [32]. There are two main methodological strategies to graft a polymer brush: *(i)* "grafting to" and *(ii)* "grafting from" (see figure 1.4).

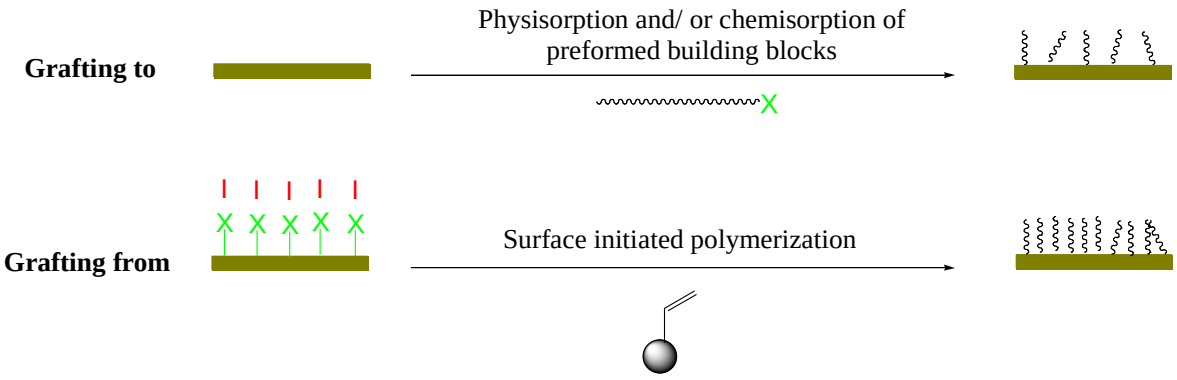

Figure 1.7. *Adaptable approaches to grafting polymer brushes on a wide range of materials:* "Grafting to" - Physisorption and/or chemisorptions of functionalized polymers on pretreated surfaces; "Grafting from" – Surface initiated polymerization of monomers on surfaces where initiators was pre-immobilized.

(i) Grafting to - low density - mushroom regime

In *"grating to"* methods, the polymer chains that were functionalized with reactive functional groups are grafted to a surface. The common reactive functional groups include thiols, silanes, amino or carboxylic groups. This technique usually shows low grafting density due to "excluded volume effect". The repulsion between already grafted polymer chains and the incoming new one from solution can perturb its attachment onto a surface [33]. In this case, the polymer chains are tethered on surfaces in a low-density, mushroom regime.

(ii) Grafting from – high density – brush regime

In *"grafting from"* methods, the monomers are polymerized from surfaces that were previously modified with initiators. This strategy shows much higher grafting density compared to that of "grafting to" strategy. With the advances in polymer synthetic

methodologies and their adaptation to surface chemistry, these methods allow us to graft polymer chains on a variety of material surfaces with controllable properties. They can be implemented with almost all available polymerization techniques: ring opening metathesis polymerization (ROMP), nitroxide-mediated polymerization (NMP), atom transfer radical polymerization (ATRP), single-electron transfer living radical polymerization (SET-LRP), or reversible addition fragmentation chain transfer (RAFT) polymerization [32]. In this case, the polymer chains are tethered on surfaces in brush regime where they are stretched away from grafting surfaces like bristles in a brush [34].

Polymer brush has been studied in many decades. It was first noted as densely tethered polymer chains on interfaces in 1976 by Alexander and de Gennes [33]. These scientists have established the foundation for theoretical analysis based on scaling theory to study polymer brushes. They have pointed out the "**excluded volume effect**" (a kind of steric effect) in which the repulsion is set up between polymer chains due to spatial confinement. At sufficiently high grafting density of polymer chains on surfaces, an entropy barrier is established. That energy fence forces polymer chains to repulse each others, stretch away from surfaces, as well as repel external objects that approach surfaces. Therefore, polymer brushes exhibit anti-fouling properties and minimize the adsorption of molecules on solid surfaces.

1.1.3.3. Adsorbed polymer layers

Polymers can adsorb from solution onto surfaces if the interaction between the polymer and the surface is more favorable than that of the solvent with the surface and/or the polymer [35]. This can be accomplished either (i) by the adsorption of certain neutral polymers on specific surfaces or (ii) by the adsorption of polyelectrolytes (ionic or anionic) on charged surfaces.

(i) Neutral Polymers:

Some neutral polymers (e.g., PS, PDMA, PHEA, PEO, etc) show the ability to adsorb physically on solid surfaces (e.g., silica, glass) [36]. It was believed that the attractive interactions (e.g., Van der Waals forces, dipolar forces, hydrogen bonds, and etc) between polymer chains and the surface are the origin of polymer adsorption. The tendency of polymer chains (adsorb to surface or not) is determined by the nature of surface, absorbing polymer, and solvency condition [35]. If the polymer prefers the surface to the solvent,

polymer chains are adsorbed to. On the other hand, we have polymer depletion if the polymer prefers the solvent to the surface. Figure 1.5 represents the differences between adsorption and depletion of polymer chains on a surface. We can see the surface energy drop in adsorption case that indicates the presence of adsorbed polymer chains on a surface. In contrast, the slow increase in surface energy implies that polymer chains can't attach to the surface in depletion case.

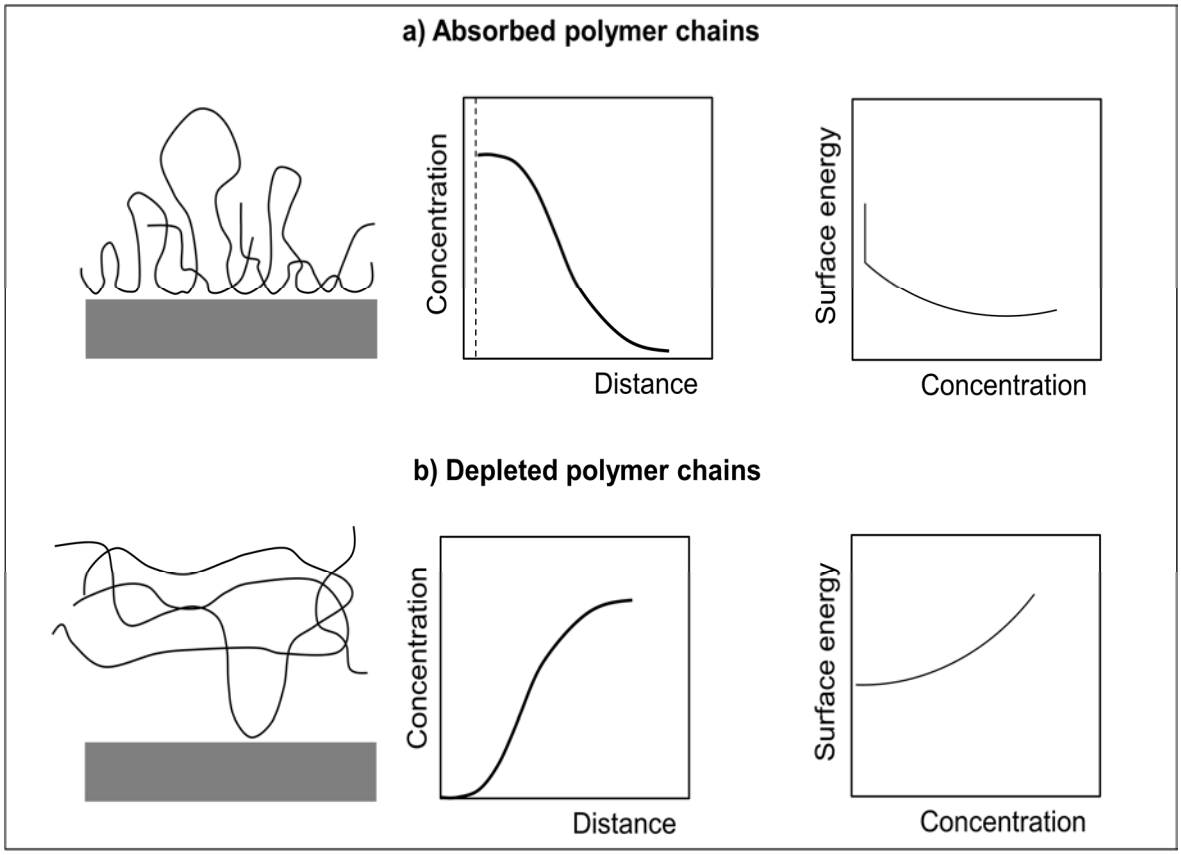

Figure 1. 8. *Adsorption and Depletion of polymer chains on surface*: a) Illustration of absorbed polymer chains, concentration profile and surface energy profile; b) Illustration of depleted polymer chains, concentration profile, and surface energy profile. Source: De Gennes [35].

An important application of polymer adsorption is the introduction of polymer to silica surface of a capillary. This is typically realized by rinsing the capillary with a solution containing the polymer of interest. The goal of introducing neutral polymers to the capillary is to eliminate sample-wall interactions as well as to stabilize Electro-Osmotic

Flow. For this purpose, hydrophilic neutral polymers (e.g., polysaccharide, PVA, PEO, PVP, PDMA) seem to be good candidates [37].

(ii) Polyelectrolytes:

Polyelectrolytes are polymers with ionizable groups (anions or cations) [38]. In polar solution (e.g., water), these ionizable groups can dissociate, providing charges on polymer chains. When a charged surface is put in a contact with a polyelectrolyte, the electrostatic interactions between those charged species of polymer chains and the surface are established. The electrostatic interaction which is generally stronger than other interactions (e.g., Van der Waals, dipolar forces, and hydrogen bonds) plays major role in governing polymer adsorption in this case.

The most important parameters controlling the adsorption behavior of polyelectrolytes at surfaces are: the charge density of the polymer chains (or degree of ionization); the net surface charge density; and the ionic strength [35]. In the situation where polyelectrolytes adsorbing on a surface of opposite charge, one can expect virtually any polymer chain to be adsorbed. For the adsorption of polyelectrolytes having the same sign as the surface, the absorbed amount of polymer chains is obviously less than that in the former case. The adsorption of polyelectrolytes generally decreases with the increase in ionic strength. Café et al., (1982) has studied the influence of ionic strength on the adsorption of sodium carboxymethyl cellulose and poly(acrylic acid) on barium sulfate surface and found that the increased ionic strength at alkaline pH allowed more polymer chains to adsorb to surface [39].

To achieve thicker polyelectrolyte films, Decher et al., has proposed the superposition of multiple polymer layers on a surface [40, 41]. He has performed the adsorption of consecutively alternating monolayers of anionic polyelectrolyte (polyalyaminehydrochloride) and cationic polyelectrolyte (sodium salt of polystyrene sulfonate) on aminopropylsilanized quartz that was previously protonated with acidic solution (as shown in figure 1.6).

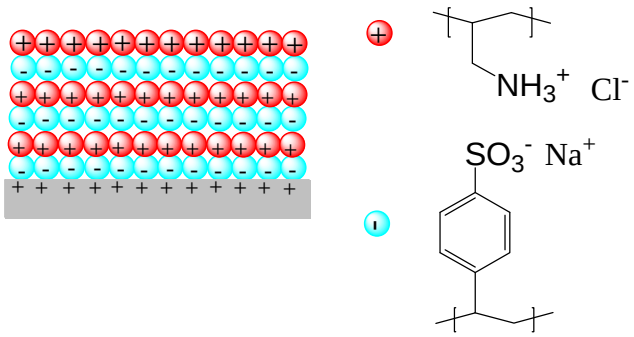

Figure 1. 9. *Example of adsorption of polyelectrolytes on surfaces*: Consecutively alternating adsorption of polyalyaminehydrochloride (in red) and sodium salt of polystyrene sulfonate (in cyan) on protonated aminopropylsilanized fused quartz [40].

1.1.4. A microchannel - scaling laws (importance of Surface to Volume ratio)

Microfluidics is a young discipline that studies the fluid flows circulating in artificial microsystems [42]. Since its introduction in 1990s, a vast of microfluidic systems has been fabricated, for example, electrophoretic separation systems, or micromixers, DNA amplifiers, microcytometers, and chemical microreactors. These systems were employing **integrated microchannels** as transportations of fluid flows. We discuss here some physical phenomena in those microchannels, and above all we evaluate the competition between facial phenomena and bulk phenomena in down-scaling.

1.1.4.1. Scaling laws in down-scaling: the predominance of surface forces on volume forces

To study physical phenomena in microchannels, it is important to consider **scaling laws**. *A scaling law signifies the law of the variation of physical quantities with the size **l** of a system or an object* [42]. The general rule of thumb for scaling laws is: When reducing the size ***l*** to a certain value, *the quantities that are associated with the weaker exponent become dominant*. As a result, the volume forces ($\sim l^3$) become negligible with respect to surface forces ($\sim l^2$) in micro- or nano- systems (see figure 1.7). With the predominance of facial forces on bulk forces, some traditional phenomena, that we are used to at macroscale, disappear while a series of new phenomena occur in these systems.

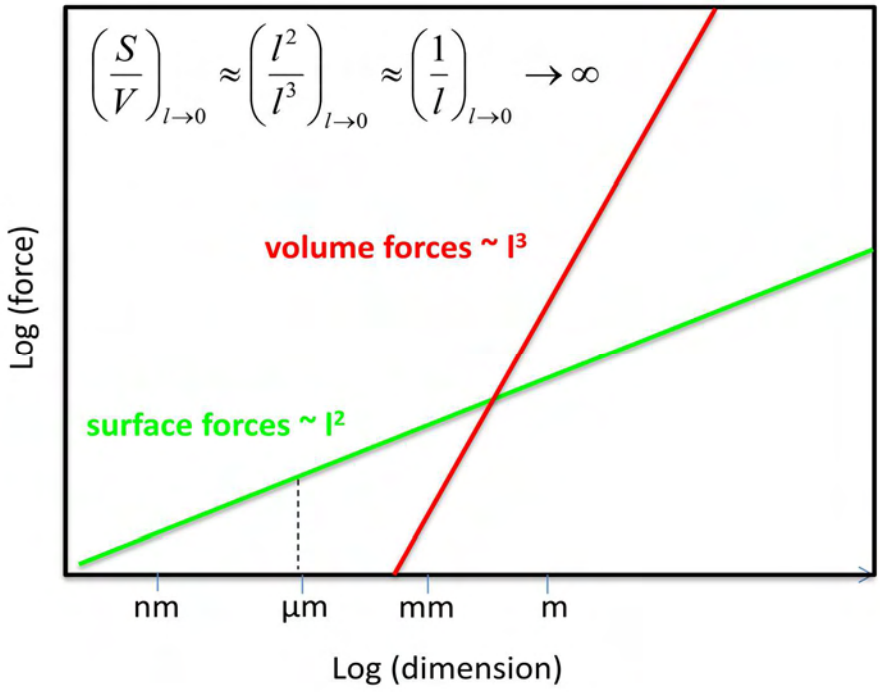

Figure 1.10. *Scaling laws in down-scaling: the predominance of surface forces on volume forces.*

1.1.4.2. Dimensionless numbers in microfluidics

The relative importance of physical phenomena in microfluidic systems is generally evaluated by dimensionless numbers. Two most often mentioned numbers in microfluidics are: **Reynolds** number (relating inertial forces to viscous forces) and **Peclet** number (relating convection to diffusion). We will discuss here how these dimensionless numbers scale with the typical length of a microfluidic system, i.e. channel size, and how they indicate physical changes in down-scaling.

(i) Reynolds numbers: dominance of viscous stress

The Reynolds number is defined as the ratio of inertial forces and viscous forces: $R_e = \frac{f_i}{f_v} = \frac{Ul}{\eta}$ where f_i is the inertial centrifugal force density, f_v is the viscous force density, l is the spatial scale, U is the characteristic velocity of the fluid, and η is its kinematic viscosity [42].

When a fluid flows through a microchannel, typical fluid velocities do not exceed a centimeter per second and widths of channels are on the order of tens or hundreds of

micrometers; it follows that, in general, Reynolds numbers in microfluidic systems do not exceed 10^0 [42]. As a result, the viscous forces are dominant over inertial forces.

In the situation where viscous forces overwhelm inertial forces, the fluids flow slowly in parallel layers without interruption between fluid layers. That simple fluid regime is known as *laminar flow* [43]. The simplification of fluid dynamics provides us the possibility to conduct precisely controllable processes, i.e. chemical reactions in laminar flow reactor.

(ii) Péclet numbers: dominance of diffusion

The dispersion Peclet number (P_e) characterizes the relation between transport of solute due to convection and diffusion. In the case of a microchannel, it is given by $P_e = \frac{Z}{l} = \frac{Ul}{D}$, where Z is the moving distance of fluid (relating convection), U is the characteristic flow velocity, l is the size of the system, and D is the diffusion coefficient of the solute [42].

In practice, microfluidic systems work at the average values of Peclet number (between 0.1 and 100) and *diffusion* is the major mixing mechanism of fluid [43]. As a result, the mixing velocity is slow in microchannels. In addition, the Taylor dispersion that spreads molecules along the direction of the flow is pronounced as ($D_z \propto P_e^2 D$) and it contributes to fluid mixing in microchannels [44].

1.1.4.3. Adsorption phenomena

Adsorption is the phenomenon of the accumulation of a substance at surfaces. In microsystems, the adsorption of biological samples on surfaces of microchannels is a major concern.

It was known that biomolecules, e.g. proteins, can strongly adsorb to silica surfaces, leading, for instance, to considerable peak broadening and asymmetry in electrophoretic separations [45] and/or to sample loss in microfluidic devices. Such adsorption is stemmed from electrostatic and / or dipolar interactions between proteins and silica surface. Indeed, the silica surface becomes negatively charged in contact with electrolytes at pH greater than 2 due to presence of silanol groups. Therefore, electrostatic interactions might occur between silanol groups on surface and proteins that generally contain charged species [46].

Proteins can also physically adsorb to PDMS surfaces [47], interfering with the usability of PDMS-based microfluidic devices. Hydrophobic and porous surfaces like PDMS are known to be favorable for protein adsorption [48].

As mentioned above, the miniaturization of a system tends to enhance interfacial phenomena, in general, and surface adsorption, in particular. It's clear that the adsorption at solid/liquid interfaces must be minimized to avoid a sample loss and the deterioration of analytical performances of microfluidic systems.

1.1.5. Microfluidic devices (lab-on-chips)

1.1.5.1. Commercialization of microfluidic devices

Lab-on-chip (LOC), also called "micro total analysis system (μTAS)", is a newly emerging field that represents a breakthrough in biomedical analysis and diagnosis. From historical point of view, lab-on-chips (LOCs) emerged from efforts to control liquid flow at subnanoliter scale in the early 1990s. Over the last twenty-five years, hundreds of microfluidic research groups and tens of microfluidic related companies have been established. iSTAT blood analyzer (from Abbott Point of Care, USA) is among the first commercially successful LOC products. This LOC device is an advanced blood analyzer that provides real-time, lab-quality results within minutes, using only several blood drops. Such a device is equipped with different cartridges which contain variety of chemically sensitive biosensors on a silicon chip, allowing a comprehensive menu of specific diagnostic tests (chemistries, hematology, blood gases, coagulation, and cardiac markers). Another interesting microfluidic device is the glucose meter (from Bayer Healthcare, Germany), which uses multiple strips integrated with optical detectors in a single package for diabetic patients. The DNA and peptide analyzer from Agilent Technologies permit the identification of an object (e.g., a virus) from characteristic sequences of genes. The future development of LOCs will provide us with a variety of fluidic devices for diverse biomedical applications.

1.1.5.2. Advantages of miniaturization and integration

Miniaturization and integration of microfluidic devices lead to many benefits. *Firstly*, the cost of fabrication of microfluidic devices decreased significantly by reducing the consumption of manufacturing materials. *Secondly*, the portability of miniaturized and

integrated devices is easier. *Thirdly*, it is obvious that the consumption of reagents and analytes can be reduced significantly by decreasing the volume of a test. *Lastly*, the time of analysis can be decreased by integrating multiple tasks on the same microfluidic platform and performing analyses in serial and / or parallel manner.

Additionally, the predominance of surface phenomena on volume phenomena (mentioned in section 1.1.4.1) offers entirely new applications that are inaccessible to fluidic systems at macroscale. For instance, passive liquid actuation based on capillary forces that is employed, for instance, in capillary **test strips** would not work on macroscale. Other cases in which we take advantage of working on microscale are, electro-osmotic flow actuation, hydrophobic valves in microfluidic devices [49], and surface immobilized enzymes in enzymatic reactors and/or single cell studies in fluidic systems [50].

1.1.5.3. Microfabrication of microfluidic devices

Depending on targeted application and cost of devices, different materials, i.e. silicon, glass, quartz, metals and polymers can be employed in manufacturing. The choice of manufacturing technique must be compatible with the chosen material. We present here current microfabrication techniques that are widely used to fabricate microfluidic devices.

(i) The choice of materials

In the early days of LOCs, **silicon** and **glass** were major materials for manufacturing microfluidic devices [51]. The use of those well-known materials allows us to enjoy the benefits of well-developed and broadly utilized techniques in microelectronics, i.e. *photolithography and etching*. Despite of their relatively high price, these materials are still required for fabrication of some active elements (e.g., thermal actuators and detectors) that can suffer from high temperature. Weak thermal expansion (coefficient of thermal expansion $\alpha \sim 2.33\times10^{-6}$ at room temperature, for silicon) inhibits the distortion of microstructures as heating. Silicon is a good conductor that allows the fast thermal dissipation which is really important in miniaturized systems.

The **metals** (e.g., Au, Ag, Cu) are necessary for construction of active elements that are electrically conductive (e.g., electrodes, magnetic coils) in LOCs. Metal- based microstructures are generally formed by *electron lithography techniques*. [52].

In several years, the **polymers** (epoxy, SU8, COC, PDMS, and etc) that are much cheaper than silicon and glass have become the materials of choice for manufacturing low-price LOCs [53]. Polymer – based microstructures can be formed by various fabrication techniques: *molding, casting, and etc*.

To satisfy the low cost of device, Charlot et.al, (2008) has currently proposed to fabricate LOCs by integrating active elements (Si, metals) into a system of channels made of cheap materials, such as PDMS and/or SU8 and calling them hybrid microfluidic devices or hybrid LOCs [54].

(ii) Photolithography

Photolithography is a process that plays a central role in microfabrication. This technique is utilized to design defined microstructures on a substrate. It is realized by using the light (X-ray, electron, or photon) to transfer geometric pattern from a photomask to a photoresist on a substrate [53]. Typically, a photolithography process groups together following steps: fabrication of a photomask; deposit of a photoresist on a substrate; and transfer of a pattern from photomask to photoresist.

Fabrication of a photomask: A photomask is a transparent plate on which a defined opaque pattern is deposited. In practice, photomasks are generally quartz plates covered with defined patterns in chrome. Taking benefits from the development of electronic lithography techniques, these techniques are often used to fabricate photomask with a precision on the order of a fraction of a micrometer [42].

Deposit of a photoresist on a substrate: A photoresist film is prepared on a solid substrate (silicon or glass) that is ready for a pattern transfer. The highly photosensitive resists, i.e. SU8 and AZ-series, are among the materials of choice [42]. The deposit is made using spin coating technique in which a layer of photoresist is deposited on a spinning surface. A drop of photoresist solution at certain volume (3-4 ml, in practice) is first dispensed at the center of a substrate. The substrate is then rotated at high velocities (several thousand rpm) to allow the spreading of the photoresist over its surface. After a sufficient rotation time (a few minutes), a layer of photoresist with a stable thickness is formed on a substrate. The thickness of the obtained film varies with the viscosity, initial concentration of photoresist solution, and rotation velocity of the substrate. At the end of this step, the resist is heated slightly (i.e., 90°C, 2 minutes) to completely remove a solvent.

Pattern transfer from photomask to photoresist: The resist film is exposed to a light beam crossing the photomask. The prepared photoresist film is previously aligned with the photomask in an aligner (e.g., MA-6 mask aligner from SUSS MicroTec, Germany). The light beam initiates reactions in the photoresist, therefore change its solubility in certain solvents.

There are two types of resists: positive (e.g., AZ-series) and negative (e.g., SU8). In the former case, the irradiated areas become soluble and removable by an organic solvent, while the non-irradiated areas are polymerized and insoluble. In the later case, the irradiated areas become insoluble while the other areas can be dissolved and removed by an organic solvent.

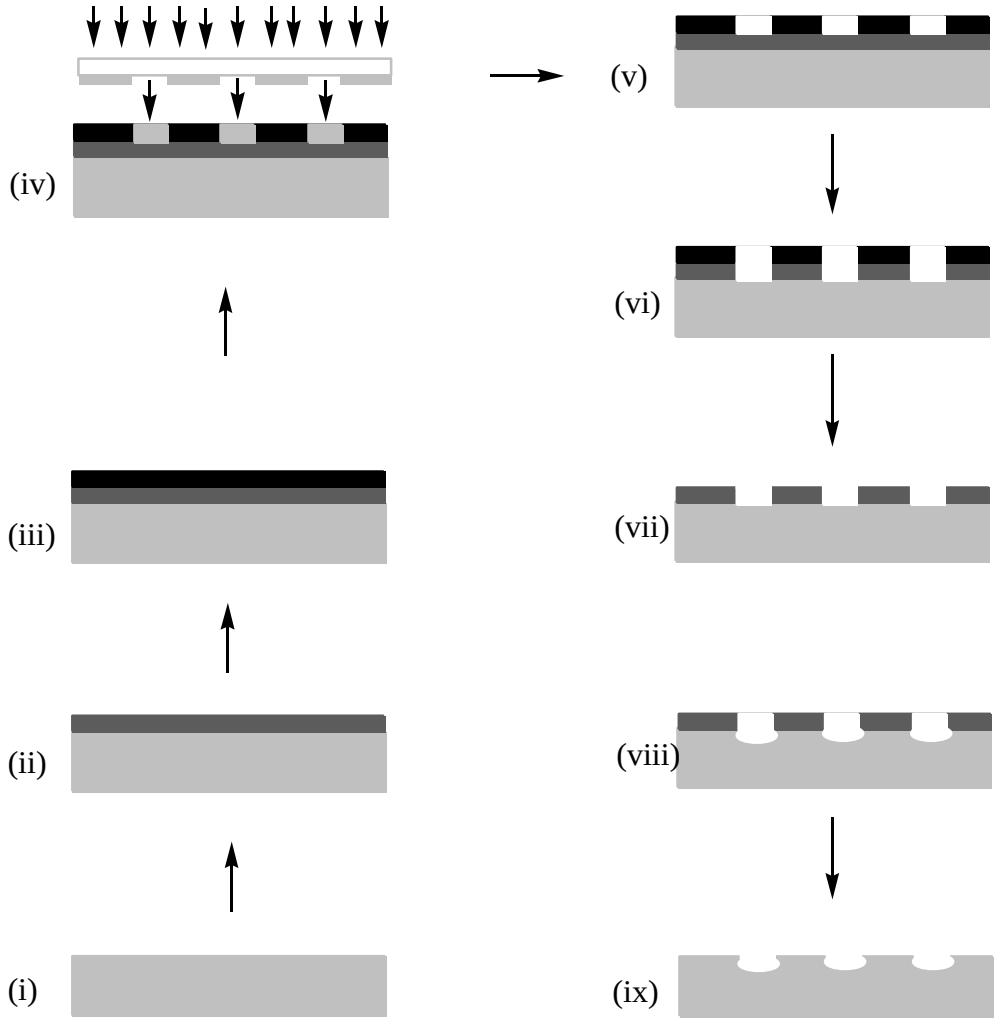

Figure 1.11. *Illustration of Wet etching of glass: (i)* Clean substrate; *(ii)* Deposit protection material; *(iii)* Deposit photoresist using spin coating; *(iv)* Expose the resist to UV radiation through a mask (UV radiation only transmits through transparent areas); *(v)* Develop the photoresist (exposed areas are eliminated in case of positive resist while remained in the case of negative resist); *(vi)* Etch protective material and *(vii)* remove the resist from the substrate; *(viii)* Etch the glass; *(ix)* Remove mask material from the substrate. Source: P. Abgrall and A-M Gué [53].

(iii) Etching

Etching belongs to bulk micromachining technologies that form micro-patterns in the substrate itself. In this technique, microstructures are etched on substrate by using a proper physicochemical method. It can be achieved by either wet etching (use of chemicals, i.e. HF or KOH) or dry etching (use of ionized gas, plasma) [53].

Figure 1.8 shows an example of wet etching of glass. First, the micro patterns on the substrate are defined by photolithographically (i→v). The desired microstructures on the substrate are obtained by etching of the glass substrate and removing the protective material (vi→ix).

(iv) Molding

Molding is a replication technique that is widely used for polymer-based microfluidic devices. The molding that employs PDMS offers an elegant solution for microfabrication. The benefits of PDMS-based LOCs are: visualization of flows in transparent PDMS channels; variable elasticity depending on PDMS/ reticulating agent; water tightness of microfluidic connections due to elastomeric property of PDMS; self-adhesion to glass, silicon or PE due to temporary hydrophilicity of oxidized PDMS surface (after oxygen plasma treatment or immersion in a strong base); and easy peeling off from substrates due to low surface energy.

Figure 1.9 describes molding process that is often used in clean room to manufacture PDMS- based LOCs. We have used this process to fabricate PDMS microchannels that were used in this work (chapter 4). The SU8 mold was first patterned by photolithography (i), the PDMS was then molded on SU8 mold, peeled off from substrate (ii), and finally the formed channels in the PDMS substrate are closed by a glass plate after O_2 plasma treatment (iii).

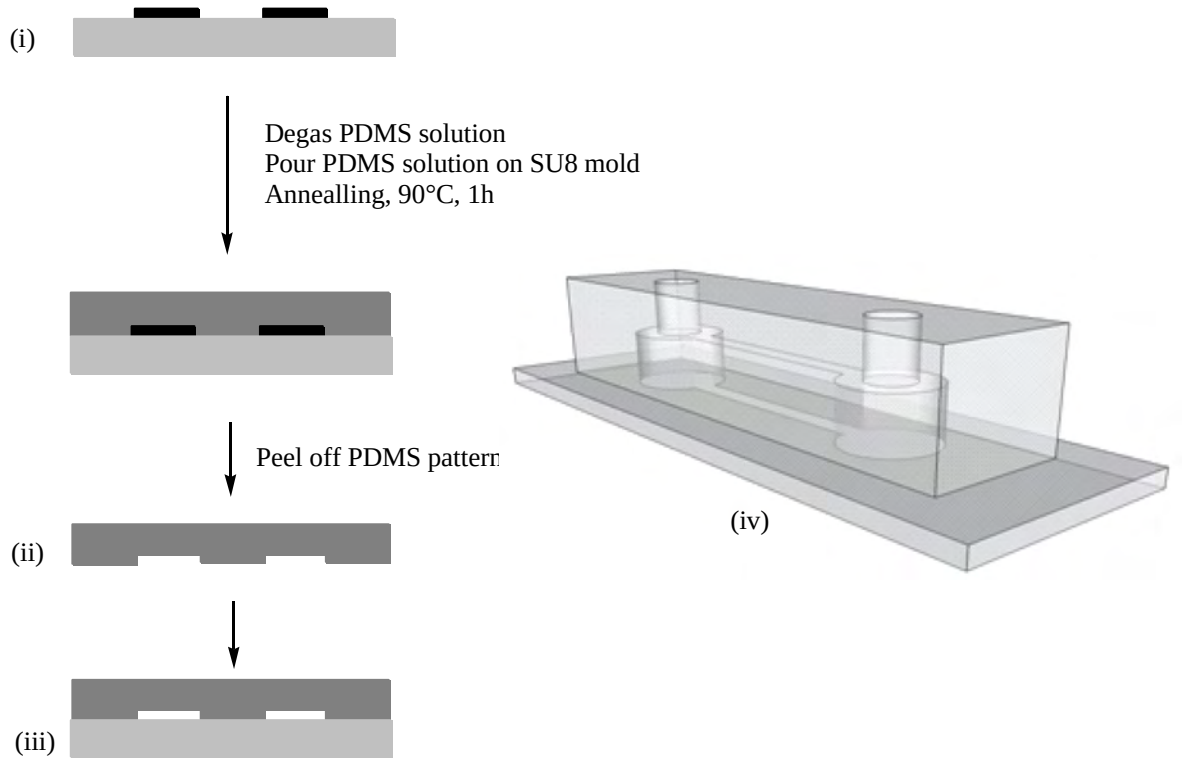

Figure 1. 12. *Illustration of Molding process of PDMS microchannels (i)* SU8 mold is photolithographically patterned; *(ii)* PDMS pattern is casted with using SU8 mold; *(iii)* PDMS pattern is sealed by glass wafer with using plasma treatment; *(iv)* An example of 1D microchannel (H×W×L = 10µm×300µm×3cm). Protocol developed by LAAS laboratory.

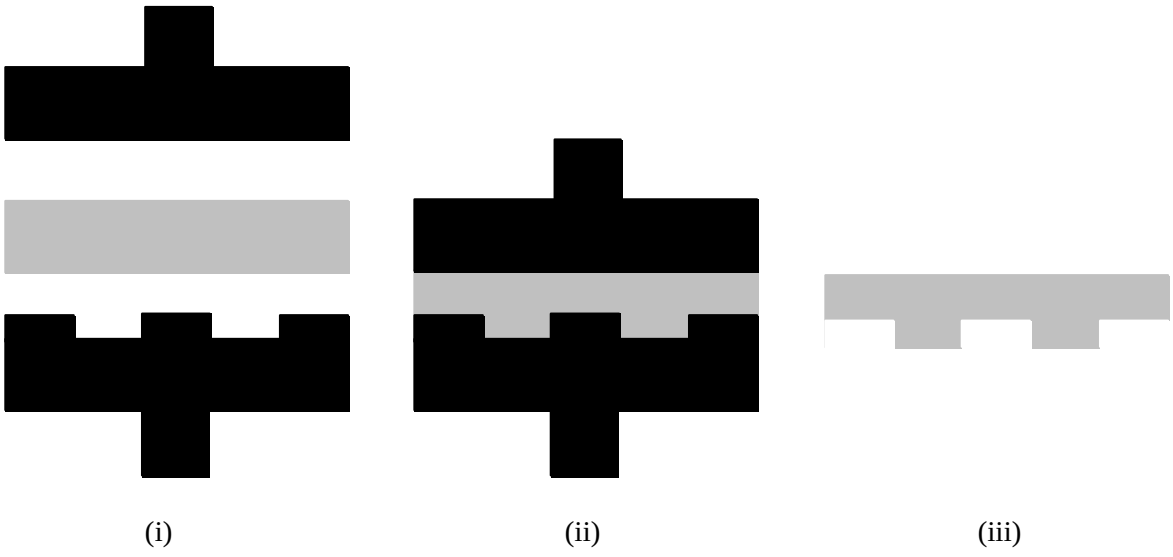

Figure 1. 13. Illustration of casting process: (i) Heating; (ii) Embossing; (iii) Demolding.

(v) Casting

Casting is another replication technique that can be applied to manufacture polymer-based LOCs. In this technique, the polymer is pressed into a heated deformable material, then cooled, and finally separated to obtain a defined microstructure.

Figure 1.10 illustrates the principle of casting technique. The mold (a rigid material, i.e. silicon or a metal) is first heated to high temperature (e.g., 170°C for PMMA) at which the polymer can deform considerably under pressure. The polymer is then pressed by heated mold at high pressure (tens of bars) to form patterns on it (*embossing*). Then the polymer bulk is removed from the mold and left cooling until a stable solid structure is obtained (*demolding*). The commonly employed casting materials include PMMA, PC, PE, PET, PVC, PEEK [42].

1.1.6. Conclusions

We have shown here that solid / liquid interfaces (SLIs) play a crucial role in many different processes in biology, chemistry and physics. Along the same lines, we also put in the evidence that SLIs become extremely important for small objects, such as particles and/or nano- and micro-channels. This can be explained through scaling laws as the volume forces decay much faster than the surface ones, with decreasing size of an object. It has been well known for many years that SLIs play a crucial role in microfluidic devices and that their role will grow even more as we move to nano-fluidics. Consequently, several approaches to the modification of SLIs have been developed over the years and they are based on formation of more or less organized organic layers on a solid surface. We have described the major modification schemes of the SLIs, such as the formation of self-assembled monolayers on silicon and/or metal surfaces, formation of end-tethered polymers brushes and adsorption of neutral or charged polyelectrolytes on various surfaces. All these approaches have their advantages and disadvantages but they all can be characterized by the requirement of a surface specificity, i.e., the surface chemistry dictates the material of choice that will be modified. The situation becomes even more difficult or even impossible to realize when surfaces of microfluidic devices built from several different materials have to be functionalized.

We have developed in this thesis work a surface modification scheme that is substrate independent (works on all solid surfaces) while it offers a great variability and choice in the physic-chemical-biological properties of the modified surfaces, spanning from passive non-fouling, through stimuli-responsive to biologically active solid/liquid interfaces.

References

[1] Alberts B., Johnson A., Lewis J., *Molecular biology of the cell*, 4th ed., Garland Science Press, USA (2002).

[2] S.J. Singer, G.L. Nicolson, Science, 1972, 175, pp 720-731.

[3] Bertil Hill, *Ion channels of excitable membranes*, 3rd ed., 2001, Sinauer Associate Publisher, USA

[4] W.D. Stein, W.R. Leib, *Transport and Diffusion across Cell Membranes*, 1986, Academic Press, USA.

[5] Thomas D. Pollard, John A. Cooper, Science, 2009, 326 (5957), pp 1208-1212.

[6] Sheryl P. Denker, Derek C. Huang, John Orlowski, Heinz Furthmayr, Diane L Barber, Molecular Cell, 2000, 6(6), pp 1425-1436.

[7] *(a)* Alan Fersht, *Structure and Mechanism in Protein Science: A Guide to Enzyme Catalysis and Protein Folding*, W. H. Freeman Press, USA (1998); *(b)* Robert A. Copeland, *Enzymes: A Practical Introduction to Structure, Mechanism, and Data Analysis*, Wiley Publisher, USA (2000).

[8] *(a)* Holmquist M., Current Protein and Peptide Science, 2000, **1**(2), pp 209-235; *(b)* R. M. C. Dawson, On the mechanism of action of phospholipase A, Biochem J., 1963, 88(3), pp 414–423.

[9] Barry M Gubiner, Cell, 1996, 84(3), pp 345-357.

[10] Marinos C., Dalakas M.D., Neurology, 1998, **51** (6), Suppl 5 S2-S8.

[11] *(a)* Edward Bittar, *Membranes and Cell Signaling*, 1997, JAI press, England; *(b)* C.M. Revankar, D.F. Cimino, L.A. Sklar, J.B. Arterburn, E.R. Prossnitz, Science, 2005, 307 (5715), pp 1625-1630; *(c)* Stephen S. G. Ferguson, Pharmacological Reviews, 2001, 53(1), pp 1-24.

[12] J.H. Duncan Bassett, Graham R. Williams, Trends in Endocrinology and Metabolism, 2003, 14(8), pp 356-364.

[13] *(a)* C.A. Ferreira, S. Aeiyach, A. Coulaud, P.C. Lacaze, J. Appl. Electrochem., 1999, 29, pp 259–263; *(b)* G.A. Smitha, O.I. Jude, Polymer, 2001, 42(24), pp 9665–9669; *(c)* T. Tüken, G. Arslan, B.Yazici, M. Erbil, Prog. Org. Coatings, 2004, 49(2), pp 153–159.

[14] Allen J. Bard, Larry R. Faulkner, Electrochemical Methods: Fundamentals and Applications, 2rd ed., Wiley Publisher, USA (2000).

[15] Michel Boudart, J. Mol. Catalysis, 1985, 30 (1-2), pp 27-38.

[16] J. M. Thomas, W. J. Thomas, Principles and *Practice of Heterogeneous Catalysis*, Wiley Publisher, USA (1996).

[17] C.M. John, J.T. Arthur, Biomaterials, 2000, 21(23), pp 2335–2346.

[18] Freed L.E., Vunjak-Novakovic G., Biron R.J., Eagles D.B., Lesnoy D.C., Barlow S.K., Langer R., Biotechnology, 1994, 12(7), pp 689-693.

[19] Patrick Tabeling, *Introduction to Microfluidics*, Oxford University Press, UK (2005).

[20] F. Tagliaro, G. Manetto, F. Crivellente, F.P. Smith, Forensic Sci. Int., 1998, 92 (2-3), pp 75–88.

[21] H. Stellan, J. Chromatogr. A, 1985, 347, pp 191–198.

[22] (a) Ken K.C. Yeung, Charles A. Lucy, Anal. Chem., 1997, 69 (17), pp 3435–3441; (b) John K. Towns , Fred E. Regnier, Anal. Chem., 1991, 63 (11), pp 1126–1132; (c) R. Nehmé , C. Perrin, Methods Mol. Biol., 1996, 984, pp 191-206.

[23] U. Abraham, Chem. Rev., 1996, 96, pp 1533–1554.

[24] G.E. Poirier, E.D. Pylant, Science, 1996, 272, pp 1145–1148.

[25] *(a)* D.B. Colin, E. Joe, M.W. George, J. Am. Chem. Soc., 1989, 111(18), pp 7155–7164; (b) G.N. Ralph, L.A. David, J. Am. Chem. Soc., 1983, 105(13), pp 4481–4483.

[26] *(a)* D.B. Colin, M.W. George, Science 240, 1988, pp 62–63; *(b)* D.P. Marc, B.B. Thomas, L.A. David, E.D. Christopher, J. Am. Chem. Soc., 1987, 109(12), pp 3559–3568 (1987).

[27] *(a)* Th. Wink, S. J. van Zuilen, A. Bult and W. P. van Bennekom, Analyst, 1997, 122, pp 43R-50R; *(b)* Anne L. Plant, Langmuir, 1993, 9 (11), pp 2764–2767.

[28] O. Steffen, J.R. Bart, N.R. David, Angew. Chem. Int. Ed., 2005, 44(39), pp 6282–6304.

[29] H. Claudia, H. Stephanie, S.S. Ulrich, Chem. Soc. Rev., 2010, 39, pp 2323–2334.

[30] S. Jacob, J. Am. Chem. Soc., 1980, 102(1), pp 92–98.

[31] Mingxian Huang, Eva Dubrovcakova-Schneiderman, Milos V. Novotny, Hafeez O. Fatunmbi, Mary J. Wirth, J. Microcolumn Separations, 1994, 6(6), pp 571–576.

[32] A. Omar, J. Polym. Sci. Part Polym. Chem., 2012, 50 (16), pp 3225–3258.

[33] *(a)* P.G. De Gennes, J. Physic Paris, 1976, 37, pp 1445–1452 ; *(b)* S. Alexander, Physic Paris, 1977, 38(8), pp 977–981; *(c)* M. Daoud, P.G. De Gennes, J. Physic Paris, 1977, 38(1), pp 85–93; *(d)* P.G. De Gennes, Macromolecules, 1980, 13(5), pp 1069–1075; *(e)* P.G. De Gennes, Macromolecules, 1981, 14(6), pp 1637–1644; *(f)* P.G. De Gennes, Macromolecules, 1982, 15(2), pp 492–500; *(g)* P.G. De Gennes, J Phys Lett, 1983, 44, pp 241–246.

[34] (a) S.T. Milner, Eur. Lett., 1988, 7(8), pp 695–699; (b) S.T. Milner, T.A. Witten, M.E. Cates, Macromolecules, 1988, 21(8), pp 2610–2619; (c) S.T. Milner, T.A. Witten, M.E. Cates, Eur. Lett, 1988, 5(5), pp 413–418.

[35] P.G. De Gennes, Adv. Colloid. In. Sci., 1987, 27(3-4), pp 189–209.

[36] Eugène Papirer, Adsorption of polymer on silica surfaces, Marcel Dekker, USA (2000), pp 463.

[37] Horvath J., Dolník V., Electrophoresis, 2001, 22(4), pp 644-655.

[38] Andrey V. Dobrynina, Michael Rubinstein, Prog. Polym. Sci.,2005, **30**, pp 1049–1118.

[39] M.C. Cafe, I.D. Robb, J. Colloid. Interface Sci., 1982, 86(2), pp 411-421.

[40] Gero Decher, Science, 1997, 277 (5330), pp 1232-1237.

[41] G. Decher, J. D. Hong, J. Schmitt, Thin Solid Films, , 1992, 210/211, pp 831-835.

[42] Patrick Tabeling, *Introduction to Microfluidics*, Oxford University press (2005).

[43] H.A. Stone, A.D. Stroock, A. Ajdari, Annu. Rev. Fluid Mech., 2004, 36, pp 381–411.

[44] Geoffrey Taylor, Dispersion of solute matter in solvent flowing slowly through a tube, Proc. R. Soc. Lond. A, **219**,186-203 (1953).

[45] M. Graf, R. Galera Garia, H. Wätzig, Electrophoresis, 2005, 26(12), pp 2409–2417.

[46] Irina Gitlin, Jeffrey D. Carbeck, George M. Whitesides, Angew. Chem. Int. Ed., 2006, 45, pp 3022 – 3060.

[47] J. Cooper McDonald, George M. Whitesides, Acc. Chem. Res., 2002, 35 (7), pp 491–499.

[48] *(a)* L.J. Ho, K. Gilson, L.J. Whan, L. Hai Bang, J. Colloid. Interface Sci., 1998, 205(2), pp 323–330; *(b)* A. Yusuke, I. Hiroo, Biomaterials, 2007, 28(20), pp 3074–3082.

[49] *(a)* Shulin Zeng, Chuan-Hua Chen, James C. Mikkelsen Jr., Juan G. Santiago, Sensors and Actuators B: Chemical, 2001, 79 (2-3), pp 107-114; *(b)* Yanying Feng, Zhaoying Zhou, Xiongying Ye, Jijun Xiong, Sensors and Actuators A: Physical, 2003, 108 (1-3), pp 138-143.

[50] *(a)* Shuichi Takayama, Emanuele Ostuni, Philip LeDuc, Keiji Naruse, Donald E. Ingber, George M. Whitesides, Nature, 2001, 411, pp 1016; *(b)* McClain MA, Culbertson CT, Jacobson SC, Allbritton NL, Sims CE, Ramsey JM., Anal Chem., 2003, 75(21), pp 5646-5655; *(c)* Anna Tourovskaia, Thomas Barber, Bronwyn T. Wickes, Danny Hirdes, Boris Grin, David G. Castner, Kevin E. Healy, Albert Folch, Langmuir, 2003, 19, 4754-4764; *(d)* Mathieu Foquet , Jonas Korlach , Warren R. Zipfel , Watt W. Webb , Harold G. Craighead, Anal. Chem., 2004, 76 (6), pp 1618–

1626; *(e)* Munce NR, Li J, Herman PR, Lilge L., Microfabricated system for parallel single-cell capillary electrophoresis, Anal Chem. 2004 Sep 1;76(17):4983-9;

[51] *(a)* D.H Jed, Science, 1993, 261, pp 895–897; *(b)* C.J. Stephen, H. Roland, B.K. Lance, J.R. Michael, High-speed Separations on a Microchip, Anal. Chem., 1994, 66, pp 114–1118; *(c)* C.J. Stephen, W.M. Alvin, J.R. Michael, Anal. Chem., 1995, 67(13), pp 2059–2063; *(d)* J. Zhi-Jian, F. Qun, F. Zhao-Lun, Anal. Chem., 2004, 76(18), pp 5597–5602; *(e)* R.F. Bryan, T.B. Michael, Anal. Chem., 2005, 77, pp 5706–5710.

[52] Holger Beckera, Laurie E. Locasciob, Talanta, 2002, 56, pp 267–287.

[53] P. Abgrall and A-M Gué, J. Micromech. Microeng., 2007, 17, R15-R49.

[54] S. Charlot, A.M. Gué, J. Tasselli, A. Marty, P. Abgrall, D. Estève, J. Micromech. Microeng., 2008, 18(1), pp 1–8.

1.2. Mussel inspired surface chemistry

1.2.1. Introduction

The attachment of mussel to virtually any solid materials has inspired a versatile approach to the surface modification of a wide range of inorganic and organic materials, resulting in new surface modification chemistry: **Mussel inspired surface chemistry (MiSC)** [1]. This new technology is based on using biomimetic compounds of mussel proteins (the catecholamine families) as bonding adhesives while dopamine is the most widely used. The principle of this surface chemistry is the deposition of oxidized products of those biomimetic adhesives (e.g., DOPA) on solid surfaces. In this section, we will present the basic principles of MiSC, including oxidation of dopamine and deposition regime of DOPA (oxidized product of dopamine), as well as the state-of-the-art of MiSC.

1.2.2. Principles of mussel inspired surface chemistry

1.2.2.1. Mussel adhesion

Mussel is a talented mollusk that can tether to any solid surfaces in high binding strength under wet condition in the sea, using its adhesive proteins. To deal with the shear forces created by waves under tidal conditions, mussel needs to anchor itself to something fixed in the ocean. To do that, this invertebrate has built a foam plaque on the fixed objects that it found and then adheres to them permanently. The mussel plaque is actually made of Mytilus edulis foot proteins (Mefts) that are secreted by mussel and sent to the solid surfaces by mussel byssus. Depending on the surfaces for adhesion, the bond strength of the mussel attachment can be between (1×10^6) to (10×10^6) Nm^{-2} [2]. Very interestingly, the mussel adhesion works on any solid surfaces such as rocks, ship hulls, oil platforms and pipelines. No substrate specificity is required for the mussel attachment. One more interesting thing is the impervious property (or underwater behavior) of mussel adhesion. In general, water and moisture has been supposed to be contaminant to adhesion; however mussel can firmly secure its byssus threads to surfaces even in aqueous environment, using its water-resistant adhesive proteins. Further studies found that the mussel adhesion is attributed from the cross-links in catecholamine. It is indicated from the biochemical analysis that the main components in mussel plaque are catecholamine compounds (mostly, post-translationally modified L-DOPA[1]) and catechol oxidase [2]. These compounds undergo a series of redox reactions to form a complex mixture of cross-linked matrix. Understanding the adhesion of mussel offers the innovations in the technology of surface modification / functionalization.

1.2.2.2. Oxidation of dopamine

In alkaline solution, dopamine in particular, and catecholamines in general, can spontaneously be oxidized into catechol products that are similar to mussel proteins. Messersmith et al., (2007) [1] has proposed a reaction scheme to explain the oxidation of dopamine. According to his report, the oxidation of dopamine can be divided into two steps: *(i)* Formation of catechol radicals; and *(ii)* Formation of cross-links between catechol radicals (known as curing or tanning).

[1] L-DOPA : 3,4-dihyroxyphenyl-L-alanine

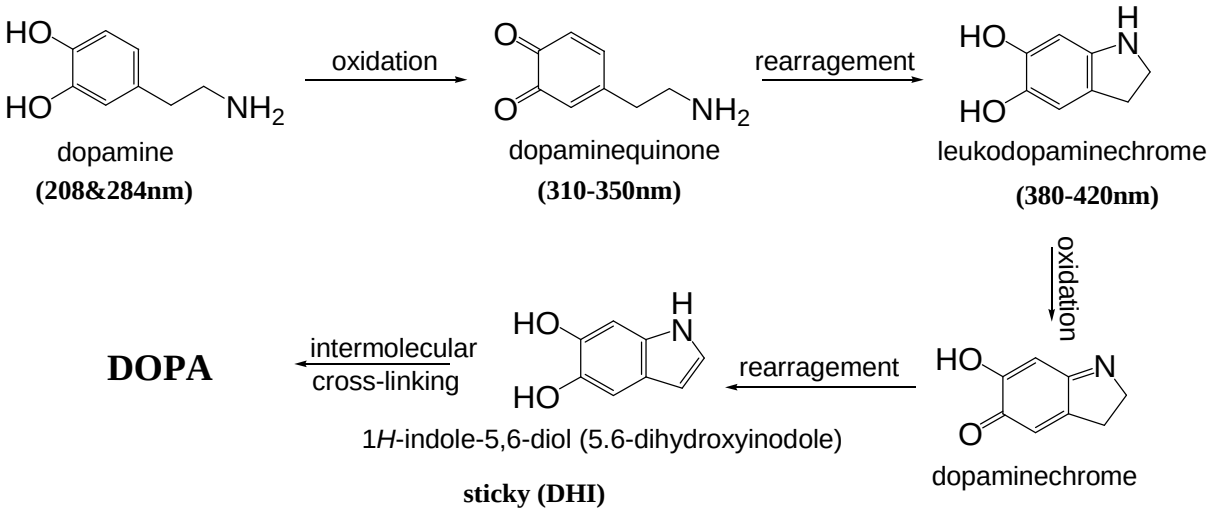

Scheme 1.1. *Oxidation of dopamine:* The intramolecular cyclization through complex redox reactions provides many intermediated products (quinones, chromes, indoles) [1]. The final product (DOPA) is multifunctional glue.

(*i) Formation of catechol radicals*: In alkaline solution, Dopamine (DOP) undergoes intramolecular cyclization through a series of complex redox reactions (as seen in the scheme 1.1). A variety of intermediate compounds (quinones, chromes, indoles…) are produced during these reactions. The products with planar structure (e.g., 5,6 dihydroxyindole (DHI) and its derivatives) are supposed to act as catechol radicals that allow their adhesion on surfaces [3]. They are able to be conjugated together in a cross-linking net.

(ii) Formation of cross-links between catechol radicals: Next, DHI and its derivatives are conjugated together to create the final product in a process named curing (or tanning). The final product is named DOPA. Until now, it is still disputed if the curing process of DOPA is covalent polymerization or hierarchical supramolecular aggregation of monomers [4]. In the past, DOPA was believed to be a polymer whose cross-linking is caused by addition polymerization of unsaturated hydrocarbon. That's why this material was known as polydopamine (the name spontaneously implies a polymeric nature) in early days of MiSC. However, no experimental proof is available at present to support this hypothesis. In contrary, Daniel et al., [5] has recently proved the later hypothesis that DOPA forms a "stacked structure" in which molecules are organized through non-covalent interactions including charge transfer, π-stacking and hydrogen bonding of monomers (scheme 1.2). This structure results in the high stability and insolubility of DOPA coating. Lee et al., [6]

also suggested that there are both covalent and non-covalent bindings in DOPA. The physically self-assembled multimers of $(DOP)_nDHI$ having the planar geometry is tightly entrapped within covalently polymerized DOPA net (scheme 1.3).

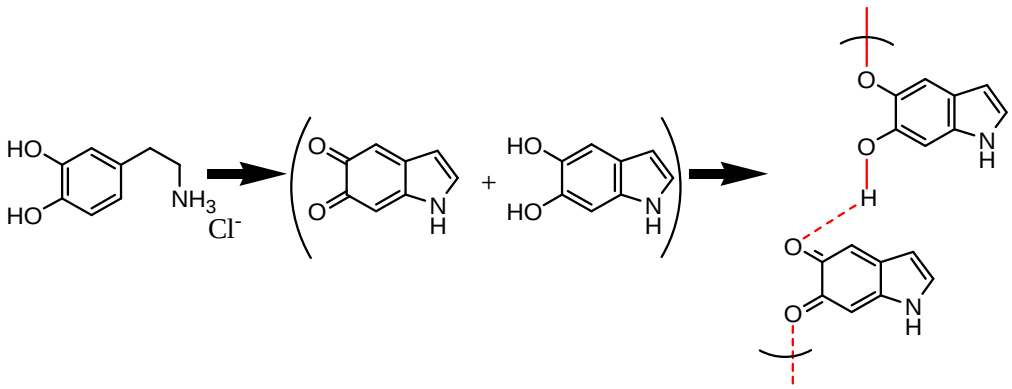

Scheme 1.2. *Strong non-covalent bond in DOPA from hydrogen bond [5].*

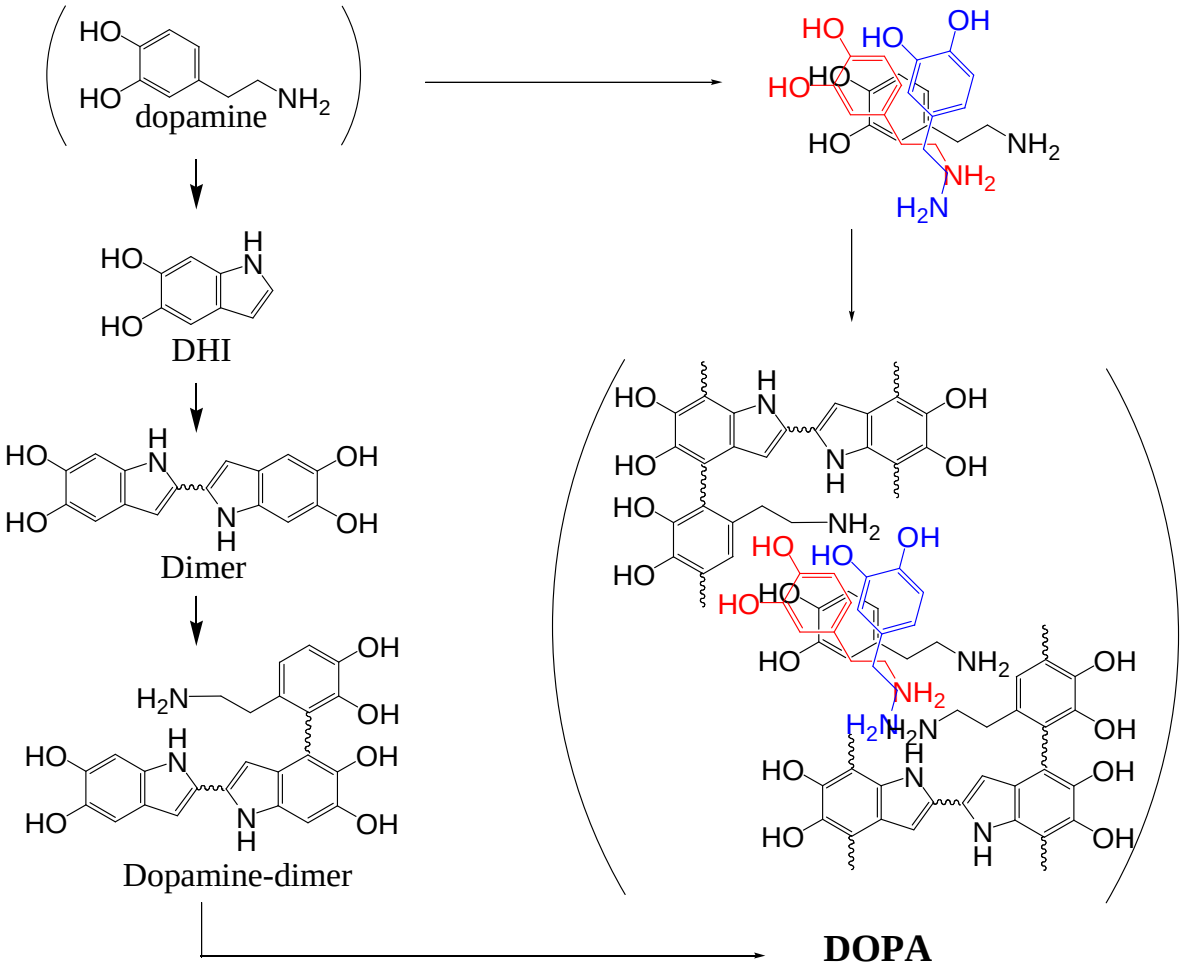

Scheme 1.3. *Mix of non-covalent and covalent bonding in DOPA [6].*

1.2.2.3. Deposition regime of DOPA-type films

It has been known that catechol is the only functional element required for adhesion of DOPA-type adhesives [7]. Here we present two assumptions about deposition regimes of DOPA-type films that have been proposed recently in literature.

The first hypothesis about deposition of DOPA-type films is: *The affinity between DOPA and surfaces are resulted from the strong non-covalent bonding*. Scheme 1.4 illustrates the attachment of DOPA to oxides (TiO_2 and SiO_2) by chemical affinity, either coordination bonding in chelating or hydrogen bonding. It was known for long time that catechol compounds possess remarkable affinity for metal ions that leads to formation of coordination bonding between catechol compounds and oxide surfaces (TiO_2, SiO_2, Fe_2O_3) [8]. Recently, it was also reported that hydrogen bonding between catechol compounds with different materials might be the reason for the attachment of DOPA to surfaces [9].

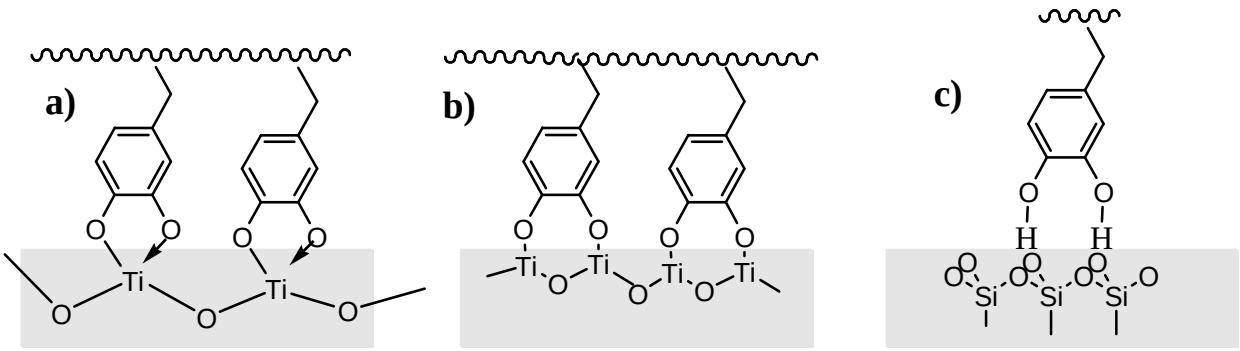

Scheme 1.4 *Attachment of DOPA to surfaces by chemical affinity:* a) The chelation of Ti ions by catechol molecules in aqueous solutions; b) Dehydration Ti-OH substrate and formation of chelate bidentate bonding for catechol molecules on titanium dioxide substrate; c) Hydrogen bonding of the phenolic groups to the oxygen atoms of the cleaved mica surfaces [8, 9].

Bernsmann et al., [3] proposed that *the growth of DOPA film originates from the adsorption of catechol radicals and is then followed by the formation of a 3-D cross-linking net* (Scheme 1.5). Firstly, the intermediate oxidized products (mostly DHI and its derivatives) that exhibit planar structures can accumulate together to form oligomers.

Consequently, these oligomers can attach on a substrate to form “phenolic radical” islands, and continue to accumulate together to form cross-linking net and totally cover the surface.

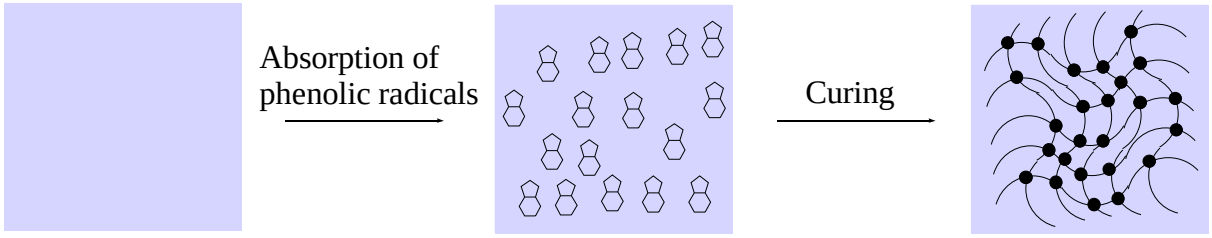

Scheme 1.5. *Attachment of DOPA to surface by adsorption of catechol radicals:* The oxidized products of dopamine (mostly, DHI and its derivatives) are adsorbed on surface and consequently conjugated together to form a continuous film on surface (DOPA film).

1.2.3. Properties of DOPA

We consider here the properties of bulk DOPA molecules and DOPA-type thin films:

(i) DOPA *shares a lot of commons with well-known melanin* (known as the natural photoprotectant of the human skin). Firstly, DOPA is very dark in color and shows very high absorbance in visible range ($\varepsilon \sim 2.6\text{-}3.0\times10^{6}$ m^{-1} at 589nm [3]). Secondly, DOPA shows properties of photo-semiconductors (monotonic absorption spectrum over the whole UV-vis region, low conductivity of $0.25 \rightarrow 1.3\times10^{-10}$ Scm^{-1} [10] and decreasing resistance with the temperature). Regarding to its similarity in structure and behavior with melanin, DOPA is also called pseudo-melanin.

(ii) DOPA is *multifunctional glue* that can attach different molecules of interest to any solid surfaces [1, 11, 12]. DOPA can tether to any material surfaces including noble metals (Au, Ag, Pt, Pd), metals with native oxide surfaces (Cu, stainless steel, NiTi alloy), oxides (TiO_2, SiO_2, Al_2O_3, Nb_2O_5), semiconductors (GaAs, Si_3N_4), glass, quart, ceramics (glass, Hap), synthetic polymers (PS, PE, PC, PET, PDMS, PEEK, PU), etc. DOPA can also adhere on one of the most anti-adhesive surfaces as polytetrafluoreethylene (PTFE) [13] or super-hydrophobic surfaces as fluorosilane coated anodic aluminum oxide membrane (AAO). Alternatively, different molecules (especially amines, thiols, metals) can be grafted on DOPA coating [1].

(iii) With respect to morphology, DOPA film shows very *rough* surface with presence of unavoidable aggregation on the scale of 10^2 nm [3]. Accompanying with unsmooth topography, DOPA is believed to be amorphous material with porous structure. To our knowledge, no quantitative investigation of the pore size distribution has been performed yet.

(iv) The static water contact angle measurement demonstrated that the surface energy of DOPA coatings depends on the surface of the original substrates, i.e., the contact angle values on hydrophilic surfaces are in the range of 50-60° [1, 11] while they become much higher on hydrophobic surfaces. For instance, the contact angles of PE and PTFE surface decreases from 127±6° to only 92.8±1.2° and from 124±3.4° to 80.6±5.0° after modification with DOPA, respectively [12]. Additionally, the hydrophilicity of DOPA coated surfaces increases with an increasing thickness of the DOPA films [14].

(vi) DOPA films display a *pH-dependent permselectivity*. Isoelectric point (pI) of such films was found to be close to 4 [15]. These films are permeable to cationic probe at low pH (pH=3) and impermeable to the probe at high pH (pH=11) whereas this is reversed in case of anionic probe.

(vii) DOPA films show *strong mechanical and chemical stability* [4]. For example, DOPA films deposited on silica are stable in the presence of a physiological buffer for at least 4 days. The stability is also excellent at pH 1: only 14% of film erosion was found within 54 h. In contrast, the films spontaneously delaminate within 15 min of exposure to sodium hydroxide solution at pH 13, most probably in relation to the increased solubility of “DOPA-like materials” in basic media [3].

1.2.4. Effect of oxidation conditions on formation of DOPA-type films

The oxidation of dopamine is the key to the deposition of DOPA-type films on surfaces. Therefore, the control of oxidation kinetics is very important in order to control the quality of DOPA-type films.

The first protocol to achieve DOPA films was proposed by Lee [1] where very thin adherent DOPA is formed on surfaces through a simple immersion of substrates into alkaline solution (marine pH 8.5) of dopamine.

In several years, the effect of oxidation conditions (e.g., pH, temperature, dopamine concentration, solvent and buffer use) on deposition of DOPA-type films has been studied. The oxidation of DOPA film was found to be a pH-dependent process [16] in which the equilibrium is shifted to the reactant when the pH decreases. An alkaline pH (pH 7.5→9.0) is mandatory to promote deposition of DOPA films, while higher temperature leads to thicker and rougher films [3]. Interestingly, there is no significant effect of nature of buffer on oxidation kinetics of DOP and deposition kinetics of DOPA film [17]. The most widely used buffer is Tris base (pK_a 8.07) titrated to pH 8.5 by HCl. Some other alkaline buffers (pK_a 7.20-8.35), such as biscine and phosphate buffer have also been reported in the literature [16, 17].

Recently, it was demonstrated that the excess of oxygen feed can lead to highly homogeneous thin DOPA-type films (Rms_{oxygen}=0.52 nm compared to Rms_{air}=2.58 nm) via accelerated reaction kinetics [18].

At last, oxidizing agents (e.g., cupric sulphate, ammonium persulfate) have currently been utilized to oxidize dopamine [17, 19].

1.2.5. Applications of mussel inspired surface chemistry

The discovery of mussel inspired surface chemistry is a technological breakthrough to overcome the difficulties in surface specific chemistry of current approaches for surface functionalization / modification. Owning the versatile adhesion, DOPA film was used as a “double-face tape” which can adhere to any solid surfaces by one end and allow the attachment of certain functional molecules to the other end for decoration of surfaces. Here are some examples:

(i) The reduction of metal ions on DOPA coating was exploited to deposit uniform metal coatings onto substrates by *electroless metallization*. For example, the deposition of silver nanoparticles on an object can be conducted through its immersion to solution of silver nitrate of that object previously modified with DOPA film.

(ii) DOPA coatings can be also modified, through e.g., Michael addition with amines or Schiff base reactions with thiols, with organic ad-layers [1]. A significant amount of research has been performed to graft anti-fouling polymers (e.g., PEG, peptoids, zwitterionics) onto surfaces via MiSC [20].

(iii) DOPA coating was also utilized for *immobilization of biomolecules* on surfaces. For example, DOPA-PEG-biotin coatings can facilitate biofunctionalization of wide range of materials with peptides, proteins or other biomolecules via biotin-avidin interactions [21].

(iv) A new family of *injectable citrate-based mussel inspired bioadhesives* (iCMBAs) has been synthesized by Mehdizadeh and coworkers at University of Texas (USA) in 2012 [22]. iCMBAs are PEG-based oglimers that have been functionalized with catechol-containing compounds in one-step polycondensation. These new biomedical adhesives outperform clinically used fibrin glue in wet tissue adhesion (they are 2.5-8.0 folds stronger than fibrin glue). They can be used as biomimetic sealants that stop bleeding instantly, which is quite challenging to do with fibrin glue.

(v) MiSC can provide a versatile platform technology for developing *scaffold materials* for tissue engineering [23]. For instance, Tsai et al., (2011) demonstrated that the deposition of a DOPA layer on 3D porous scaffolds is a promising strategy for cartilage tissue engineering, and may be applied to other types of tissue engineering [24].

(vi) DOPA was used for biofunctionalization to incorporating sensitive biological molecules (antibodies, enzymes, nucleic acids, cells) on surfaces of *biosensors*. For example, DOPA film was employed as a platform to functionalize carbon nano-tubes (CNTs) with folic acid (CNTs@PDA-FA), allowing detection of folate receptor positive tumor cells by specific recognition [25].

(vii) In last five years, MiSC has been applied for the modification of inner wall of capillary, allowing an enhancement of CE separation of proteins via controllable EOF and decreased adsorption. Messersmith et al., (2012) used MiSC for the covalent immobilization of trypsine onto silica or titania monolithic supports for protein digestion [26].

(viii) Lee and coworkers [27] fabricated a new surface tension confined droplet 2D, gravity-driven micro-fluidic device, called "*polydopamine micro-fluidic system*". Spatially controlled modification of the AAO surface through DOPA coating generates hydrophilic microlines on superhydrophobic surface, allowing the gravity-driven movement of droplet with low dragging force. This microfluidic device enables one to control movements of droplets as well as droplet mixing.

(ix) MiSC was also utilized as a simple and universal platform for *micro-contact printing* [28]. Tsai developed tunable micro-patterned substrates based on DOPA deposition via micro-contact printing with PDMS stamp for biomedical applications [29]. The DOPA patterns printed on cytophobic and non-fouling substrates were used to form patterns of cells or proteins. DOPA imprints reacted with nucleophile amines or thiols to conjugate PEG for creating non-fouling area on surfaces.

1.2.6. Conclusions

MiSC opens a new strategy in surface science. This surface chemistry is based on oxidation of catecholic compounds (e.g., dopamine) that have structural similarity with mussel adhesive proteins. The oxidized products of these compounds can act as multifunctional glue that can easily attach to virtually any material surfaces (e.g., metals, semiconductors, oxides, plastics, polymers, etc). Therefore, MiSC is an elegant solution to overcome all difficulties of specific surface chemistry in functionalizing / modifying materials surfaces.

Additionally, in MiSC, functionalizing organic molecules (e.g., polymer chains) with amino end-group can help to promote their attachment to grafting sites on surfaces. Chain transfer atom polymerization (CTRP) is among the effective methods to synthesize amino terminated water soluble polymers. In the next sections of this thesis (chapter 3, 4, 5), we are going to develop a protocol that is based on MiSC to graft amine terminated polymers that is synthesized by CTRP on different materials surfaces commonly used in hybrid devices.

References

[1] H. Lee, S.M. Pellatore, P.B. Messersmith, Science, 2007, 318, pp 426–430.

[2] G.S Heather, F.R. Francisco, Mar. Biotechnol., 2007, 9(6), pp 661–681.

[3] F. Bernsmann, A. Ponche, C. Ringwald, J. Hemmerlé, J. Raya, B. Bechinger, J.C. Voegel, P. Schaaf, V. Ball, J. Phys. Chem. C, 2009, 113(19), pp 8234–8242.

[4] V. Ball, D.D. Frari, M. Michel, M.J. Buehler, V. Toniazzo, M.K. Singh, Jose Gracio, David Ruch, Bio. Nano Sci., 2012, 2(1), pp 16–34.

[5] D.R. Dreyer, D.J. Miller, B.D. Freeman, D.R. Paul, C.W. Bielawski, Langmuir, 2012, 28(18), pp 6428–6435.

[6] S. Hong, Y.S. Na, S. Choi, I.T. Song, W.Y. Kim, H. Lee, Adv. Funct. Mater., 2012, 22(22), pp 4711–4717.

[7] Y. Qian, Z. Feng, L. Weimin, Chem. Soc. Rev., 2011, 40, pp 4244–4258.

[8] *(a)* J. Moser, S. Punchihewa, O.P. Infelta, M. Graetzel, Langmuir, 1991, 7(12), pp 3012–3018; *(b)* B.A Borgias, S.R. Cooper, Y.B. Koh, K.N. Raymond, Inorg. Chem., 1984, 23(8), pp 1009–1016; *(c)* T. Rajh, L.X. Chen, K. Lukas, T. Liu, M.C. Thurnauer, D.M. Tiede, J. Phys. Chem. B, 2002, 106(41), pp 10543–10552; *(d)* M. Vega-Arroyo, P.R. LeBreton, T. Rajh, P. Zapol, L.A Curtiss, Chem. Phys. Lett., 2005, 406(4-6), pp 306–311; *(e)* T. Rajh, J.M. Nedeljkovic, L.X. Chen, O. Poluektov, M.C. Thurnauer, J. Phys. Chem. B, 1999, 103(18), pp 3515-3519; *(f)* P.C. Redfern, P. Zapol, L.A. Curtiss, T. Rajh, M.C. Thurnauer, J. Phys. Chem. B, 2003, 107(41), pp 11419–11427; *(g)* J.L. Dalsin, Lijun Lin, S. Tosatti, J. Voros, M. Textor, P.B. Messersmith, Langmuir, 2005, 21, pp 640–646; *(h)* X. Fan, L. Lin, P.B. Messersmith, Compos. Sci. Technol., 2006, 66, pp 1195–1201.

[9] Shao-Chun Li, Jian-guo Wang, Peter Jacobson, X.Q. Gong, A. Selloni, Y. Diebold, J. Am. Chem. Soc., 2009, 131(3), pp 980–984.

[10] Vincent Ball, Colloids Surfaces Physicochem. Eng. Asp., 2010, 363(1-3), pp 92–97.

[11] K. Kang, I. Choi, Y. Nam, Biomaterials, 2011, 32(27), pp 374–6380.

[12] S.H. Ku, J. Ryu, S.K. Hong, H. Lee, C.B. Park, Biomaterials, 2010, 31(9), pp 2535–2541.

[13] J. Jiang, Liping Zhu, Lijing Zhu, Baku Zhu, Y. Xu, Langmuir, 2011, 27(23), pp 14180–14187.

[14] P.G. Ognen, P. Stepan, H. Milan, C. Dagmer, P. Vladimir, R. Frantisek, Biomacromolecules, 2011, 12(9), pp 3232–3242.

[15] V. Ball, Colloids Surfaces Physicochem. Eng. Asp., 2010, 363(1-3), 92–97.

[16] V. Ball, D.D. Frari, V. Toniazzo, D. Ruch, J. Colloid Interface Sci., 2012, 386(1), pp 366–372.

[17] F. Bernsmann, V. Ball, F. Addiego, A. Ponche, M. Michel, J.J. de Almeida Gracio, V. Toniazzo, D. Ruch, Langmuir, 2011, 27(6), 2819–2825.

[18] H.W. Kim, B.D. McCloskey, T.H. Choi, C. Lee, M.J. Kim, B.D. Freeman, H.B. Park, Appl. Mater. Interfaces, 2013, 5(2), 233–238.

[19] Q. Wei, F. Zhang, J. Li, B. Li, C. Zhao, Polym. Chem., 2010, 1, pp 1430–1433.

[20] *(a)* J.K. Dalsin, P.B. Messersmith, Mater. Today, 2005, 8, pp 38-46; *(b)* A.R. Statz, A.E. Barron, P.B. Messersmith, Soft Matter 4,2008, pp 131-139; *(c)* A.R. Statz, J. Kuang, C. Ren, A.E Barron, I. Szleifer, P.B. Messersmith, Biointerphases, 2009, 4, pp 22-32; *(c)* A.R. Statz, R.J. Meagher, A.E Barron, P.B. Messersmith, J. Am. Chem. Soc., 2005, 127, pp 7972–7973; *(d)* N.D. Brault, C. Gao, H. Xue, M. Piliarik, J. Homola, Biosens. Bioelectron., 2010, 25, pp 2276–2282; *(e)* C. Gao, G. Li, H. Xue, W. Yang, F. Zhang, S. Jiang, Biomaterials, 2010, 31, pp 1486–1492; *(f)* R. Gunawan, J. King, B.P. Lee, P.B. Messersmith, W. Miller, Langmuir, 2007, 23, pp 10635–10643.

[21] Haeshin Lee, Junsung Rho, Phillip B. Messersmith, Adv Mater., 2009, 21(4), pp 431-434.

[22] M. Mehdizadeh, H. Weng, D. Gyawali, L. Tang, J. Yang, Biomaterials, 2012, 33(32), pp 7972–7983.

[23] *(a)* E. Ko, K. Yang, J. Shin, S.W. Cho, Biomacromolecules, 2013, 14(9), pp 3202-3213; *(b)* K. Yang, J.S Lee, Y.B. Lee, H. Shin, S.H. Um, J.B. Kim, K.I. Park, H. Lee, Biomaterials, 2012, 33(29), pp 6952-6964; *(c)* J. Tian, S.Y. Deng, D.L. Li, D. Shan, W. he, X.J. Zhang, Y. Shi, Biosensors and Bioelectronics, 2013, 49, pp 466-471; *(d)* J. Ryu, S.H. Ku, M. Lee, C.B. Park, Soft Matter, 2011, 7, pp 7201–7206; *(e)* L. M. Hamming, X.W. Fan, P.B. Messersmith, L.C. Brinson, Compos. Sci. Technol., 2008, 68(9), pp 2042–2048; *(f)* J. Ryu, S.H. Ku, H. lee, C.B. Park, Adv. Funct. Mater., 2010, 20(13), pp 2132–2139; *(g)* K.J. jeong, L. Wang, C.F. Stefanescu, M.W. Lawlor, J. Polat, C.H. Dohlman, R.S. Langer, D.S. Kohane, Soft Matter, 2011, 7, pp 8305–8312; *(h)* Y.B. Lee, Y.M. Shin, J.H. lee, I. jun, J.K. Kang, J.C. Park, H. Shin, Biomaterials, 2012, 33(33), pp 8343–8352; *(i)* K. Yang, J.S. Lee, J. Kim, Y.B. Lee, H. Shin, S.H. Um, J.B. kim, K.I. Park, H. Lee, S.W. Cho, Biomaterials, 2012, 33(29), pp 6952–6964; *(k)* S. M. Kang, S. Park, D. Kim, S.Y. Park,, R.S Ruoff, H. Lee, Adv. Funct. Mater., 2011, 21(1), 108–112.

[24] W.B. Tsai, W.T. Chen, H.W. Chien, W.H. Kuo, M.J. Wang, Acta Biomater 7(12), 4187-4194 (2011).

[25] T.T. Zheng, R. Zhang, L. Zou, J.J. Zhu, Analyst., 2012, 137, pp 1316–1318.

[26] J.G. Rivera, P.B. Messersmith, J. Sep. Sci., 2012, 35(12), pp 1514–1520.

[27] I. You, S. M. Kang, S. Lee, Y. O. Cho, J. B. Kim, S. B. Lee, Y. S. Nam, H. Lee, Angew. Chem. Int. Ed., 2012, 51, pp 6126-6130.

[28] *(a)* J. Liu, Q. Ye, B. Yu, X. Wang, F. Zhou, Chem. Commun., 2012, 48(3), pp 398–400; *(b)* Q.P. Ho, S.L. Wang, M.J. Wang, Appl. Mater. Interfaces, 2011, 3, pp 496–4503.

[29] H.W. Chien, W.H. Kuo, M.J. Wang, S.W. Tsai, W.B. Tsai, Langmuir, 2012, 28, pp 5775-5782.

Chapter 2: Amine terminated polymers

2.1. Introduction

It is known that organic molecules that are functionalized with amino endgroup can easily be grafted to / on DOPA films [1]. In order to decorate DOPA films with polymer brushes, we have synthesized two different amine terminated polymers (polyacrylamide and poly(N-Isopropylacrylamide)) by chain transfer radical polymerization. These polymer chains were thoroughly characterized and consequently grafted on the DOPA films.

2.2. Materials

Monomers, N-Isopropylacrylamide (NIPAm, $C_6H_{11}NO$, MW 113.16, Ref. 415324-50g), Acrylamide (AM, 99+%, electrophoresis grade, $CH_2CHCONH$, MW 71.08, Ref. 14,866-0) were purchased from Sigma and used as received.

Initiators, Cysteamine hydrochloride (AET.HCl,≥98%, $C_2H_7NS.HCl$, MW 113.61, Ref. M6500) and Potassium persulfate (KPS, +99%, ACS reagent, $K_2S_2O_8$, MW 270.32, Ref. 21,622-4) were purchased from Sigma and used without any purification.

Fluorescent probe, Fluorescein 5(6) isothiocyanate (FITC, ≥90% HPLC, $C_{21}H_{11}NO_5S$, MW 389.38, Ref. 46950-250mg-F) was bought from Sigma-Aldrich and used without purification.

1-Hydroxy-benzotriazol (HOBT, +98%, purum, $C_6H_5N_3O$, MW 135.13, Ref. 54802) was purchased from Fluka.

N,N'-DicyclohexylCarbodiimide (DCC, 1.0M solution in dichloromethane, $C_6H_{11}N=C=NC_6H_{11}$, MW 206.33, d 1.247, Ref. 379115) was purchased from Sigma-Aldrich.

Patent blue VF Soidum salt (Disulfine Blue, $C_{27}H_{31}N_2NaO_6S_2$, Ref. 76357) was bought from Sigma-Aldrich.

Dialysis cassette with molecular weight cut-off (MWCO) of 3500Da was bought from Fisher Scientific.

All solutions were prepared in deionized water from a Millipore's Laboratory Water System (Simplicity UV, Millipore, France) with a resistivity of 18.2 MΩ•cm.

2.3. Experiments

2.3.1. Mechanism of chain transfer radical polymerization

The mechanism of the chain transfer radical polymerization (CTRP) is illustrated as scheme 2.1. The CTRP is generally achieved by introducing a convenient redox system [2], such as cysteamine (chain transfer atom, CTA) and potassium persulfate (initiator, KPS). The polymerization consists of three steps: initiation, propagation and termination. Firstly, the redox couple (persulfate and thiol) is dissociated in the aqueous phase to form radical initiators. In the second step (propagation), these radical initiators (with amine functional group at one end and thiol group at the other end) attack ethane monomer at weak pi bond and the growth of polymer chains begins. By that way, the amino group present in chain transfer atom is conjugated to growing polymer chains. The propagation process is continued to increase length of polymer chains until there is no more monomer or the termination takes place.

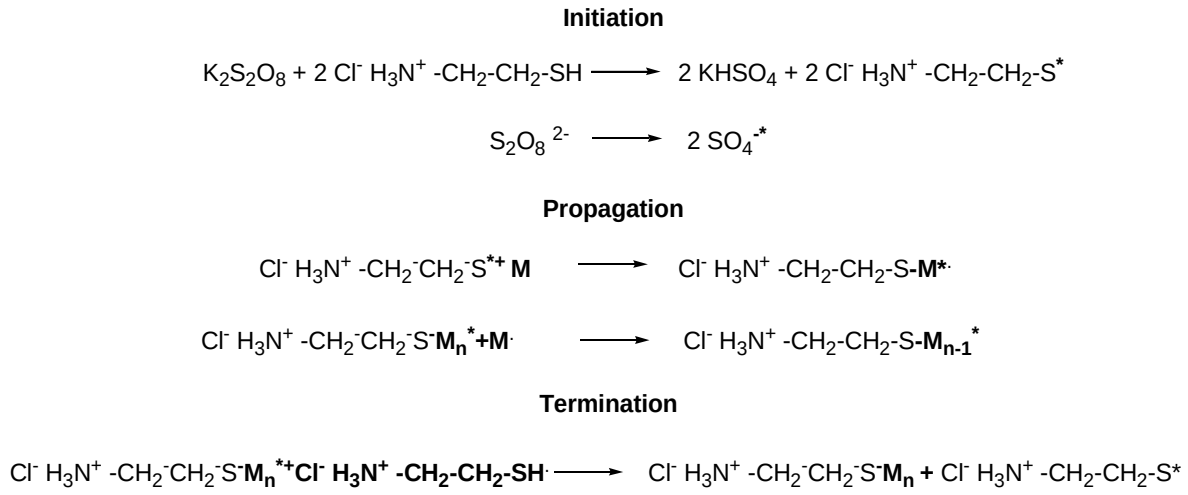

Scheme 2. 2. *Mechanism of chain transfer radical polymerization (*=radical)* [2].

It was reported that CTRP provides functional polymers with both, the functional end and desired molecular weight [2, 3]. Molecular weight (MW) of polymer increases with increase in a monomer concentration and decrease with the decreasing CTA concentration. The KPS concentration doesn't seem to have any important effect on molecular weight of synthesized polymer.

2.3.2. Procedure

Two series of amine terminated polymers (PAM and PNIPAM) were synthesized as the following procedure: The monomer was dissolved in water and the solution was bubbled with argon stream during 1-2h. The redox initiators (AET.HCl and KPS) were added separately and rapidly into degassed monomer solution under constant temperature (adjusted to (26±2°C) with a water bath). The reaction was preceded for 18-24h under constant steering and argon feed. The synthesized polymers were purified by dialysis against distilled water (dialysis cassette with molecular weight cut-off MWCO of 3500 Daltons) and freeze dried. The experimental conditions, concentrations of monomers, the chain transfer and initiator are given in Table 2.1, together with the abbreviations of synthesized polymers (PAM stands for polyacrylamide and PNI for poly (N-isopropyl acrylamide)).

Table 2. 1. *List of synthesized polymers.*

Telomer	$[M]_0$ (M)	$[AET]_0$ (M)	$[KPS]_0$ (M)	Telomer	$[M]_0$ (M)	$[AET]_0$ (M)	$[KPS]_0$ (M)
PAM5	0,85	0,042	0,017	PNI5	0,85	0,042	0,017
PAMd	0,64	0,026	0,013	PNId	0,64	0,026	0,013
PAM10	1,28	0,026	0,013	PNI10	1,28	0,026	0,013
PAMc	2,56	0,026	0,013	PNIi	1,28	0,021	0,013
PAM13	1,24	0,025	0,025	PNIa	1,28	0,013	0,013
				PNI13	1,24	0,025	0,025

2.4. Results and discussions

The synthesized polyacrylamide and poly(N-isopropyl acrylamide) were thoroughly characterized before their utilization for surface modification. The results of these characterization studies and the appropriate discussion are given below.

2.4.1. Fourier transform infrared spectroscopy (FTIR)

The infrared spectra of monomers, initiators and synthesized polymer were measured using the FTIR Spectrometer in the wave number region from 4000 to 500 cm^{-1}. Samples were mixed with KBr powder and compacted by pressure into pellets. The background was measured with an empty pellet holder (without sample).

FTIR spectra of synthesized polymers demonstrated the successful polymerization with the presence of characteristic peaks of polyacrylamide and derivatives: *2932* cm^{-1} ($-CH_2-$), *1673* cm^{-1} (C=O), *1415* cm^{-1} (C-N). The absence of the peaks concerning to vinyl group (1641 cm^{-1} and 989 cm^{-1}) indicated high purity of synthesized polymers. However, no significant signal of terminal amine group was obtained on FTIR spectra, probably due to the low concentration of the amine group (one group per a chain).

2.4.2. Nuclear Magnetic Resonance (NMR)

The synthesized polymers were also characterized by ^1H NMR on a Bruker Avance 300 spectrometer (Bruker, Germany) at 300MHz. In general, the polymer and reactive are dissolved in deuterium oxide with concentration of 20mg/600µl.

The conversion of polymerization, calculated from ^1H NMR of unpurified polymer solutions, was found to be very high (up to *80-95*%).

^1H NMR spectra of purified polymers showed the well-structured polymers with high purification. Figure 2.1 represents ^1H NMR spectra of purified PAMc and PNIPAMc. The presence of broaden multiple peak related to methylene group (PNIPAM *2.50-0.50* ppm; PAM *2.60-0.50* ppm) instead of vinyl group (*5.65-6.20* ppm) demonstrated that polymers have been successfully synthesized and recovered with high purity. The presence of consecutive chemical shifts (*3.60 - 2.50* ppm) concerning to aliphatic end-group [4] on ^1H NMR spectra demonstrated that synthesized polymers have been functionalized. Amine

terminated polymers with various molecular weights have been synthesized at different concentrations of monomers and initiators.

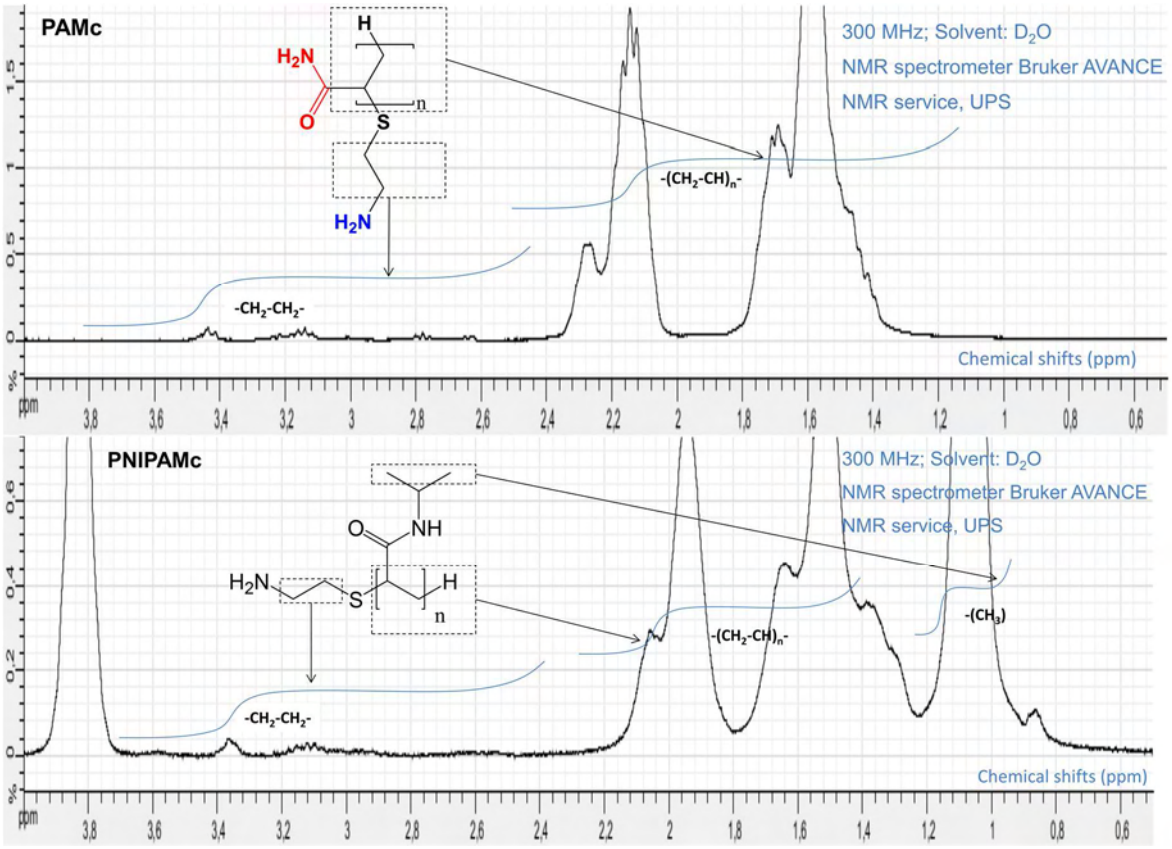

Figure 2. 1. *^{1}H NMR spectra of PAMc (top) and PNIPAMc (bottom):* The synthesized polymers have functional groups at the end of linear polymer chains.

^{1}H NMR spectra of all synthesized polymers are illustrated in figure 2.2 (PAM) and figure 2.3 (PNIPAM). The increase in intensity of end-dead peak as increasing AET concentration or decreasing monomer concentration indicated the decrease in molecular weight of synthesized polymers. The exact molecular weights of these polymers will be further determined by SEC (see 2.4.4, chapter 2).

^{13}C NMR spectra of PAM and PNIPAM are represented in figure 2.4 and 2.5, respectively. It is shown that the polymers were successfully synthesized, which is indicated by the presence of peaks related to saturated carbons –CH_2-CH- (*42-34* ppm) and C=O (*179* ppm) as well as the disappearance of vinyl peak (*140-120* ppm).

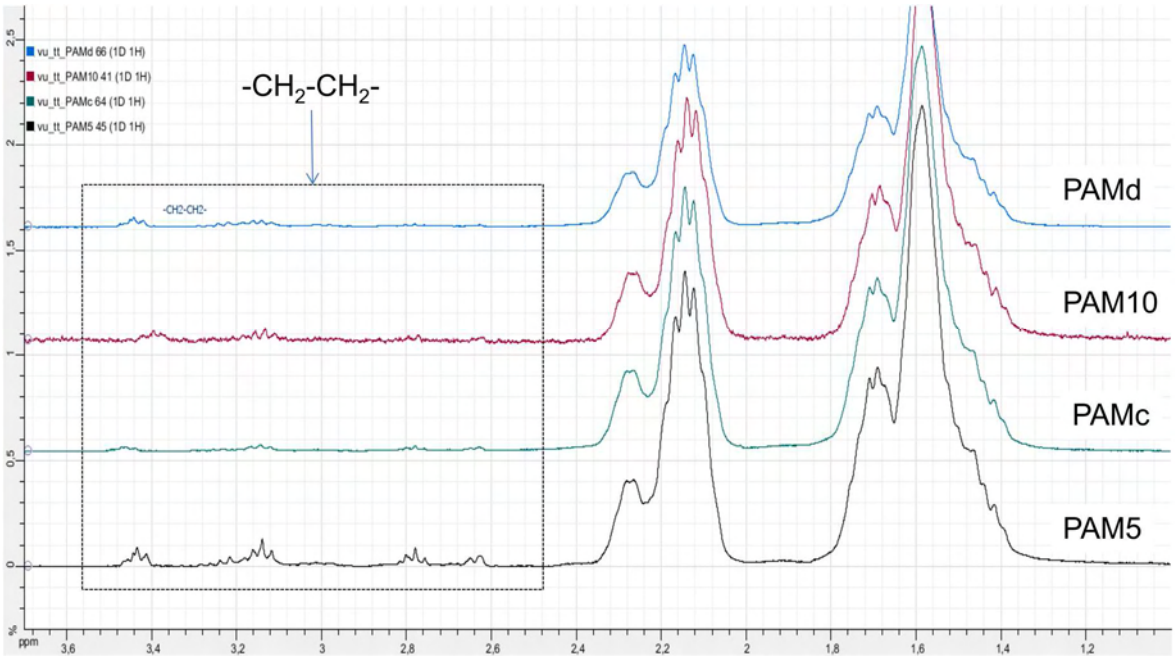

Figure 2.2. *^{1}H NMR spectra of PAM synthesized at different monomer concentrations and initiator concentrations*: PAMc (black), PAM10 (cyan), PAMd (red), PAM5 (blue).

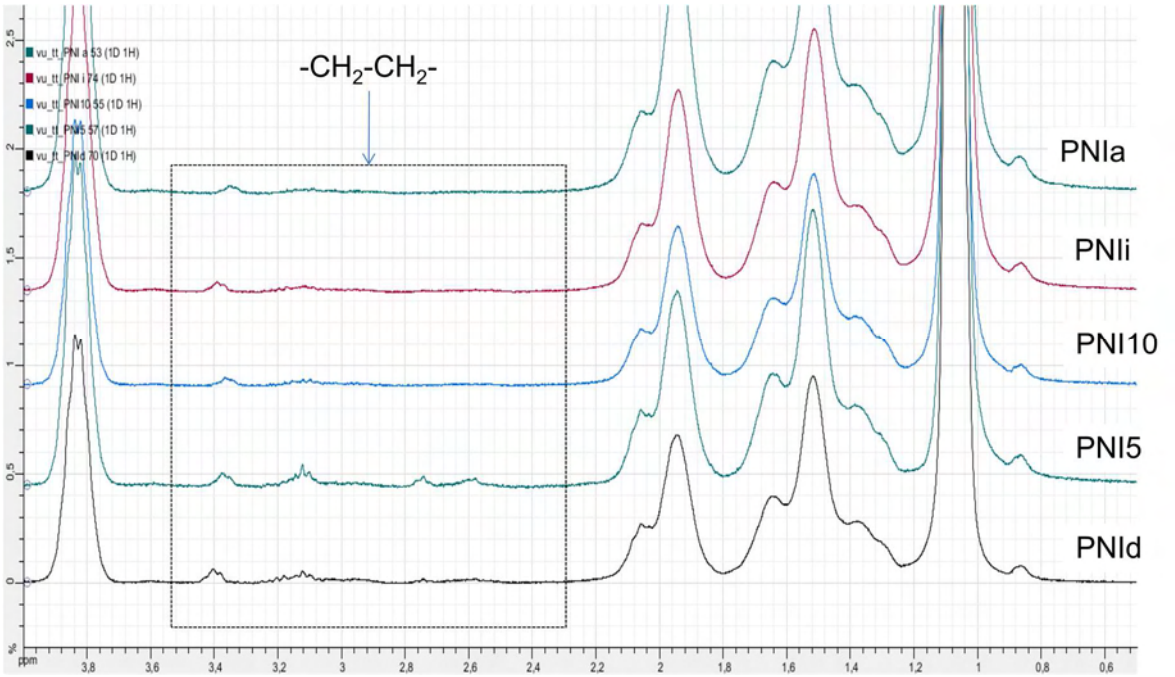

Figure 2.3. *^{1}H NMR spectra of PNIPAM synthesized at different monomer concentrations and different initiator concentrations:* PNIa (black), PNIi (light cyan), PNI10 (blue), PNI5 (red), PNId (bold cyan).

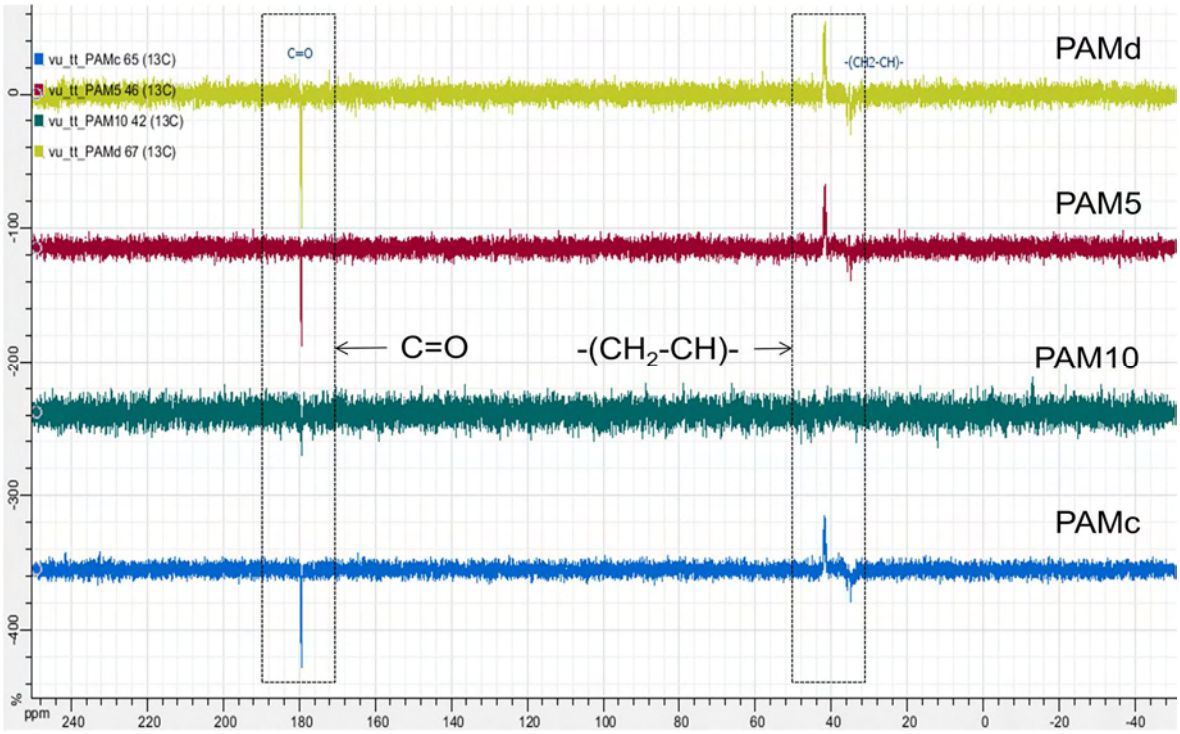

Figure 2.4. *^{13}C NMR spectra of PAM synthesized at different monomer concentrations and initiator concentrations:* PAMc (blue), PAM10 (cyan), PAMd (red), PAM5 (green).

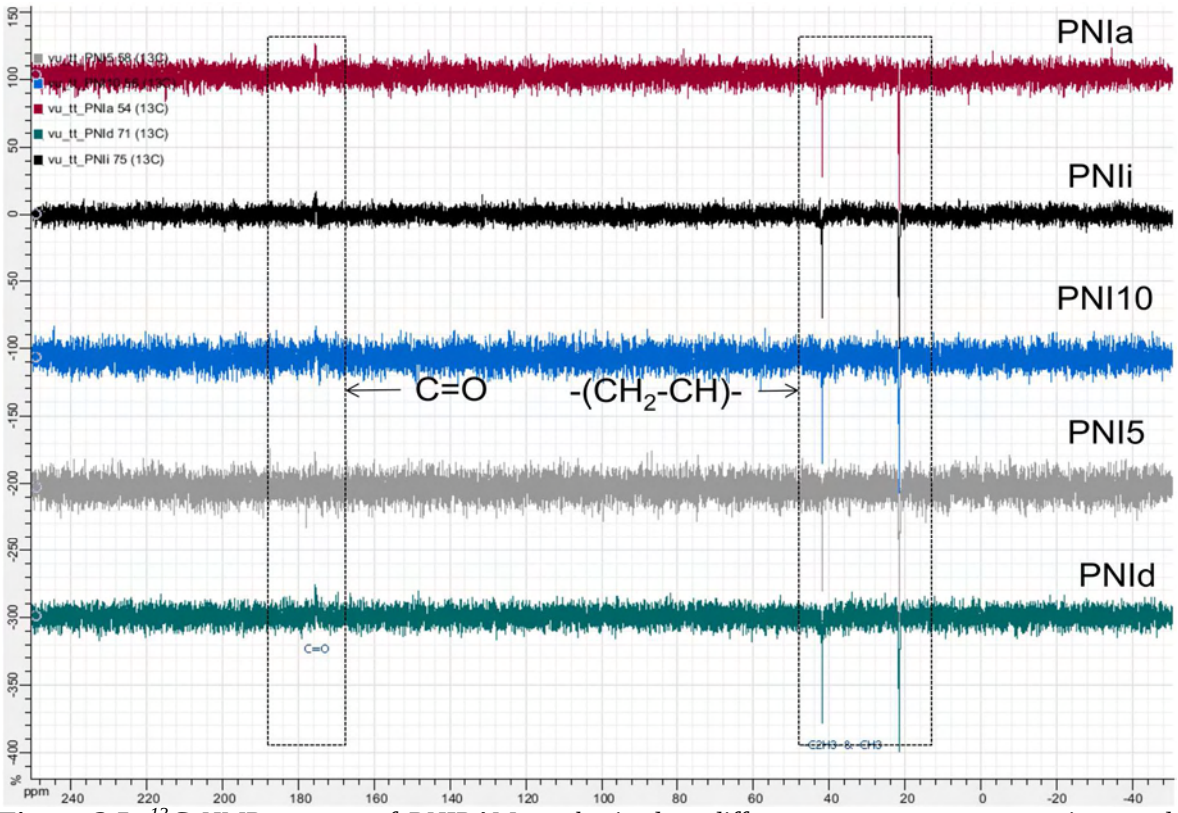

Figure 2.5. *^{13}C NMR spectra of PNIPAM synthesized at different monomer concentrations and different initiator concentrations:* PNIa (cyan), PNIi (grey), PNI10 (blue), PNI5 (black), PNId (red).

2.4.3. Matrix-assisted laser desorption/ionization-Time of Flight (MALDI-TOF)

The combination of nuclear magnetic resonance and mass spectroscopy based techniques is a powerful methodology for generating information of end-group structures [5]. Here, we used MALDI-TOF mass spectroscopy in addition to NMR analysis (mentioned above) to study structure of PNIPAM.

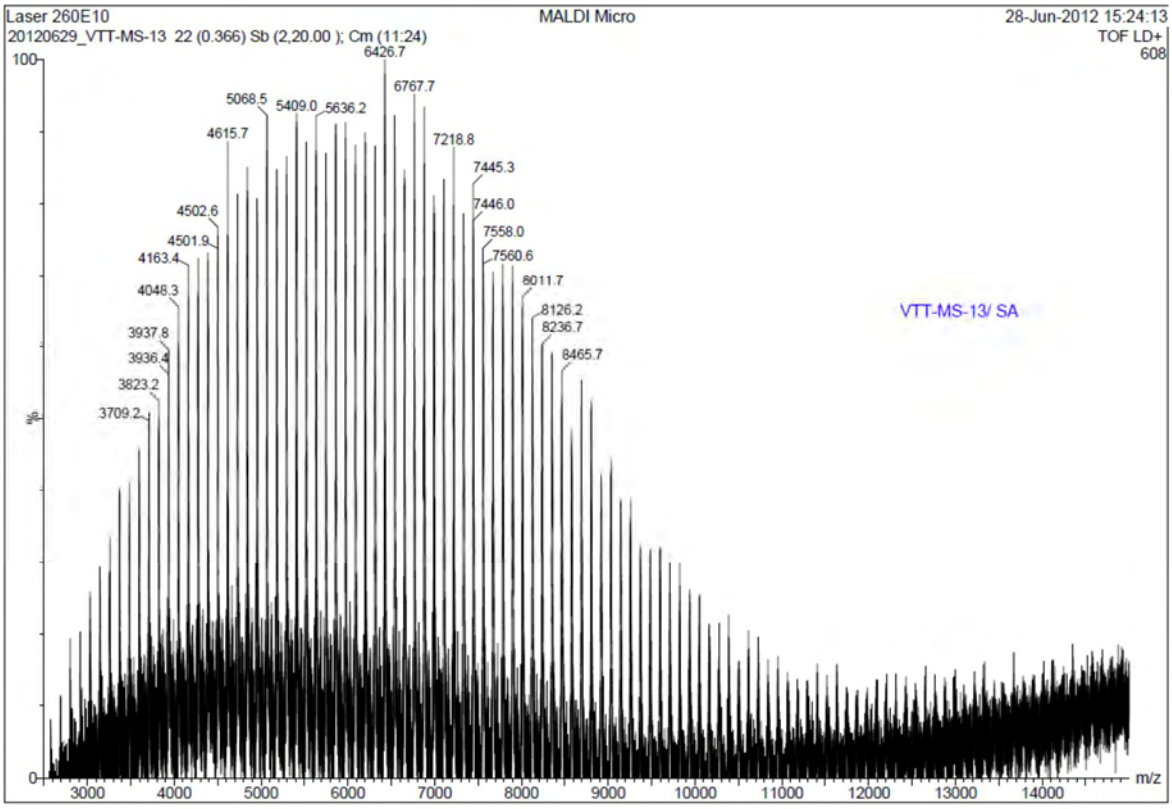

Figure 2. 6. *MALDI-TOF of amine terminated PNIPAM*: the repeating unit corresponds to the multiples of NIPAM monomer (Mw 113) with addition of one amino end-group per a fragment (Mw 71). Matrix: *Sinapinic acid matrix.*

MALDI-TOF mass spectroscopy with 2,5-dihydroxybenzoic acid (DHB) and sinapinic acid (SA) as matrix in addition of suitable salts, such as NaI, NaCl, was used to determine the average molecular weight, its distribution and the structure of the polymer fragments. The sample at concentration of 10mg/ml in THF was mixed either with DHB in THF (50mg/ml) and NaCl/NaI in MeOH (10mg/ml) with portion of 1/30/2 or with SA

(10mg/ml) in H_2O 0.1%/CH_3CN with portion of 1/3. The polyacrylamide chains are insoluble in organic solvents and they were not analyzed by MALDI-TOF-MS.

It can be seen from the figure 2.6 that the repeating unit corresponds to the multiples of NIPAM monomer (Mw 113) with addition of one amino end-group per a fragment (Mw 71). The MW_n measured by MALDI-TOF is smaller than that in SEC measurements (about 3kDa for DHB matrix and 5kDa for sinapinic acid). The size-discrimination at the higher end in MALDI-TOF experiments is originated from the difficult ionization of high molecular weight fragments.

2.4.4. Size Exclusion Chromatography (SEC)

Size exclusion chromatography (SEC) was equipped with a refractometric detector (Shimadzu, Japan) and a static light scattering detector (Mini Dawn^{TM} Treos, Wyatt Technology Europe GmbH, Germany). The chromatography was conducted at a flow rate of 0.5 ml / min, using 2 columns (Shodex OH Pack SB 804 HQ and SB 802.5 HQ) and aqueous buffer of 0.1M $NaNO_3$ pH 7 with 200ppm NaN_3 as static and mobile phase, respectively. The sample was diluted in the mobile phase to a final concentration of 5-6 mg / ml and injected into the columns.

The SEC analyses provided more precise values of the molecular weights of synthesized polymers than MALDI-TOF. It can be seen from table 2.2, the molecular weights of synthesized polymers span in the range of *5000-15000 Da*. This size distribution is relatively high; interestingly it is greater for PAM chains than for PNIPAM chains. The large size distribution might be useful to generate dense polymer brushes by grafting short and long chains next to each other and minimizing the excluded volume interaction problem[2]. The increase in monomer concentration or decrease in initiator concentration led to increase in molecular weight of polymer (table 2.2).

[2] Excluded volume effect: the already grafted polymer chains on a surface impede the attachment of the polymer chains approaching that surface.

Table 2. 2. *Molecular weights (determined from SEC) of synthesized polymers.*

	Initial conditions			SEC	
Telomer	$[Monomer]_0$ (M)	$[AET]_0$ (M)	$[KPS]_0$ (M)	MW (Da)	I_p
PAM5	0,85	0,042	0,017	4577	1,297
PAMd	0,64	0,026	0,013	6435	1,185
PAM10	1,28	0,026	0,013	8620	1,344
PAMc	2,56	0,026	0,013	15080	1,433
PNId	0,64	0,026	0,013	5150	1,23
PNI5	0,85	0,042	0,017	5227	1,16
PNI10	1,28	0,026	0,013	8561	1,14
PNIi	1,28	0,021	0,013	8950	1,10
PNIa	1,28	0,013	0,013	12970	1,06

2.4.5. Fluorescence labeling

FITC conjugation with synthesized polymers was used to demonstrate the reactivity of amino group in the *polyacrylamide* chain. Fluorescein isothiocyanate (FITC) is widely used to attach a fluorescent label to proteins [6]. Isothiocyanate group in this compound is known to be very sensitive to amines in proteins [7]. Here, we use this fluorophore to qualitatively evaluate the amino group in our functionalized polymers. TLC and ^{1}H NMR were used to study the polymer that was modified with FITC.

Labeling of the amino group on the polyacrylamide with FITC dye was performed by Oppermann's method [8]: we dissolved the amino-terminated polyacrylamide (AmPAM) in 0.01M Na_2CO_3 (pH 11.0) to a final concentration of 50 mg / ml and we added to this solution a five-fold molar excess, according to the total number of amine moieties in the reaction mixture, of FITC in anhydrous DMF (20mg / 200µl). The AmPAM was conjugated with the FITC dye in dark room during 24 hrs under permanent stirring. The reaction is illustrated in the scheme 2.2.

TLC of polyacrylamide modified with FITC was performed with (*$CHCl_3$/MeOH=7/3*) eluent and UV detection at *365* nm. The first spot in the Fig. 2.7.b (on the left) corresponds to the FITC alone (R_f is equal to 0.9, in agreement with literature [9]) and the third spot (on your right) positioned at the starting line corresponds to the purified FITC-AmPAM conjugate. In the middle, we can see the mixture of FITC and FITC-AmPAM conjugate. These results pretty clearly demonstrate, on the qualitative level, the presence and the reactivity of the amino group in the polymer chains.

Additionally, ^{1}H NMR spectrum of modified polymer was also studied to confirm the conjugation. As seen in the Fig. 2.7.c, there are peaks corresponding to aromatic groups (b, *6.61-7.86* ppm) on ^{1}H NMR spectrum of FITC-AmPAM conjugate. These results are in agreement with the previous works that studied the FITC labeling of other polymers [10].

From the results obtained on TLC plate and ^{1}H NMR spectrum, it can be concluded that our polymer has been successfully modified with FITC probe.

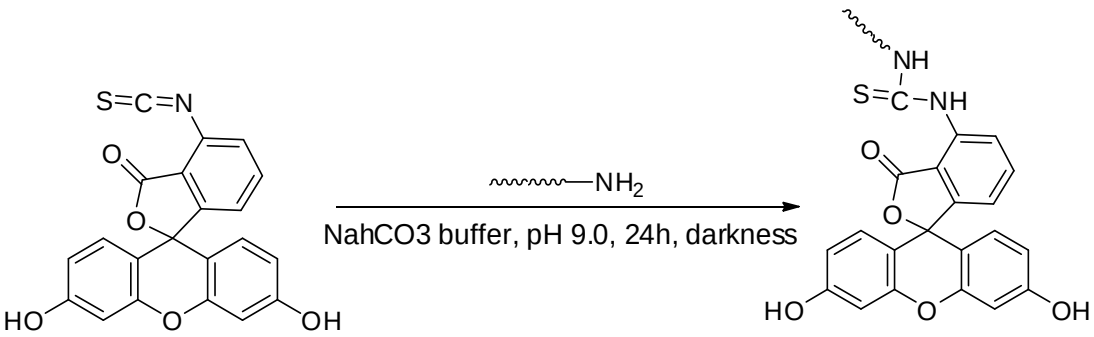

Scheme 2.2. *Conjugation of amine terminated polymer with FITC.*

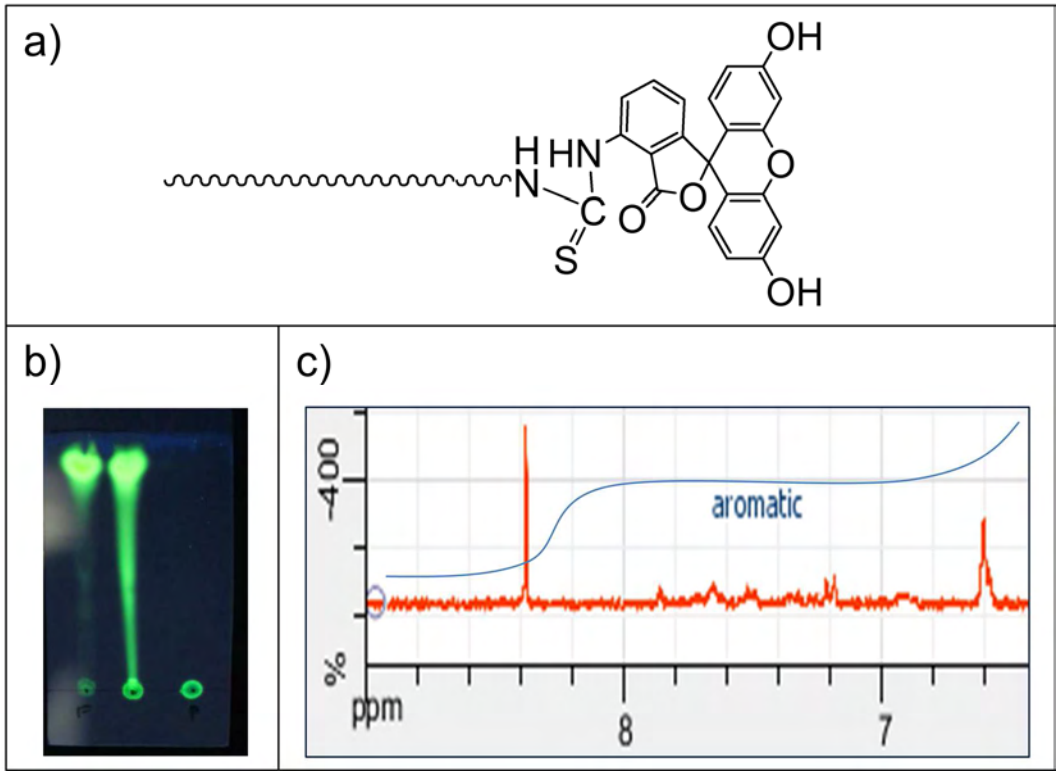

Figure 2.7. *FITC conjugated polyacrylamide:* a) Structural formula; b) TLC with eluent $CHCl_3$/MeOH=7/3 and UV stain of 365nm; c) ^1H NMR in D_2O (δ: 6.61-7.86ppm).

2.4.6. DCC/HOBT mediated amidation

In another approach, we used *amidation* of functional polymer with acrylic acid to qualitatively prove the presence of amino group in *poly(N-Isopropylacrylamide)* chain [11, 12] (see Scheme 2.3). First, the acrylic acid was activated by using DCC: HOBT (689mg, 5.1mM) was suspended in anhydrous DCM (10ml) and added to a solution of (i) DCC (5.3ml, 5.3mM) and (ii) acrylic acid (341µl, 4.98mM) in DCM (15ml). The reaction was stirred for 1.5h at room temperature. The precipitated dicyclohexylurea (DCU) was discarded by filtration. TLC was used to monitor reaction with using eluent of Cyc/AcOEt (5/5). The visualization of the TLC plates was accomplished in UV at 254nm. Then, 1g of amino terminated polymer was dissolved in anhydrous DCM (5ml) and added dropwise to the filtrated solution of the activated acrylic acid. The reaction was preceded during 15h and final product was gained by precipitation in excess Et_2O and evaporation in vacuum during 1h.

It can be seen from ^{13}C NMR spectrum (Fig. 2.8), a peak corresponding to the vinyl group appeared in the spectrum of the polymer modified with acrylic acid. This indicates that the esterification was successful.

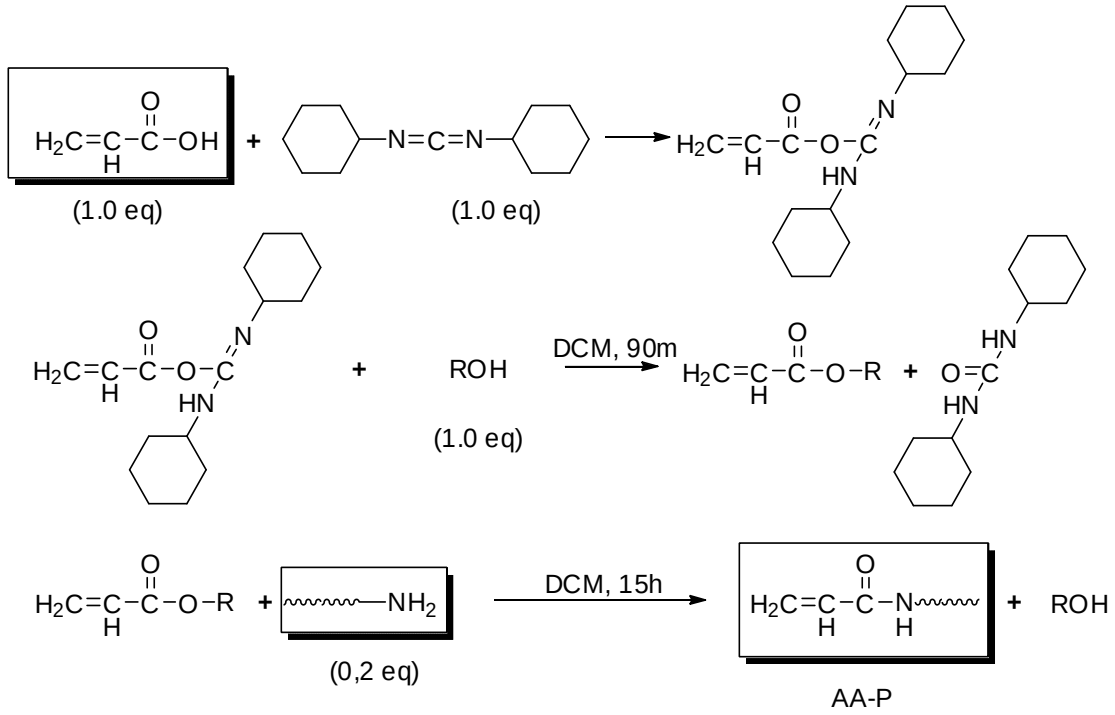

Scheme 2.3. *HOBT/DCC-mediated amidation between amine terminated PNIPAM and acrylic acid.*

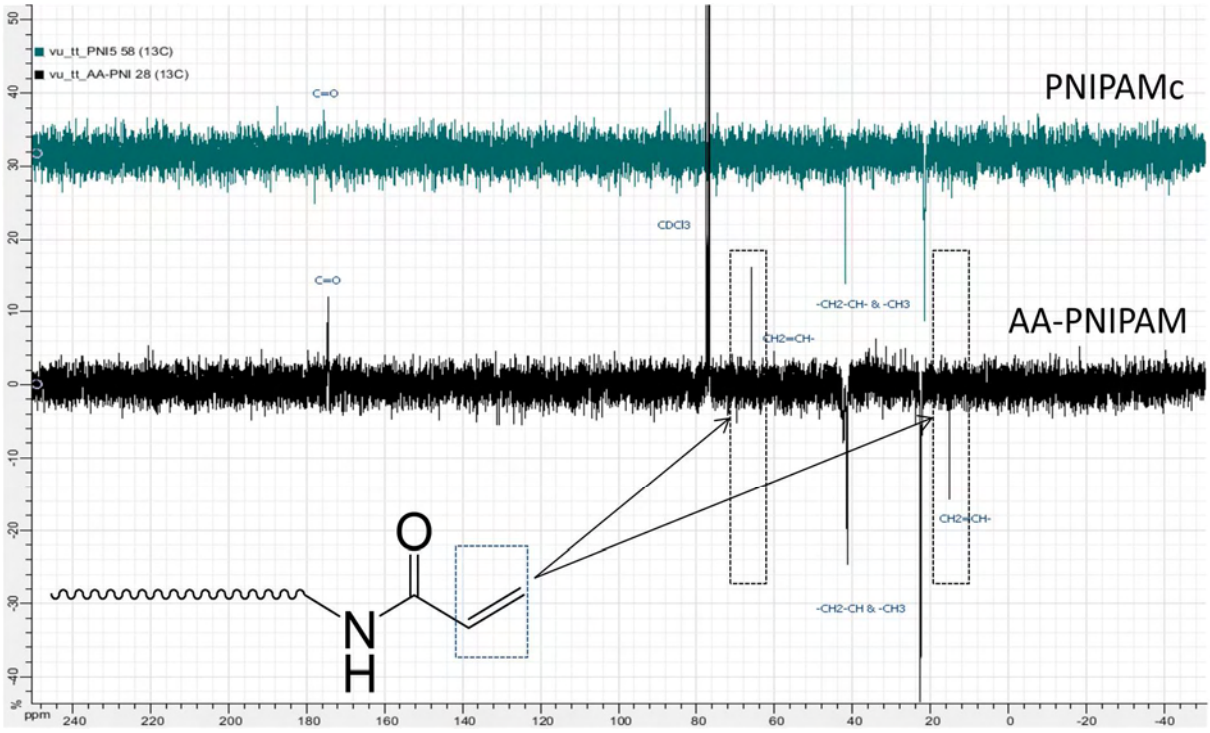

Figure 2.8. *^{13}C NMR spectra (in $CDCl_3$) of unmodified PNIPAM and PNIPAM modified with acrylic acid*: HOBT/DCC mediated amidation of PNIa with acrylic acid was conducted at RT in DCM for 15h.

2.5. Conclusion

We synthesized several AmPAM and AmPNIPAM polymer chains by employing a redox system of cysteamine and potassium persulfate. The structure of synthesized polymers was thoroughly characterized by FITR, NMR and MALDI-TOF. The presence and the reactivity of the amino end-group was evaluated by conjugation of the AmPAM chains with FITC and consequent TLC, ^{1}H NMR analysis; by reaction of AmPNIPAM chains with acrylic acid in the presence of DCC and consequent ^{13}C NMR analysis. The molecular weight of the polymers was determined by MALDI-TOF and SEC. The results of SEC are more realistic due to the size-discrimination in MALDI/TOF analyses. The chosen polymerization protocol allowed us to synthesize well-structured polymers with amino end-group and controllable molecular weight that were consequently utilize for decorating various solid surfaces with polymer brushes.

References

[1] H. Lee, S.M. Pellatore, P.B. Messersmith, Science, 2007, 318 (5849), pp 426–430.

[2] Alain Durand, Dominique Hourdet, Polymer, 1999, 40 (17), pp 4941–4951.

[3] (a) Georges Bokias, Alain Durand, Dominique Hourdet, Macromol. Chem. Phys., 1998, 199(7), pp 1387–1392; (b) A. G. De Boos, Polymer, 1973, 14(11), pp 587-588; (c) Vera Ushakova, Evgenji Panarin, Elisabetta Ranucci, Fabio Bignotti, Paolo Ferruti, Macromol. Chem. Phys., 1995, 196(9), pp 2927-2939.

[4] Laurence Petit, Carole Karakasyan, Nadège Pantoustier, Dominique Hourdet, Polymer, 2008, 48, pp 7098-7112.

[5] A.T. Jackson, D.F. Robertson, Comprehensive Analytical chemistry, Vol. 53, Chap. 5, pp. 17, Elsevier press (2008).

[6] (a) Schreiber A.B., Haimovich J., Methods Enzymol., 1983, 93, pp 147-155; (b) Harlow E., Lane D., Antibodies a Laboratory Manual, pp 353-355, Cold Spring harbor Laboratory (1988).

[7] Green F.J., Sigma-Aldrich Handbook of Stains, Dyes and Indicators, pp 377 (1990).

[8] Sebastian Seiffert, Wilhelm Oppermann, Macromol. Chem. Phys., 2007, 208, pp 1744–1752.

[9] Amy Junnila, D. Scott Bohle, Roger Prichard,Inna Perepichkaand Carla Spina, Bioconjugate Chem., 2007, 18, pp 1818–1823.

[10] HeuiKyoung Cho, Saifullah Lone, DaeDuk Kim, Joon Ho Choi, Sung Wook Choi, Jin Hun Cho, Jung Hyun Kim, In Woo Cheong, Polymer, 2009, 50, pp 2357–2364.

[11] F. Albericio, R. Chinchilla, D.J. Dodsworth, C. Najera, Org. Prep. Proc. Int. 33 202 (2001); Oleg Marder, F. Albericio, Chim. Oggi, 2003, 31, pp 35-40.

[12] Senthil Govindaraji, Philippe Nakache, Vered Marks, Zvika Pomerantz, Arie Zaban, Jean-Paul Lellouche, J. Org. Chem., 2006, 71, pp 9139-9143.

Chapter 3: Optimization of oxidation of dopamine

3.1. Introduction

The oxidation kinetics of dopamine (DOP) is supposed to be the critical parameter to improve efficiency of surface modification in MiSC [1]. Therefore, this chapter is focused on the investigation of the effect of oxidation kinetics on the deposition kinetics of DOPA (oxidized dopamine) thin films and on the analysis of the surface properties (e.g., topography and wettability) to find out optimal condition for building up high-quality DOPA films for subsequent grafting.

3.2. Materials

Chemicals

Dopamine (DOP) in the form of hydrochloride salt and tris(hydroxymethyl)-aminomethane (Tris base, crystalline, ≥99.9%), Ammonium persulfate (AP, ACS reagent, ≥98.0%) were purchased from Sigma-Aldrich (refs H8502, T1503 and 248614) and used without any further purification. Acrylamide (AM, electrophoresis grade, ≥99.0%), 2-aminoethanethiol hydrochloride (AET, ≥98.0%) and potassium peroxodisulfate (KPS, ACS reagent, ≥99.0%) were purchased from Sigma-Aldrich (refs 148660, M6500 and 216224) and used as received. All solutions were prepared in deionized water from a Millipore Q Plus system with a resistivity of 18.2kΩ•cm.

Flat wafers

Flat wafers of various materials (silicon oxide, coverslips, silicon, gold, copper, SU8, PDMS) were prepared. Coverslips (22×22mm) were purchased from Sigma-Aldrich. Standard one side polished silicon wafers, Silicon oxide wafers (d~600nm) and gold coated wafers (d=50-150nm) were supplied by LAAS laboratory. The growth of copper layer on silicon wafer was performed by UNIVEC 450C plasma sputtering at LAAS laboratory. SU-8, commonly used epoxy-based negative photoresist was deposited on clean silicon wafer by spin-coating at the thickness of 800nm. Polydimethylsiloxane (PDMS) was mixed with curing agent at proportion of 10/1, degassed with nitrogen for 1h, then coated on clean silicon wafer by spin-coating, and finally, annealed at 90°C in oven for 1h. All wafers were cut into (1×3cm) areas.

3.3. Experiments

To prepare the dopamine (DOP) solutions, a given amount of DOP was weighed and dissolved in 50mM Tris.HCl buffer (pH 8.5) under desired oxidation conditions just before this solution was put in contact with substrates. This high concentration of buffer inhibited the pH drop (δpH~0.3) caused by oxidation of DOP. All experiments were conducted in alkaline aqueous solution to promote the oxidation of DOP. In case an oxidant was used to induce deposition, pH was slightly adjusted to be 9.0.

All wafers were sonicated in iso-propanol (IPA) and deionized water (Milli Q system, Millipore) for 2 minutes, rinsed with water, and finally, blow dried before use. Then, clean surfaces were quickly immersed into oxidizing dopamine solution. All substrates were kept upright to avoid formation of micro-particles on surfaces. Then, these surfaces were rinsed with Millipore water and dried by Nitrogen stream before storage or use. All experiments were performed at room temperature (20-22°C). The coating procedures could be repeated to increase the coating thickness as fresh DOP solutions were supplied. The deposits obtained by putting solid substrates in contact with freshly prepared DOP solutions were named DOPA films.

The oxidation kinetics of dopamine (DOP) is supposed to be the critical parameter to improve efficiency of surface modification in MiSC. Therefore, we studied here the effect of oxidation conditions on oxidation kinetics of dopamine as well as the deposition kinetics, and the surface morphology. We have investigated 3 oxidation conditions of dopamine: air bubbling, oxygen bubbling, and oxidant induced oxidation:

Air bubbling: Substrates were immersed in a dilute aqueous solution of DOP (2mg/ml, in Tris.HCl 50mM, pH 8.5). The deposition was conducted in open glass big-col beaker by dipping under convection (stirring) to ensure a continuous oxygen flow for oxidized-polymerization through the water-air interface.

Oxygen bubbling: The DOP solution was prepared by dissolving a 2mg/ml DOP in 50mM Tris.HCl buffer solution (pH 8.5) then oxygenated continuously for several hours.

Oxidant induced oxidation: Ammonium persulfate at concentration of 1mg/ml was used as oxidant to promote the oxidation of degassed DOP (2mg/ml) solution in Tris.HCl buffer solution (50mM, pH 9.0).

3.4. Characterizations

3.4.1. UV-Vis absorption

The kinetics of oxidized polymerization of DOP has been studied by UV-Vis absorption. The UV-Vis spectra of twenty-fold dilution of reaction solutions were recorded by Specord 205 (Anlytik Jena, Germany) in the range of 250-700nm. The absorbance of DOP solution at 282nm increases linearly versus DOP concentration in the chosen range. A calibration curve (absorbance at 282nm as a function of concentration) of DOP aqueous solution was built in the range of 0.02-0.20mg/ml. All DOP solutions were prepared in degassed Millipore water. The DOP consumption was determined from absorption spectra (after baseline subtraction) in comparison with calibration curve of DOP.

3.4.2. Water contact angle

Water contact angles were measured by static sessile drop method using the GBX digidrop goniometer (GBX, France) to determine the surface energy. For each static contact angle measurement, a drop of certain volume was dispensed from the height of 1cm with low speed. After that, the needle was brought down into the drop from the top center. The images of the drop were recorded by Windrop software and analyzed by triangulation method in terms of contact angle. All measurements were performed in ambient air at the room temperature.

3.4.3. Atomic force microscopy (AFM)

The surface morphology and topography were evaluated by a Nanoscope V Multimode scanning probe microscope (Bruker, Germany) in the tapping mode. The advantages of the tapping mode, compared to contact mode, are the elimination of a large part of permanent shearing forces and the causing of less damage to the sample surface, even with stiffer probes. In this AFM mode, cantilever oscillates at a frequency lower and close to resonance frequency. Single lever silicon probe (force constant of $3Nm^{-1}$ and resonance frequency of 70-90 kHz) was chosen as cantilever for all measurements in compatibility with soft polymeric films.

The images were captured in the retrace direction at a scan rate of 0.2-1.0 Hz with a set point voltage ranging between 1.4 and 2.0 (as high as possible). Scan size was 1×1, 10×10 μm^2 and image resolution was 512 samples per line. Phase and amplitude image were

recorded in order to reflect the chemical and geometric heterogeneity of polymer layers. AFM measurements were conducted in ambient conditions without any special environmental setup in the AFM instrument. Typical variations at room temperature of several degrees have negligible effects on the results. AFM images were first-order flattened to remove horizontal artifacts. Roughness was determined by an analysis of the AFM height image employing Nanoscope Software version 7.0. Roughness of bare flat wafers was measured in order to compare with modified substrates.

Notably, the AFM tip may be contaminated by the sample due to the periodical contact between the tip and the sticky DOPA films or high surface energy PAM films. To neglect artifacts related to polymer debris mounted on AFM cantilever, contaminated tips were immersed in piranha solution, 70% H_2SO_4 and 30% H_2O_2, at room temperature [2, 3] for 30 minutes then ozone dehydrated before scans using ultra-violet Ozone cleaning systems (UVOCS).

The thickness of deposited layer on hard wafers (silicon oxide or silicon) was determined by AFM measurement after removing partly the deposited layer. The polymer layer was scratched all the way down to the substrate with a sharp metallic object which didn't damage the surface topography of the glass [4]. Visible scratches on the substrate would have been easily detected due to the sub-nanometric high resolution in the vertical direction of AFM. The depth of polymer layer was estimated by section analysis across the scratched area.

3.4.4. Nano analyser

The aggregation of DOPA in reaction solution was confirmed by Beckman Coulter Delsa(TM) Nano Zeta Potential and Submicron Particle Size Analyzer. The Delsa-Nano series from Beckman Coulter is a new generation of instruments that use photon correlation spectroscopy (PCS), which determines particle size by measuring the rate of fluctuations in laser light intensity scattered by particles as they diffuse through a fluid, for size analysis measurements (size range 0.6nm-7µm). All measurements were conducted at room temperature in Millipore water (refractive index n =1.3328, viscosity η=0.8878).

3.5. Results and discussions

The DOPA films were developed in three different ways (described in 3.3, chapter 3): (i) air bubbling, (ii) oxygen bubbling and (iii) ammonium persulfate induction. Silicon oxide was chosen as a first substrate to be modified by the DOPA film due to facilities in characterization.

3.5.1. Intrinsic huge aggregates and high roughness of DOPA films

The formation of aggregations in oxidizing dopamine solution which tends to incorporate into surface deposition and leads to rough surface morphology seems to be unavoidable. In efforts to prepare DOPA thin films with high uniformity, we deposited these films on silicon oxide in sealed reactor where the oxidation velocity of dopamine is set to be as low as possible. From a kinetic thin-film deposition viewpoint, it was believed that high deposition rate generally results in increased surface roughness compared to low deposition rate [5]. The clean substrate was immersed into dopamine solution at concentration of 2mg/ml buffered with Tris.HCl buffer pH 8.5 (widely used oxidation condition of dopamine in literature). After 24h of deposition, the formed films was rinsed with DI water, and then blown dry for further characterization. AFM was used to evaluate the homogeneity of deposited films. At the same time, the size of colloidal particles of aggregates formed in reaction solution was also measured by nano-particle analyzer using light scattering method.

As seen from figure 3.1, a very thin DOPA film (d~10nm) was formed on flat silicon wafer but with very high roughness of 3,61±0,54nm. This result is really counterintuitive in comparison with theories about deposition kinetics of thin films. The slow oxidation leads to very rough surfaces instead of homogeneous films as it should do, conflicting to our expectation. Logically, we wondered if more DOPA aggregates, potential source of defects in deposition on surfaces, were formed during inhibited oxidation. The particle size distribution, as evidenced by light scattering, showed no significant difference between oxidizing solution in sealed and opened reactor. Particles with a hydrodynamic diameter of several cents nanometers appear within less than 10 minute of oxidation of dopamine solution in both cases and gradually grow and reach size of micrometer during several tens of minutes, leading to a shift to micro-scale of size distributions. This suggested that the origin of defects on the surfaces might lie at not only the aggregation of DOPA particles

but also at something else. It was believed that the adsorption of oxidizing products (mainly DHI and its derivatives) initiates the growth of DOPA films [6]. The fully conjugated planar structures of these compounds causes improved molecular stacking based on their non-covalent or covalent bonds in cross-linking net of DOPA films. Here, we suggest that the lack of oxygen in sealed reactor may not only inhibit the growth of DOPA grains but it can also reduce considerably the formation of such initiators, leading to formation of thinner but rougher depositions.

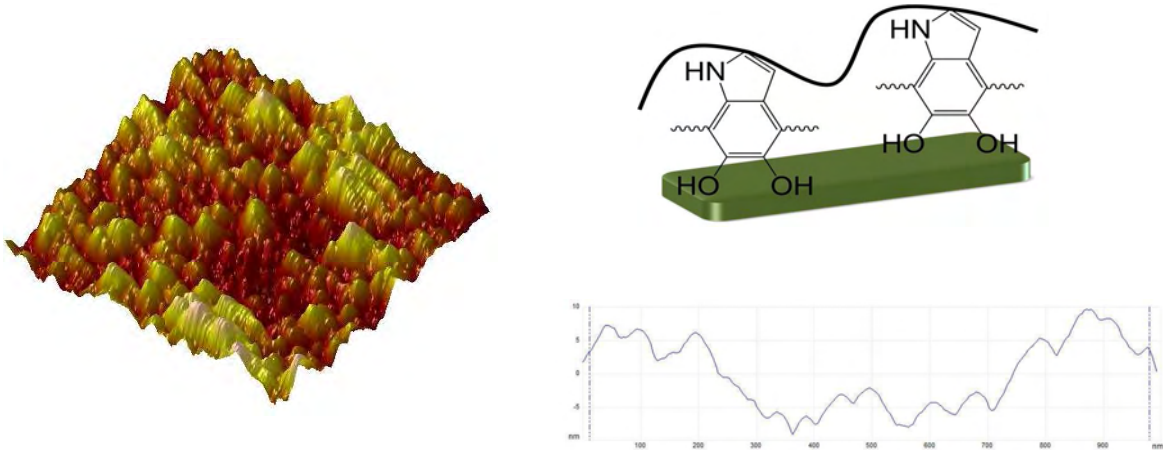

Figure 3.1. *AFM measurements of DOPA film deposited in sealed reactor:* The deposition was conducted on silicon oxide wafer dipped in DOP solution (2mg/ml) buffered Tris 50mM pH 8.5 for 24h. The lack of oxygen in sealed reactor led to slow oxidation speed, thus forming very rough deposition (left). The cross-section analysis was shown (right, bottom). This comes from the low density of phenolic radicals adsorbed on surface (right, top).

In brief, the intrinsic defects formed during deposition of DOPA films is unavoidable problem in mussel inspired surface modification. The reduction in oxidation velocity didn't generate uniform thin films, but in contrast, gave rise to incredibly rough depositions. These results suggested us to optimize DOPA films in opposite strategy by which the acceleration of oxidation kinetics will be applied to homogenize these surfaces.

3.5.2. Effect of oxidation conditions on oxidation kinetics, deposition kinetics and surface morphology

As aforementioned results about effect of oxygen concentration on surface morphology of DOPA films, the more homogeneous films should be obtained at high oxidation speed. We, therefore, achieved DOPA films in rich-oxygen conditions such as using excess oxygen supply or using oxidant as oxidizing agents. In this report, the inexpensive oxidant

(eg. ammonium persulfate) was firstly chosen as an oxidizing agent. All experiments were performed at a constant concentration of dopamine (2mg/ml, corresponding to 10.6mM).

3.5.2.1. Effect of oxidation condition on Oxidation kinetics

The oxidation kinetics of DOP solutions was investigated by UV-Vis absorption measurements in changing the oxidation condition.

The oxidation of dopamine was spontaneously indicated by a very quick change in color of solution from clear and transparent to dark as the reaction proceeds to completion, correspond to absorbance of oxidized products of DOP. Apparently, this color change in case of oxidant induction takes place quite fast compared to the oxidation under pure oxygen (oxygen bubbling), and extremely fast compared to that under ambient condition (air bubbling) due to increase in oxidation speed.

Interestingly, the detailed UV-Vis analysis shows the same spectra shape in three used oxidation conditions. A monotonic absorption spectrum of DOPA over the whole visible Ultraviolet region that was observed, explains the very dark color of DOPA films. A valley at 310-320nm and a broaden peak located at ~420nm were observed which correspond to quinones and chromes (intermediate oxidized products), respectively. These observations indicated that dopamine oxidation in all used conditions follows the same mechanism described in Messersmith scheme [7]. These observations suggested that the excess amount of oxygen or the replacement of oxygen by ammonium persulfate to initiate oxidation only accelerated oxidation but didn't change the oxidation mechanism.

We determined the DOP consumption from UV-Vis absorption spectra, by employing our calibration curve, in order to evaluate the oxidation kinetics. Surprisingly, the complete dopamine consumption (~ 98%) was observed after 1h of oxidation in the presence of ammonium persulfate (1 mg/ml), whereas the highest dopamine consumption was only 38% in the air bubbled and 60% in the oxygen bubbled solution. These findings are contradictory with the above conclusion that suggested the same oxidation mechanism for all three cases. We believe that the reaction mechanism is definitely affected by the presence of the oxidizing agent. It is known that oxidation of dopamine using oxygen as oxidizing agent is pH-dependent process (overall oxidation reaction: $\mathbf{DOPH^+ + 2O_2 <-> DOPchrome + H^+ + 2H_2O_2}$, as suggested by Herlinger [1]). In such a case, the oxidation of dopamine is reversible reaction where chemical equilibrium is reached as pH of solution

reaches a certain values, in spite of continuous oxygen or dopamine supply. This equilibrium is shifted to the reactant when the pH decreases and hence the deposition of DOPA does not occur in acidic conditions. The alkaline pH is the mandatory to promote the oxidation of DOP in aqueous condition in air and in the excess of oxygen. In contrast, the oxidation of dopamine when using ammonium persulfate as oxidizing agent is irreversible reaction whose termination takes place only when no more dopamine is supplied. This also explains the formation of dopamine deposition in acidic solutions, when Lewis acids (ammonium persulfate or copper sulfate) are used as oxidizing agents [8, 9].

3.5.2.2. Effect of oxidation condition on deposition kinetics

The deposition kinetics of DOPA on silicon oxide substrates was investigated by AFM. Silicon oxide was chosen as a model substrate in this investigation because of its very flat surfaces (R_{ms} = 0,142nm). Figure 3.2 illustrated the evolution of DOPA thin films built up in three oxidation conditions (air bubbling, oxygen bubbling, oxidant induced oxidation).

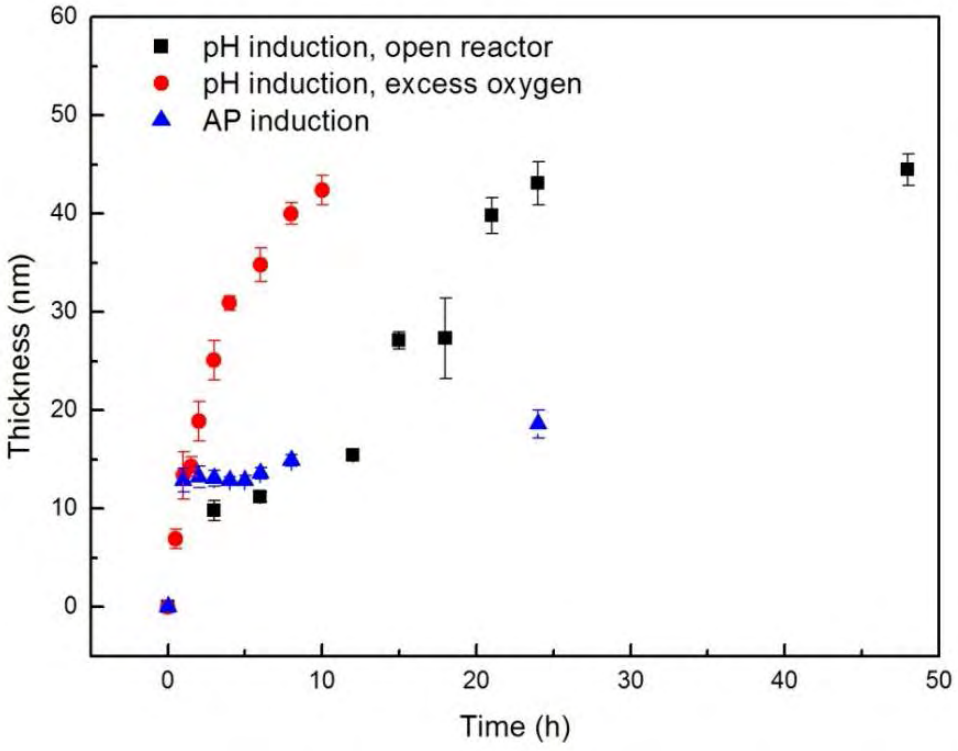

Figure 3. 2. *Evolution of DOPA film on silicon oxide wafer in various oxidation conditions:* air bubbling (square), oxygen bubbling (round), oxidant (triangle).

It was found that the deposition kinetics of DOPA when using oxygen as oxidizing agent could be satisfactorily fitted with an exponential decay function: **$d(t) = d_{max}.(1-\exp(-t/\alpha))$** whereas, d_{max} is the maximal thickness and $1/\alpha$ is the *kinetic constant*. Therefore, the *deposition velocity* is determined:

$$v = \frac{d(d(t))}{dt} = \frac{e^{-t/\alpha}}{\alpha} d_{\max} = \frac{d_{\max} - d(t) + d_0}{\alpha} \text{ and } v_0 = v(t=0) = \frac{d_{\max}}{\alpha}$$

Note also that the thickness of deposition isn't reproducible due to the difficulties to control oxygen amount, which results in a significant error. The values of kinetic constant and initial velocity of deposition were determined from fitted curve are (fig. 3.3): *α =14.9 (h)* and *v_0=2.9±0.2* (nm/h) (air bubbling); *α =4.09 (h)* and *v_0=10.4±0.6* (nm/h) (oxygen bubbling).

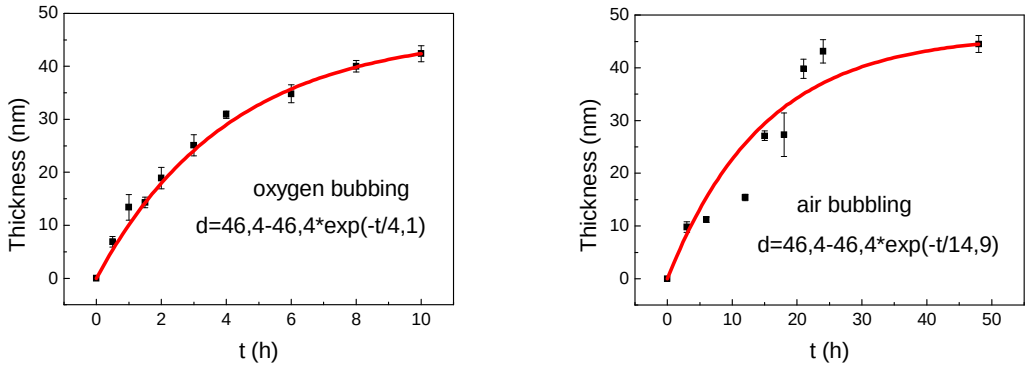

Figure 3.3. *Deposition kinetic analysis of DOPA films in various oxidation conditions:* oxygen bubbling (left), air bubbling (right). The deposition speed increased up to 4 folders at high oxygen concentration.

When using ammonium persulfate as oxidizing agent, a thin film of thickness about 8nm was deposited on surface within 15 minutes, corresponding to deposition velocity of 32nm/h. Nevertheless, this value increased slightly with deposition time, up to 13±1nm after 1h of deposition, then kept constant for many hours, compared to the maximum thickness of 40-45nm for air and oxygen induced depositions [6, 8, 10]. The exact reason why the DOPA films in case of oxidant induction didn't keep growing is still questionable for us at this moment. Alternatively, the thicker films could be obtained by multi-immersions of modified substrate into freshly prepared DOP solution until the desired thickness is reached. We did test the deposition of oxidant induced multi-layers of DOPA on silicon oxide substrates, and found that its thickness increase linearly with the number

of immersion steps (8-9nm/layer), allowing a growth regime that is proportional to the reaction time.

3.5.2.3. Effect of oxidation condition on surface morphology

As mentioned above, we supposed that the acceleration of oxidation of dopamine would produce high-quality DOPA films with considerably smooth morphology. To evaluate the effect of oxidation condition on surface topography, DOPA films prepared in chosen conditions were characterized by AFM. As seen in figure 3.4, only a few aggregates were observed on modified surfaces in the presence of ammonium persulfate, much less than that in case of oxygen bubbling and that of air bubbling.

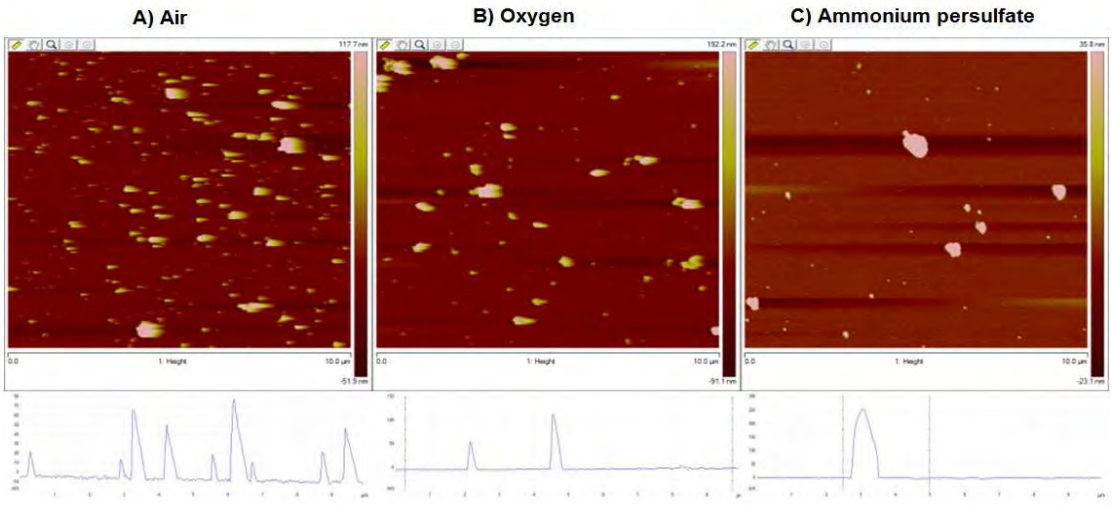

Figure 3.4. *AFM topography of DOPA films on silicon oxide wafer in various oxidation conditions:* in air bubbling (A); oxygen bubbling (B); oxidant induction (C). The use of oxidizing agent generated smoother surfaces.

In fact, Hyo et al., (2013) have reported the same results, demonstrating that the high oxygen concentration in the dopamine solution led to highly homogeneous, thin deposition on any material surfaces via accelerated reaction kinetics [11]. He suggested that the quicker oxidation under excess oxygen supply resulted in a much higher concentration of final phenolic oxidation products (DHI and its derivatives) with fully conjugated planar structures, thus leading to formation of smoother depositions. Herein, the ultra-smooth films obtained by ammonium persulfate initiation were studied for the first time in our work. The use of oxidant led to formation of uniform films with much smaller roughness (1.05nm), comparing to that in oxygen bubbling (1.63nm) and air bubbling (2.44nm). We

suggest that the effect of ammonium persulfate on morphology of DOPA films is two-fold, (i) as oxidizing agent to accelerate oxidation reaction and (ii) also at its role as Lewis acid to promote self-Michael additions between oxidizing products of dopamine, thus increasing the curing yield of DOPA films.

3.5.3. Versatility of pseudo-melanin film

The facile introduction of a wide variety of desired properties onto virtually any material surface is an ultimate goal in surface chemistry. The versatility of DOPA adhesives suggested the incorporation of structurally diverse molecules onto any materials. Here, the DOPA deposition was applied on various wetting substrates including silicon oxide, coverslip, copper, gold, SU8, PDMS (hydrophobic surface) and silicon. These materials were chosen as test materials since they are often used in biochemical essays and micro-fluidic systems. The aforementioned substrates were modified with DOPA film by immersing the substrates into an aqueous DOP solution (2mg/ml in 50mM Tris.HCl buffer) in mentioned oxidation conditions. We measured the change in water contact angle to confirm the film formation.

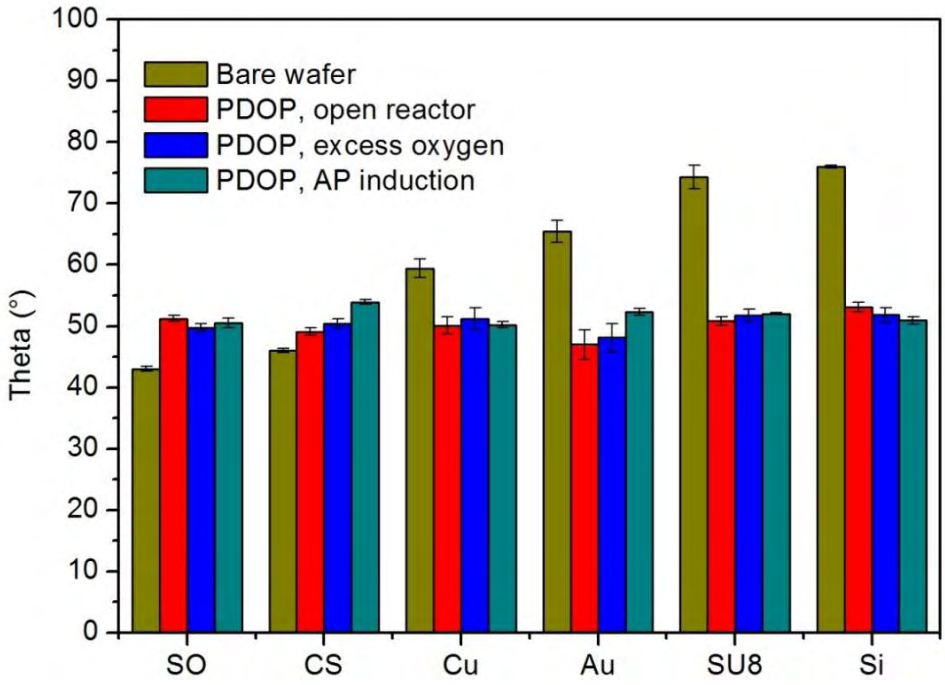

Figure 3.5. *Wettability of DOPA film on various substrates:* in air bubbling (red); in oxygen bubbling (blue); in presence of ammonium persulfate (cyan). The WCA converged to a narrow range of 50-55° though difference in initial wettability of bare surfaces.

As seen from figure 3.5 the water contact angles of DOPA coatings on hydrophilic surfaces converged into narrow region (50-55°) though the initial contact angles were ranging between 40° and 80°. The measured contact angle values are very similar to those previously reported in the literature [7, 13].

The water contact angle on non-modified PDMS substrate was 110° while it decreased to 92.6° after the DOPA film deposition. These results suggest that the PDMS substrate was covered by DOPA film; however, probably there were many defects on the PDMS surface coming from the very different stiffness of the DOPA film and the PDMS substrate. At present, we cannot provide a better explanation as to why the water contact angle on modified PDMS substrate did not decrease to 40-50°, however, dynamic contact angle measurements will be performed in the future to get a better insight into the surface chemical heterogeneity on the PDMS.

These results demonstrate the adhesion capability of DOPA films on virtually any solid surfaces. This finding opens a route for homogenization of multi-component fluidic devices, suggesting its potential applications in nano- and micro- fluidic systems.

3.6. Conclusion

In conclusion, the effect of oxidizing agent on properties of DOPA films was investigated. The surfaces modified with DOPA were thoroughly studied by atomic force microscopy and water contact angle measurements. The increase in deposition velocity, accompanying with increase in oxidation speed, has shown ability to improve surface morphology for further applications. An ultralow roughness and much less aggregates were observed in case of oxidant induced deposition of DOPA. The deeper studies of deposition kinetics should be conducted to find out the origin of the difference in deposition mechanism in addition of oxidant. Here, we will choose this oxidation condition as the optimization for the DOPA assisted surface modification (see publications in chapter 4). Above all, the use of oxidant instead of oxygen to fabricate high-quality surface coatings are very appealing for the modifications of channels in micro-fluidic systems, in which the control of oxygen flow is extremely difficult.

References

[1] P.G. Ognen, P. Stepan, H. Milan, C. Dagmer, P. Vladimir, R. Frantisek, Biomacromolecules, 2011, 12(9), pp 3232–3242.

[2]L. Sirghi, O. Kylian, D. Gilliland, G. Ceccone, F. Rossi, J. Phys. Chem. B, 2006, 110(51), pp 25975–25981.

[3]Y.S. Lo, N.D. Huefner, W.S. Chan, P. Dryden, B. Hagenhoff, T.P. Beebe, Langmuir, 1999, 15(19), pp 6522–6526.

[4]H.Dvir, J. Jopp, M. Gottlied, J. Colloid. Interface Sci., 2006, 304(1), pp 58–66.

[5] R.F. Xiao, N.B. Ming, Phys. Rev. E, 1994, 49(5), pp 4720–4723.

[6]F. Bernsmann, A. Ponche, C. Ringwald, J. Hemmerlé, J. Raya, B. Bechinger, J.C. Voegel, P. Schaaf, V. Ball, J. Phys. Chem. C, 2009, 113(19), pp 8234–8242.

[7]H. Lee, S.M. Pellatore, P.B. Messersmith, Science, 2007, 318, pp 426–430.

[8]F. Bernsmann, V. Ball, F. Addiego, A. Ponche, M. Michel, J.J. de Almeida Gracio, V. Toniazzo, D. Ruch, Langmuir, 2011, 27(6), pp 2819–2825.

[9]Q. Wei, F. Zhang, J. Li, B. Li, C. Zhao, Polym. Chem., 2010, 1, pp 1430–1433.

[10] V. Ball, D.D. Frari, V. Toniazzo, D. Ruch, J. Colloid Interface Sci., 2012, 386(1), pp 366–372.

[11] H.W. Kim, B.D. McCloskey, T.H. Choi, C. Lee, M.J. Kim, B.D. Freeman, H.B. Park, Appl. Mater. Interfaces, 2013, 5(2), pp 233–238.

[12] Falk Bernsmann, Melanin Made by Dopamine Oxidation: Thin Films and Interactions with Polyelectrolyte Multilayers, thesis, Université de Strabourg, Strabourg, France (2010).

[13] K. Kang, I. Choi, Y. Nam, Biomaterials, 2011, 32(27), pp 6374–6380.

[14] F. Yang, B. Zhao, The Open Surface Science Journal, 2011, 3, pp 115-122.

Chapter 4: Monitoring wettability of heterogeneous material surfaces in fluidic devices

Introduction

Here, optimized one-pot approach for mussel-inspired surface chemistry developed by our group (see chapter 3) will be applied to control wettability of fluidic materials through polymer coatings. The adhesive versatility of mussels for almost surfaces allowed us to achieve a substrate-independent route for grafting end-functionalized polyacrylamide chains onto any solid surfaces. The polymer was functionalized with amino group in chain transfer polymerization (see chapter 2). The modified surfaces were thoroughly characterized by water contact angle, atomic force microscopy and cyclic voltammetry. The protein adsorption of fluorescently modified albumin on surfaces wetted by polyacrylamide brushes was evaluated by fluorescence microscope. It was found that the surface modified with polyacrylamide is anti-fouling. In addition to the substrate independency of this approach, that is extremely appealing for the development of hybrid micro- and nano-fluidic devices, this method works in a low-viscosity regime and, therefore, is also extremely interesting for surface modification of nanometric-sized channels.

Sensors and Actuators B 196 (2014) 64–70

Contents lists available at ScienceDirect

Sensors and Actuators B: Chemical

journal homepage: www.elsevier.com/locate/snb

A new and easy surface functionalization technnology for monitoring wettability in heterogeneous nano- and microfluidic devices

Thi Thu Vu[a,b], Marc Fouet[c], Anne-Marie Gue[c], Jan Sudor[a,b,*]

[a] Université de Toulouse, UPS; UMR 152 Pharma-Dev, Université Toulouse 3, Faculté des Sciences Pharmaceutiques, F-31062 Toulouse Cedex 09, France
[b] Institut de Recherche pour le Développement (IRD), UMR 152 Pharma-Dev, F-31062 Toulouse Cedex 09, France
[c] LAAS-CNRS, 7 Avenue du Colonel Roche, F-31077 Toulouse Cedex 4, France

ARTICLE INFO

Article history:
Received 22 October 2013
Received in revised form
19 December 2013
Accepted 24 January 2014
Available online 30 January 2014

Keywords:
Solid/liquid interfaces
Wettability
Microfluidics
Dopamine
Polyacrylamide brush
Anti-fouling

ABSTRACT

We have developed a new and easy surface functionalization technology for monitoring wettability in heterogeneous nano- and microfluidic devices. This technology is based on mussel inspired, dopamine chemistry and it permits to end-graft hydrophilic polymer brushes onto virtually any surface in a low-viscosity regime. We have successfully modified a variety of different solid surfaces, such as Si, SiO_2, Ag, Cu, SU8 and PDMS. The modified surfaces were characterized by water contact angle measurements, atomic force microscopy, cyclic voltammetry and by electrokinetic measurements. The adsorption of proteins on the unmodified and modified surfaces was probed with fluorescently labeled albumin. We clearly demonstrated that the studied surfaces became non-fouling when modified with a hydrophilic, polyacrylamide brush, while they remained protein adsorbing when unmodified and/or modified with the dopamine film only. We believe that this universal surface modification approach will be extremely useful in nano- and micro-fluidic devices build from a variety of different materials.

© 2014 Elsevier B.V. All rights reserved.

1. Introduction

To fabricate complex microfluidic devices, various solid materials, spanning from silicon, glass and plastics can be employed. The material of choice is often governed by the specific requirements of a given application while the price of the device can also play a crucial role. Chariot et al. [1] have demonstrated that the cost of a microfluidic device can be dramatically reduced by applying hybrid technology in which silicon-based actuators are incorporated into non-expensive polymeric materials [1]. Fulcrand et al. [2,3] have employed this technology for integrating metallic-based, magnetic coils into polymeric microfluidic systems. On the other hand, it is well known that decreasing the size of any fluidic device leads invariably into increase of the surface-to-volume ratio. This often imposes the necessity to perform laborious, chemical or physical tailoring of the surfaces, especially in the micro- and nanofluidic devices dedicated to biological applications [4]. In general, surface modification approaches are developed case-by-case. They depend only on the properties of the modified materials and tethering molecules. The methods most commonly employed for the functional modification of solid surfaces include the formation of self-assembled monolayers (SAM) on metals [5–7], silane-based chemistry on silicon and glass substrates [8,9] and polyelectrolyte layer-by-layer assembly on charged surfaces [10–12]. It is clear that with these state-of-the-art surface modification approaches, it would be impossible to homogenize the surface properties in multicomponent or hybrid fluidic devices, integrating silicon, glass, metals, photoresists (e.g., SU8) and elastomers (e.g., polydimethoxysilane, PDMS) together.

In this study, we present a substrate-independent route for grafting end-functionalized polyacrylamide chains onto any solid surfaces through mussel inspired chemistry [13]. The adhesive versatility of mussels for almost any wet surfaces may lie in the amino acid composition of proteins found in the attachment layers that are rich in 3,4-dihydroxy-L-phenylalanine (DOPA) [13,14]. DOPA spontaneously oxidizes, under alkaline conditions, and forms highly reactive products that further polymerize and self-organize on any solid surface that leads to a formation of thin-layer coating that can be additionally modified with various molecules of interest [15–19]. It has been shown in the literature that amines, thiols and carboxyl groups react with DOPA films [13].

We have synthesized a variety of amino-terminated polyacrylamide (AmPAM) and polyacrylamide derivative chains of different

Abbreviations: SAM, self-assembled monolayer; PDMS, polydimethylsiloxane; DOPA, polydopamine; AmPAM, amine terminated polyacrylamide; FITC, fluorescein isothiocyanate; DHI, 5,6-dihydroxyindole; AP, ammonium persulfate.

* Corresponding author at: Université de Toulouse, UPS; UMR 152 Pharma-Dev, Faculté des Sciences Pharmaceutiques, Université Toulouse 3, F-31062 Toulouse Cedex 09, France. Tel.: +33562259804; fax: +33562259802.
E-mail address: jan.sudor1@univ-tlse3.fr (J. Sudor).

0925-4005/$ – see front matter © 2014 Elsevier B.V. All rights reserved.
http://dx.doi.org/10.1016/j.snb.2014.01.085

molecular weights. The polyacrylamide chains were end-tethered on different materials via a one-pot, DOPA approach [20,21] and the modified surfaces were thoroughly characterized. We have shown that the adsorption of fluorescently modified albumin decreased dramatically on the DOPA-AmPAM surfaces compared to unmodified or only DOPA modified surfaces. In addition to the substrate independency of this approach, that is extremely appealing for the development of hybrid micro- and nanofluidic devices, this method works in a low-viscosity regime and, therefore, is also extremely interesting for surface modification of nanometric-sized channels.

2. Experimental

2.1. Materials

Dopamine (DOPA) in the form of hydrochloride salt, tris(hydroxymethyl)-aminomethane (tris base, crystalline, ≥99.9%), Acrylamide (AM, electrophoresis grade, ≥99.0%), 2-aminoethanethiol hydrochloride (AET, ≥98.0%), potassium persulfate (KPS, ACS reagent, ≥99.0%) and Ammonium persulfate (AP, ACS reagent, ≥98.0%) were all purchased from Sigma-Aldrich and used without any further purification. All solutions were prepared in deionized water from a Millipore's Laboratory Water System (Simplicity UV, Millipore, France) with a resistivity of 18.2 MΩ cm.

Flat surfaces of various materials (silicon, silicon oxide, glass, gold, copper, SU8, PDMS) were employed in this study. Simple glass coverslips (22 × 22 mm) were purchased from Sigma-Aldrich. Standard one side polished silicon wafers were purchased from BT Electronics, France. Silicon oxide wafers (d ~600 nm) and gold coated wafers (d = 50–150 nm) were prepared in a clean room of LAAS-CNRS laboratory. The growth of copper layer on silicon wafer was performed on UNIVEC 450C plasma sputtering. SU-8, an epoxy-based negative photoresist, was deposited on a clean silicon wafer by spin-coating at the thickness of 800 nm. Polydimethylsiloxane (PDMS) was mixed with curing agent at proportion of 10/1, degassed with nitrogen for 1 h, then coated on a clean silicon wafer by spin-coating, and finally, annealed at 90 °C in oven during 1 h. All wafers were cut into (1 × 3 cm) pieces. The wafers were cleaned in a sonication bath in iso-propanol (IPA) and deionized water (Milli Q system, Millipore) for 2 min, rinsed with water, and finally, air-blow dried before the use.

2.2. Synthesis of amino-terminated polyacrylamide chains (AmPAM)

The chain transfer radical polymerization of acrylamide was performed using aminoethanthiol hydrochloride (AET) and potassium persulfate (KPS) as chain transfer agent (CTA) and initiator, respectively. The redox initiators consisting AET (26 mM) and KPS (13 mM) were added separately and rapidly into degassed monomer solution (2.56 M) in a flask placed in a water bath and kept at constant temperature of 26 ± 2 °C. The reaction was proceeded for 18–24 h, constantly stirred with the magnetic stirrer and bubbled with argon. After the polymerization was completed, the polymers were purified by dialysis of the reaction medium against distilled water (dialysis cassette with molecular weight cut-off MWCO of 3.5 kDa) and recovered by freeze drying.

2.3. Characterization of AmPAM chains

2.3.1. Size exclusion chromatography of AmPAM

Size exclusion chromatography (SEC) was equipped with a refractometric detector (Shimadzu, Japan) and a static light scattering detector (Mini Dawn™ Treos, Wyatt Technology Europe GmbH, Germany). The chromatography was conducted at a flow rate of 0.5 ml/min, using 2 columns (Shodex OH Pack SB 804 HQ and SB 802.5 HQ) and aqueous buffer of 0.1 M $NaNO_3$ pH 7 with 200 ppm NaN_3 as static and mobile phase, respectively. The sample was diluted in the mobile phase to a final concentration of 5–6 mg/ml and injected into the columns. All measurements were conducted at a constant temperature of 35 °C.

2.3.2. Fourier transform infrared spectroscopy (FTIR)

The infrared spectra of monomer, initiators and synthesized polymer were measured using the FTIR Spectrometer (Spectrum One, Perkin-Elmer) in the wave number region from 4000 to 500 cm^{-1}. Samples were mixed with KBr powder and compacted by pressure into pellets. The background was measured with an empty pellet holder (without sample).

2.3.3. Nuclear magnetic resonance (NMR)

The synthesized polyacrylamide chains were also characterized by 1H NMR on a Bruker Avance 300 spectrometer (Bruker, Germany) at 300 MHz.

2.3.4. Fluorescence labeling

Labeling of the amino group on the polyacrylamide with FITC dye was performed in the following manner: we dissolved the amino-terminated polyacrylamide (AmPAM) in 0.01 M Na_2CO_3 (pH 11.0) to a final concentration of 50 mg/ml and we added to this solution a five-fold molar excess, according to the total number of amine moieties in the reaction mixture, of FITC in anhydrous DMF (20 mg/200 μl). The AmPAM was conjugated with the FITC dye in dark room during 24 h under permanent stirring.

2.4. Surface modification with DOPA-AmPAM

To modify the selected surfaces with hydrophilic polymers, such as AmPAM, we have developed a one pot approach that is easily applicable to nano- and microfluidic devices. In this way, the surfaces of interest are simply modified when in contact with an alkaline buffer (50 mM Tris.HCl, pH 9.0) solution that contains DOPA (2 mg/ml), AmPAM (1 mg/ml) and ammonium persulfate (1 mg/ml). We also modified various surfaces with DOPA coatings only. In this case, the modification protocol reminded unchanged but we did not add AmPAM into the initial solution. In general, a freshly prepared solution is injected into a microfluidic channel and/or flat substrates are immersed into this solution for several hours (usually 3 h.) and, consequently, the channels are flushed (and the flat substrates rinsed) with a deionized water and dried in a nitrogen stream prior the use or further characterization. All experiments were performed at room temperature (20–22 °C). The coating procedures could be repeated several times on the same substrate with a new DOPA (or DOPA-AmPAM) solution in order to increase the coating thickness when desired.

2.5. Characterization of the modified surfaces

2.5.1. Water contact angle (WCA) measurements

Water contact angles (WCA) were measured by static sessile drop method using the Digidrop goniometer (GBX, France) to determine the surface energy. For each static contact angle measurement, a drop of water of a certain volume was dispensed from the height of 1 cm with low speed and the contact angle was measured by using the triangulation method with the Windrop software.

2.5.2. Atomic force microscopy (AFM) measurements

The surface morphology and topography were evaluated by a Veeco scanning probe microscope in the tapping mode (Bruker, Germany). The advantages of the tapping mode as compared to

contact mode, is the elimination of a large part of permanent shearing forces, which causes less damage to the sample surface even with stiffer probes. In the tapping mode, cantilever oscillates at a frequency slightly below the resonance frequency. Single lever silicon probe (force constant of 3 N m^{-1} and resonance frequency of 70–90 kHz) was chosen as cantilever for all measurements in compatibility with probing soft polymeric films.

The images were captured in the retrace direction at a scan rate of 0.2–1.0 Hz, with a scan size of 1×1, 10×10 μm^2 and image resolution of 512 samples per line. AFM measurements were conducted at an ambient temperature without any special environmental setup. Typical variations in temperature of few degrees have negligible effects on the results. AFM images were first-order flattened to remove horizontal artifacts. Roughness was determined by an analysis of the AFM height image employing Nanoscope Software, version 7.0. Roughness of bare flat wafers was measured in order to compare with the roughness of the modified substrates.

The thickness of deposited layer on hard wafers (silicon oxide or silicon) was also determined by AFM measurement after partially removing the deposited film. The polymer layer was scratched all the way down to the substrate with a sharp metallic object which did not damage the surface topography of the substrates. Visible scratches on the substrate would have been easily detected due to the sub-nanometric height resolution in the vertical direction of AFM. The depth of polymer layer was estimated by section analysis across the scratched area.

2.5.3. Cyclic voltammetry (CV) measurements

Cyclic voltammetry (CV) measurements were performed with a SP-240 potentiostat (BioLogic, France) using a three-electrode set-up. The working electrode was from gold deposited on a silicon wafer and isolated by a layer of silicon oxide (Au/Ti/SiO_2/Si). The thickness of the gold electrode was 150 nm. The electrode was cleaned with piranha solution (H_2SO_4/H_2O_2 = 7/3) prior each use. The reference and counter electrodes were Ag/AgCl and platinum wire, respectively. A cyclic voltammetry (CV) analysis was performed between −100 and +650 mV at a scan rate of 50 mV/s. A CV curve was recorded by employing 1 mM ferrocyanide $Fe[(CN)_6]_4$ in 150 mM KCl as an electroactive probe solution.

2.5.4. Electro-kinetic surface characterization

The electro-kinetic experiments were performed on a home-built apparatus consisting of a high-voltage power supply (Supelco, PA, USA) and platinum electrodes (Goodfellow Cambridge Limited, UK). The experiments were performed at room temperature. Small bore fused silica capillaries (Polymicro Technologies, Molex, Europe) were modified with DOPA-AmPAM coatings and the change in zeta potential was determined through the measurements of the electro-osmotic flow at alkaline pH (Tris.Borate, pH 8.1) by using the method of Huang et al. [22]. The electroosmotic flow decreased dramatically, about 8-fold, when the inner surface of the capillary was modified with DOPA-AmPAM compared to the uncoated capillary, and the coating was stable over several days.

2.5.5. Protein adsorption

The absorption of protein on the uncoated, DOPA and DOPA-AmPAM coated substrates were observed by fluorescence staining, using serum bovine albumine conjugated to fluorescein isothiocyanate (Albumine-FITC conjugate) as a probe. After 18 h of incubation, fluorescence images were observed by confocal microscope (Axio, Zeiss, Germany), with objectives of 5X and 20X. A high performance solid state multi-line light source, Lumencor Light Engine (Spectra light engine, Lumencor, USA), was utilized in these experiments. The following filter set was employed for the adsorption study: excitation 470 ± 20 nm, dichroic filter at 495 nm and the emission was collected at 525 ± 25 nm. The images of the surfaces were captured by Zeiss camera (Zeiss, Germany) controlled by Andor Solis software (Andor Technology, Ireland), and analyzed by Image J (National Institutes of Health, USA).

3. Results and discussion

The objective of our work was to develop an easy and universal approach for surface modification of channels in micro- and nanofluidic devices. This approach combines three characteristics that are essential for the future of surface engineering in tiny fluidic channels: (i) the developed surfaces are non-fouling toward biological molecules (ii) the surface chemistry is independent of the substrate physico-chemical properties and, (iii) the viscosity of the reaction medium is low and ideally very close to the water viscosity, permitting the surface modification of channels with dimensions laying in the nanometer range. The surface modification approach that we have developed and optimized in our work is based on the hydrophilic polymer brushes grafted to DOPA films via end-chain amino groups.

3.1. Amine terminated polyacrylamide (AmPAM)

FTIR spectra of synthesized polymers demonstrated the successful polymerization with the presence of the peak related to –CH2-group (located at 2932 cm^{-1}) and no peaks relating to the vinyl group (1641 and 989 cm^{-1}).

The presence of the multiple peaks located in the range of 2.60–0.50, which relates to – CH2–CH – protons and the absence of the multiple peaks in the range of 5.65–6.20 (related to vinyl group) on the 1H NMR spectra confirmed the successful polymerization of the AmPAM chains. The consecutive peaks in the range from 3.60 to 2.50 probably stem from aliphatic hydrocarbon chain dead-end. These 1H NMR results are in agreement with previously reported observation on polymerization of monomers containing vinyl group synthesized by this method [23]. The polymerization conversion, determined from the 1H NMR spectra was about 80–95%.

The synthesized AmPAM chains showed reactivity with isothiocyanate group. The successful conjugation of Am-PAM with FITC was observed by 1H NMR that showed chemical shifts in the range of 6.61–7.86 which correspond to aromatic groups [24]. TLC performed with ($CHCl_3$/MeOH = 7/3) eluent depicted the complete removal of polar FITC [24] and the successful conjugation with one fluorescent spot at baseline of the modified polymer. The fluorescent detection was performed at 365 nm (Rf of FITC is of 0.90). The MW of AmPAM employed in this study, determined by size-exclusion chromatography (SEC) was 15,100 Da and the functionality (f) of synthesized polymer, calculated from 1H NMR spectra, was 0.7 (see Supporting information).

3.2. Water contact angle (WCA) measurements

The facile introduction of a wide variety of desired properties onto virtually any solid material is an ultimate goal in surface chemistry. We have demonstrated here the incorporation of amino-terminated polyacrylamide chains (Am-PAM) onto different solid surfaces (such as SiO2, glass, Cu, Au, SU8, Si and PDMS) by employing an optimized protocol for DOPA chemistry. The static WCA angle measurements (Fig. 1) show that the DOPA coating adhere to all employed surface and that independently of the value of WCA before modification, all the materials become alike, after the surface coating (except for the PDMS surface that is more hydrophobic than any other material, before and after the modification). The WCA varies between 50.5° and 53.9° (while it is 92.8° for the PDMS). The WCA decreases for all the surfaces when AmPAM is added to the DOPA solution prior contact with the solid material, suggesting

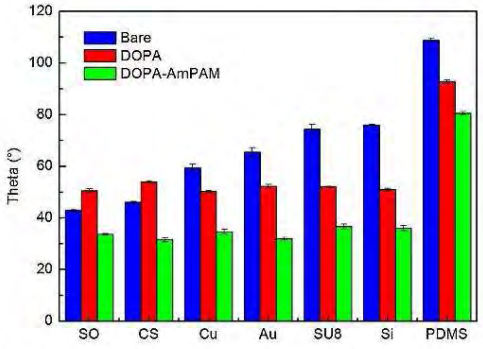

Fig. 1. Static water contact angle on various surfaces. In blue are shown water contact angles for unmodified surfaces, in red for DOPA only modified surfaces and, in green, for DOPA-AmPAM modified surfaces. (For interpretation of the references to color in this figure legend, the reader is referred to the web version of this article.)

that the polyacrylamide chains get end-tethered onto the surfaces most probably via the primary amino group. The WCA for the DOPA-AmPAM surfaces is between 31.5° and 36.6° for all the materials, except for the PDMS the WCA decreased to 80.6°. We do not have, at present, any suitable explanation for the increased hydrophobicity of the PDMS surface after the DOPA and DOPA-AmPAM modification.

3.3. Deposition kinetics and surface roughness

The composition and the size of final oxidized products of dopamine and their deposition kinetics are somewhat difficult to control. For instance, the formation of aggregates in solution which tend to incorporate into the surface film leads to a rough surface morphology. The most important factor that controls the surface morphology and uniformity is the dopamine oxidation kinetics [25–29] that can be influenced by the initial dopamine concentration, the pH of employed buffer and the presence of an oxidizing agent. It has been reported recently [28] that highly homogeneous, thin layer films are formed at the higher oxygen concentration via accelerated reaction kinetics. This inspired us to employ an oxidizing agent to promote the oxidation of dopamine in order to achieve thin films with high uniformity. To this end, we have studied the effect of ammonium persulfate on the characteristics of DOPA-AmPAM coatings in a one pot reaction scheme.

The surface morphology as well as the thickness of the coatings was investigated by AFM, the oxidation kinetics was analyzed by UV–Vis absorption and the formation of the aggregates in solution was observed by light scattering.

The oxidation of dopamine results in a very quick change in the color of the solution from clear/transparent to dark brown as the reaction proceeds to completion. We have compared the UV spectra for the three different conditions (air, oxygen and ammonium persulfate initiation of the polymerization) and we concluded that spectra shapes were almost the same for all the conditions, showing the presence of quinone and chrome compounds [13] (narrow valley at 310–320 nm, pink, and a broaden peak ~420 nm, yellow) that are intermediate products in Merssersmith scheme [13], suggesting that the presence of ammonium persulfate accelerated the oxidation but did not change the mechanism of DOPA film formation. The complete dopamine consumption (~ 98%), calculated from UV–Vis absorption, was observed after 1 h of oxidation in the presence of ammonium persulfate (1 mg/ml), whereas the highest dopamine consumption was only 38% in the air bubbled and 60% in the oxygen bubbled solution.

The colloidal particles of DOPA and DOPA-AmPAM were formed in the solution from the very beginning of ammonium persulfate induced oxidation, as evidenced by light scattering. Particles with a hydrodynamic diameter of about 100 nm appear within less than 1 min after the addition of ammonium persulfate in the DOPA solution and gradually grow and reach the micrometer size in several minutes. We have observed that the size of the aggregates somewhat decreased in the presence of AmPAM in the solution. This is probably due to continuous incorporation of AmPAM into the aggregates and, consequent, decoration of their surface with a polymer brush that prohibits their further growth.

AFM measurements were performed to study the morphology of the modified surfaces and to determine the thickness of the deposited films. Silicon oxide was chosen as the substrate due to its low surface roughness. The thickness of the AmPAM-DOPA film after 3 h of deposition was determined to be around 10 nm. The major question we wanted to address by the AFM study was the effect of oxygen, ammonium persulfate and the presence of the AmPAM on the roughness and uniformity of the deposited films. We exploited the root mean square roughness to evaluate the quality of the coatings. Representative images of $1.0 \times 1.0\ \mu m^2$ scans of all surfaces are shown in Fig. 2. It can be clearly seen from this figure that the surfaces become smoother when ammonium persulfate is used as the oxidizing agent, compared to air or oxygen only. The roughness of DOPA-AmPAM and DOPA coatings were determined to be 1.05 and 0.96 nm, instead of 2.44 and 1.92 nm when air, or 1.63 and 1.17 nm when oxygen was used as the oxidizing agent. Moreover, the density of large aggregates on the surfaces also considerably decreased in the presence of ammonium persulfate (see the Supporting information). It has been shown in the literature that the deposition of films containing DOPA is initiated by the adsorption of oxidized radicals (mostly DHI and its derivatives) on surfaces [25] and it continues by curing process in which these molecules cross-link through either covalent [30] or non-covalent binding [31]. We believe that the use of ammonium persulfate leads to the creation of many initial radicals with more uniform and decreased size and this is responsible for the decreased roughness and improved uniformity of the film deposited in our approach.

3.4. Cylic voltammetry (CV)

The coverage of DOPA and one-pot DOPA-AmPAM films on the gold substrates was additionally assessed by CV study using ferrocyanide ($K_4[Fe(CN)_6]$) as the electroactive probe. First a typical oxidation/reduction voltammogram of the ferrocyanide (presence of the oxidation and reduction peaks located at +274 and +200 mV versus Ag/AgCl reference electrode, respectively, (ΔE=74 mV) is clearly seen in Fig. 3. In contrast, the CV curves for the DOPA and DOPA-AmPAM (Fig. 3) modified gold electrodes showed dramatically decreased redox peaks, suggesting that the surface coating hindered the electroactive species to get onto the gold electrode and almost no electron exchange was established between the electrode and the solution. We calculated the specific capacitance of the DOPA and DOPA-AmPAM coatings by integrating the area under the CV curves. The specific capacitance of DOPA film was 82 $\mu F/cm^2$ while the DOPA-AmPAM was slightly increased (109 $\mu F/cm^2$) that could reflect smaller pore size of these coating. This is an important finding as it shows that these organic films on metals could potentially find an application as supercapacitors or actuators.

3.5. Protein adsorption

The non-fouling properties of our surfaces were studied with fluorescein (FITC)-albumin conjugate. The FITC-albumin conjugate

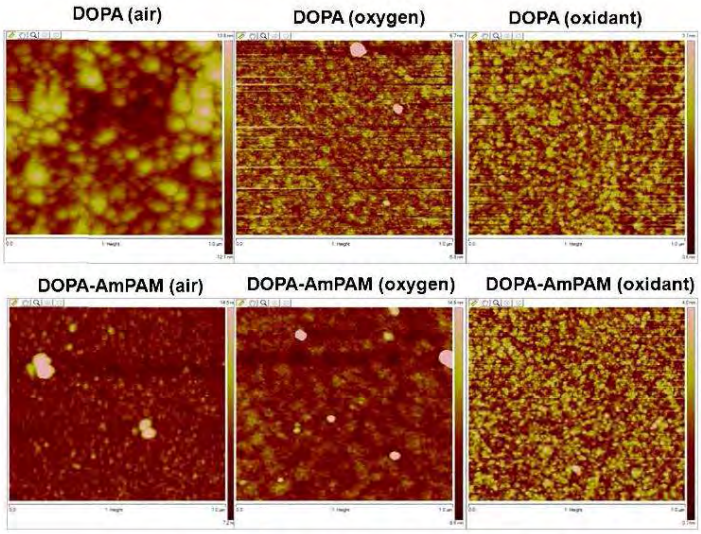

Fig. 2. AFM images of DOPA and DOPA-AmPAM modified silicon oxide surfaces.

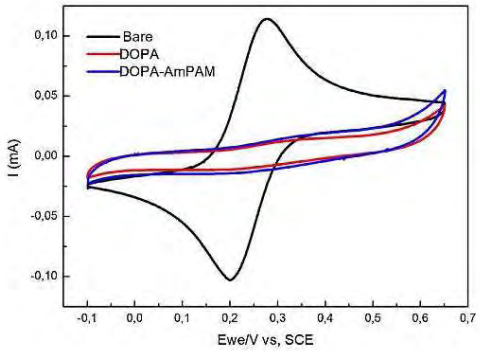

Fig. 3. Cyclic voltammogram unmodified and modified surfaces. In black are shown CV curve for unmodified surfaces, in red for DOPA only modified surfaces and, in blue, for DOPA-AmPAM modified surfaces. (For interpretation of the references to color in this figure legend, the reader is referred to the web version of this article.)

was dissolved in a buffer (pH 7.4) at the final concentration of 1 mg/ml. The unmodified and modified PDMS surfaces were dipped into the FITC-albumin solution and incubated at room temperature for several hours (18 h). After the incubation was completed, the surfaces were washed with deionized water and dried in a stream of nitrogen. We observed the remaining fluorescence signal on a microscope, employing 5× and 20× objectives. It can be seen from Fig. 4, that the unmodified and DOPA modified surfaces barely minimize the protein adsorption (see the lower part of the Fig. 4A and B) and they appear to be fluorescent after the incubation with FITC-albumin. However, the fluorescence was dramatically decreased on the DOPA-AmPAM surface (the lower left side of the Fig. 4C), suggesting that the hydrophilic PAM brush is necessary to minimize the protein adsorption. It is well know from the literature (4) that polymer brushes form an entropic barrier on the surface and prohibit proteins or other molecules of interest to get into a close proximity and to adsorb onto a given surface. We also tested SU8 substrates and obtained very similar results (not shown), suggesting that any solid surfaces can be modified with our optimized approach and to render them non-fouling.

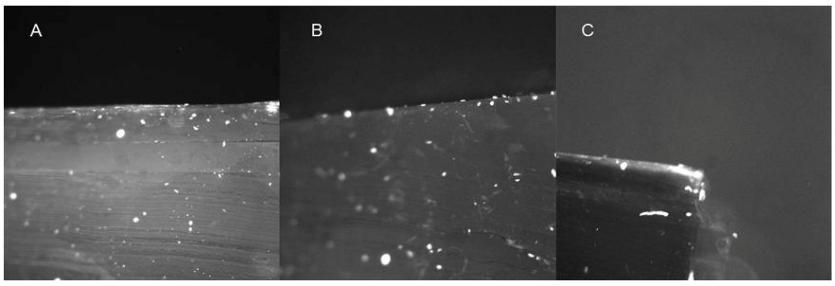

Fig. 4. Protein absorption on unmodified (A), DOPA coated (B) and DOPA-AmPAM (C) coated PDMS surfaces.

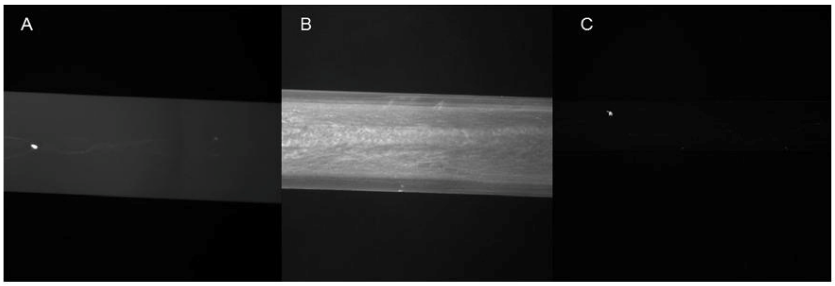

Fig. 5. Protein absorption on unmodified (A), DOPA coated (B) and DOPA-AmPAM (C) coated PDMS channels.

Along the same lines, we have also modified inner surfaces of heterogeneous microfluidic channels. The channel height and width were 10 and 300 μm and the channel length was 3 cm. The channels were built from PDMS and they were closed with a glass cover slide. The channels were filled with either dopamine solution (dopamine 2 mg/ml and ammonium persulfate 1 mg/ml in Tris.HCl buffer pH 9.0) or dopamine-AmPAM solution (dopamine 2 mg/ml, AmPAM 1 mg/ml and ammonium persulfate 1 mg/ml in Tris.HCl buffer pH 9.0). After 12 h, the channels were washed with the Tris.HCl buffer.

For the adsorption studies the unmodified, DOPA modified and DOPA-AmPAM modified channels were rinsed during 2 h (flow rate—10 μl/s) with FITC-BSA solution dissolved in PBS buffer (pH 7.4) at a concentration of 0.3 mg/ml. The FITC-BSA solution was left in the channels during 12 h and, consequently, the channels were rinsed with PBS solution for 30 min (flow rate—10 μl/s) and the remaining fluorescence was observed on the fluorescence microscope utilized in the previous studies. From the fluorescence images it is clearly seen that the FITC-BSA adsorbed on the unmodified and DOPA modified surfaces (Fig. 5A and B), while it was substantially decreased on the DOPA-AmPAM surfaces (Fig. 5C). This is in accordance with previous study on flat PDMS surfaces.

4. Conclusion

We have demonstrated the universality of our approach for the modification and functionalization of surfaces of any solid material. In this work, we were interested to exploit the non-fouling properties of the modified surfaces prepared from hydrophilic polymer brushes. We applied our strategy to the modification and homogenization of surfaces inside nano- and microfluidic channels. The advantage of the developed strategy is inherited in the substrate independent chemistry and low viscosity of the modifying medium. We have demonstrated that all the employed surfaces could be modified with DOPA or with DOPA-AmPAM coatings. The employed AmPAM chains were synthesized and characterized in our laboratory and the molecular weight was determined to be 15,100. The modified surfaces were characterized by WCA measurements, AFM, cyclic voltammetry, electro-kinetically and finally tested with fluorescently labeled albumin. The formation of DOPA and DOPA-AmPAM films on all the studied materials was clearly demonstrated in our work. The adsorption studies with the FITC-albumin conjugate showed that the fluorescently labeled albumin adsorbed on the non-modified PDMS and also on the PDMS-DOPA modified substrates; however, the adsorption was dramatically decreased on the PDMS-DOPA-AmPAM substrate. The difference in WCA between the two surfaces (DOPA and DOPA-AmPAM) was only about 12°, suggesting that the minimized adsorption of proteins on such surfaces is related to the presence of the PAM polymer brushes rather than to the overall surface energy. Similar results were obtained also on SU8 substrates (results not shown). Currently, we employ the optimized protocol for the modification of inner surface of small bore (i.d. <10 μm) capillaries that will be employed for electrophoretic separations of proteins coupled to mass spectrometry.

Acknowledgment

This work was financially supported by a doctoral fellowship to T.T. Vu from Hanoi University, Vietnam.

References

[1] S. Charlot, A.-M. Gue, J. Tasselli, A. Marty, P. Abgrall, D. Esteve, J. Micromech. Microeng. 18 (2008) 1–8.
[2] R. Fulcrand, D. Jugieu, C. Escriba, A. Bancaud, D. Bourrier, A. Boukabache, A.M. Gue, J. Micromech. Microeng. 19 (2009) 1–11.
[3] R. Fulcrand, A. Bancaud, C. Escriba, Q. He, S. Charlot, A. Boukabache, A.-M. Gué, Sens. Actuators, B 160 (2011) 1520–1528.
[4] G. Paumier, J. Sudor, A.-M. Gue, F. Vinet, M. Li, Y.J. Chabal, A. Estève, M. Djafari-Rouhani, Electrophoresis 29 (2008) 1245–1252.
[5] R.G. Nuzzo, D.L. Allara, Adsorption of bifunctional organic disulfides on gold surfaces, J. Am. Chem. Soc. 105 (1983) 4481–4483.
[6] C.D. Bain, J. Evall, G.M. Whitesides, Formation of monolayers by the coadsorption of thiols on gold: variation in the head group, tail group, and solvent, J. Am. Chem. Soc. 111 (1989) 7155–7164.
[7] M.D. Porter, T.B. Bright, D.L. Allara, C.E.D. Chidseyi, Spontaneously organized molecular assemblies: 4. Structural characterization of n-Alkyl thiol monolayers on gold by optical ellipsometry, infrared spectroscopy, and electrochemistry, J. Am. Chem. Soc. 109 (1987) 3559–3568.
[8] S. Onclin, B.J. Ravoo, D.N. Reinhoudt, Engineering silicon oxide surfaces using self-assembled monolayers, Angew. Chem. Int. Ed. 44 (2005) 6282–6304.
[9] J. Sagiv, Organized monolayers by adsorption: 1. Formation and structure of oleophobic mixed monolayers on solid surfaces, J. Am. Chem. Soc. 102 (1) (1980) 92–98.
[10] G. Decher, J. Schmitt, Fine-tuning of the film thickness of ultrathin multilayer films composed of consecutively alternating layers of anionic and cationic polyelectrolytes, Prog. Colloid Polym. Sci. 89 (1992) 160–164.
[11] G. Decher, Fuzzy nanoassemblies toward layered polymeric multicomposites, Science 277 (1997) 1232–1237.
[12] G. Decher, J.D. Hong, J. Schmitt, Buildup of ultrathin multilayer films by a self-assembly process: III. Consecutively alternating adsorption of anionic and cationic polyelectrolytes on charged surfaces, Thin Solid Films 210/211 (1992) 831–835.
[13] H. Lee, S.M. Dellatore, W.M. Miller, P.B. Messersmith, Mussel-inspired surface chemistry for multifunctional coatings, Science 318 (2007) 426–430.
[14] H.G. Silverman, F.F. Roberto, Understanding marine mussel adhesion, J. Mar. Biotechnol. 9 (2007) 661–681.
[15] O.P. Georgievski, S. Popelka, M. Houska, D. Chvostova, V. Proks, F. Rypacek, Poly(ethylene oxide) layers grafted to dopamine–melanin anchoring layer: stability and resistance to protein adsorption, Biomacromolecules 12 (2011) 3232–3242.
[16] H. Lee, J. Rho, P.B. Messersmith, Facile conjugation of biomolecules onto surfaces via mussel adhesive protein inspired coatings, Adv. Mater. 21 (2009) 431–434.
[17] V. Ball, I. Nguyen, M. Haupt, C. Oehr, C. Arnoult, V. Toniazzo, D. Ruch, The reduction of Ag^+ in metallic silver on pseudomelanin films allows for antibacterial activity but does not imply unpaired electrons, J. Colloid Interface Sci. 364 (2011) 359–365.

[18] C.Y. Li, W.C. Wang, F.J. Xu, L.Q. Zhang, W.T. Yang, Preparation of pH-sensitive membranes via dopamine-initiated atom transfer radical polymerization, J. Membr. Sci. 367 (2011) 7–13.
[19] V. Ball, D.D. Frari, M. Michel, M.J. Buehler, V. Toniazzo, M.K. Singh, J. Gracio, D. Ruch, Deposition mechanism and properties of thin polydopamine films for high added value applications in surface science at the nanoscale, BioNanoScience 2 (2012) 16–34.
[20] S.M. Kang, N.S. Hwang, J. Yeom, S.Y. Park, P.B. Messersmith, I.S. Choi, R. Langer, D.G. Anderson, H. Lee, One-step multipurpose surface functionalization by adhesive catecholamine, Adv. Funct. Mater. 22 (2012) 2949–2955.
[21] Y. Zhang, B.M. Teo, A. Postma, F. Ercole, R. Ogaki, M. Zhu, B. Städler, Highly-branched poly(*N*-isopropylacrylamide) as a component in poly(dopamine) films, J. Phys. Chem. B 117 (2013) 10504–10512.
[22] X. Huang, M.J. Gordon, R.N. Zare, Anal. Chem. 60 (1988) 1837–1838.
[23] P. Laurence, K. Carole, P. Nadège, H. Dominique, Synthesis of graft polyacrylamide with responsive self-assembling properties in aqueous media, Polymer 48 (2007) 7098–7112.
[24] J. Amy, B.D. Scott, P. Roger, P. Inna, S. Carla, Fluorescent diethylcarbamazine analogues: sites of accumulation in *Brugia malayi*, Bioconjugate Chem. 18 (2007) 1818–1823.
[25] F. Bernsmann, A. Ponche, C. Ringwald, J. Hemmerlé, J. Raya, B. Bechinger, J.C. Voegel, P. Schaaf, V. Ball, Characterization of dopamine–melanin growth on silicon oxide, J. Phys. Chem. C 113 (2009) 8234–8242.
[26] F. Bernsmann, V. Ball, F. Addiego, A. Ponche, M. Michel, J. Joaquin de Almeida Gracio, V. Toniazzo, D. Ruch, Dopamine–melanin film deposition depends on the used oxidant and buffer solution, Langmuir 27 (2011) 2819–2825.
[27] V. Ball, D.D. Frari, V. Toniazzo, D. Ruch, Kinetics of polydopamine film deposition as a function of pH and dopamine, J. Colloid Interface Sci. 386 (2012) 366–372.
[28] H.W. Kim, B.D. McCloskey, T.H. Choi, C. Lee, M.J. Kim, B.D. Freeman, H.B. Park, Oxygen concentration control of dopamine-induced high uniformity surface coating chemistry, ACS Appl. Mater. Interfaces 5 (2013) 233–238.
[29] W. Qiang, Z. Fulong, L. Jie, L. Beijia, Z. Changsheng, Oxidant-induced dopamine polymerization for multifunctional coatings, Polym. Chem. 1 (2010) 1430–1433.
[30] R.D. Daniel, J.M. Daniel, D.F. Benny, R.P. Donald, W.B. Christopher, Elucidating the structure of poly(dopamine), Langmuir 28 (2012) 6428–6435.
[31] S. Hong, Y.S. Na, S. Choi, I.T. Song, W.Y. Kim, H. Lee, Non-covalent self-assembly and covalent polymerization co-contribute to polydopamine formation, Adv. Funct. Mater. 22 (2012) 4711–4717.

Biographies

Thi Thu VU received B.S. and M.S. degrees in Solid-State Physics from the HaNoi University of Education, Ha Noi, Viet Nam in 2008 and 2010, respectively. In 2011, she was nominated for USTH fellowship from Vietnamese government to conduct her doctoral research in Material Science at Laboratory of Pharmacochemistry and Pharmacology for Development (PHARMA-DEV, UMR152), Toulouse, France. Her research interests are concerned to nanomaterials for biomedical applications, including noble metal nanoparticles and polymer thin films.

Marc A. Fouet received B.S. and M.S. degrees in chemical engineering from the École Nationale Supérieure des Industries Chimiques, Nancy (France) in 2009 and 2012, and his M.S. degree in biomedical engineering from the University Pierre et Marie Curie (Paris 6) in 2012. The same year, he started a PhD at LAAS-CNRS on 3D magnetophoretic lab on a chip for cells targeting and trapping.

Anne-Marie Gué studied physics at the National Institute for Applied Science and received her PhD degree at the University of Toulouse. She joined LAAS-CNRS in 1988 as a CNRS senior scientist. Since 1994, she is involved in the development of microtechnologies and microsystems for chemical and biological applications. She has first been working in the design and fabrication of miniaturized chemical and bio-sensors. Her activity is now focusing on microfluidic aspects. She has been the head of the CNRS Network "Micro and Nanofluidics" and is now deputy-director of LAAS-CNRS

Jan Sudor received his M.S. from Palacky University (Olomouc, Czech Republic) in 1988 and his Ph.D. in analytical chemistry and biochemistry from Indiana University (Bloomington, IN, USA) in 1997. He joined the Institute Curie (Paris, France) as a postdoctoral fellow in 1997, where he worked on new, thermo-associating separation media for DNA sequencing. Later, he spent several years at the Commissariat à l'Energie Atomique (CEA) in Grenoble, where he was involved in several projects concerning microfluidic devices dedicated to genomics, proteomics and other biological applications. More recently, he worked on stimuli-responsive, solid/liquid interfaces and their utilisation in intelligent nano- and microfluidic devices. In 2008, he was appointed as an assistant professor at the University Paul Sabatier in Toulouse and, since then, he develops various approaches for functionalization of solid/liquid interfaces based on mussel-inspired chemistry and applies them to nano- and microfluidics.

SUPPORTING INFORMATION

Table S1. AFM analysis of DOPA and AmPAM-DOPA films on silicon oxide in chosen oxidation conditions**.**

R_{ms}	air	Oxygenation	AP induction
Bare	0,25±0,04	0,25±0,04	0,25±0,04
DOPA	2,44±0,26	1,63±0,08	0,96±0,08
AmPAM-DOPA	1,92±0,14	1,17±0,05	1,05±0,06

Table S2. Water contact angle of DOPA and AmPAM-DOPA films deposited on various substrates with assistance of ammonium persulfate

Wafer	Theta 0	Theta (PDOP)	Theta (PAM)
SO	43±0,4	50,5±0,8	33,6±0,3
CS	46±0,3	53,9±0,4	31,5±0,8
Cu	59,4±1,5	50,2±0,5	34,6±0,9
Au	65,4±1,8	52,3±0,6	31,9±0,5
SU8	74,3±1,9	52±0,2	36,6±0,9
Si	76±0,2	50,9±0,6	36±1,0
PDMS	108,9±0,7	92,8±0,7	80,6±0,6

Table S3. AFM analysis of DOPA and AmPAM-DOPA films deposited on various substrates with assistance of ammonium persulfate

Wafer	Rms_{bare} (nm)	Rms_{DOPA} (nm)	$Rms_{DOPA\text{-}AmPAM}$ (nm)
SO	0,25±0,04	0,96±0,08	1,05±0,06
Au	1,55±0,32	1,45±0,21	1,56±0,31
SU8	0,63±0,05	1,0±0,12	1,01±0,10
PDMS	1,23±0,17	0,58±0,04	0,59±0,07

Conclusions

In this thesis, a new and easy surface functionalization technology has been developed for monitoring wettability of heterogeneous material surfaces in nano- and micro-fluidic devices. This technology is based on **one-pot mussel inspired surface chemistry** with the use of oxidant as oxidizing agent of dopamine, allowing us to end-graft hydrophilic polymer brushes onto virtually any surface in a low-viscosity regime. This technology is: *(i)* substrate independent (works on all solid surfaces), permitting the application of the same experimental conditions for the modification of fused-silica capillaries and/or channels made from glass, silicon, PDMS, SU8, COC and/or any other solid material, *(ii)* accomplished in aqueous solutions and, therefore, it is compatible with grafting of biologically active molecules, such as enzymes, *(iii)* easily regenerated when necessary and, *(iv)* it works in a low-viscosity regime and can be employed for functionalization of sub-micrometer sized channels.

Firstly, two series of *amine terminated polymers* (polyacrylamide and poly(N-isopropylacrylamide)) have been synthesized by chain transfer radical polymerization (CTRP). Cysteamine ($HS\text{-}CH_2\text{-}CH_2\text{-}NH_2$) and potassium persulfate ($K_2S_2O_8$) were used as chain transfer atom (CTA) and initiator, respectively. The addition of amine ended chain transfer atom (cysteamine) to growing polymer chains provides amine group at the end of polymer chains. These functional polymers are essential for the construction of nano-engineered polymer brushes on the studied substrates.

The structure of synthesized polymers was thoroughly characterized by Fourier Transform Infrared spectroscopy (FTIR), Nuclear Magnetic Resonance (NMR) and Matrix-assisted laser desorption/ionization Time-of-Flight (MALDI-TOF) mass spectrometry. It was found that the synthesized polymers are *linear and contain amino end-group*. FTIR spectra showed the characteristic peaks of polyacrylamide and its derivatives at 2932 cm^{-1} (-CH2-), 1673 cm^{-1} (C=O) and 1415 cm^{-1} (C-N). The consecutive chemical shifts (3.60-2.50 ppm) related to amino end-group were obtained on ^1H NMR spectra, suggesting the successful end-chain functionalization. ^1H NMR spectra also indicated high conversion (up to 80-95%) of polymerization and high purity of gained polymers.

Molecular weights of polymers, determined from Size Exclusion Chromatography (SEC), were found to be increased with increasing monomer concentration and decreasing

cysteamine concentration, while kept constant with varied initiator concentration. The measured Mws were in the range of *5000 -15000 Daltons.*

The *amino end-group* was qualitatively evaluated through its reaction with isothiocyanate (-N=C=S) and carboxylic acids (-COOH). ^{1}H NMR spectrum of polyacrylamide reacted with fluorescent FITC showed chemical shifts of aromatic groups (6.0-8.0 ppm), indicating the successful conjugation between amino end-group and cyanide compound. Additionally, the amidation between synthesized poly(N-Isopropylacrylamide) and acrylic acid in presence of HOBT/DCC coupling indicated the incorporation of amino end-group on polymer chains.

Secondly, the *oxidation conditions of dopamine were optimized* to achieve low-roughness DOPA films. The deposition of DOPA-type thin films on silicon oxide wafer was investigated under three different oxidation conditions (air bubbling, oxygen bubbling and oxidant induction).

The wetting of modified surfaces was studied by water contact angle measurements to confirm the presence of DOPA films. It was found that surfaces modified under chosen conditions have moderate hydrophilicity with theta values in the range of (50°-55°).

The topography of DOPA films was studied by atomic force microscopy in tapping mode. It was seen from AFM images, the surfaces modified on all examined conditions were covered by continuous thin films. The huge grains deposited on surfaces, accompanying with dark aggregations in dopamine solutions was found to be characteristics of DOPA. The slow oxidation of dopamine in sealed reactors led to very rough films, contrary to theories as well as previously experimental reports about deposition kinetics of thin films. The lack of oxygen might have reduced adsorption of phenolic radicals (which initiates the deposition of DOPA-type thin films) on surfaces, thus increased their roughness. Herein, *the use of oxidant as oxidizing agent was found to be optimal condition for surface modification by mussel inspired surface chemistry*. The presence of oxidant not only accelerated oxidation of dopamine, but also improved dramatically properties of surfaces modified with DOPA. Very smooth surfaces (roughness about 1 nanometer) with much less aggregations (several grains on the area of 10 micrometers square) were observed.

Additionally, the *deposition kinetics* of DOPA films was evaluated by atomic force microscopy in tapping mode using a scratching method. Evidently, the initial deposition velocity increased as the oxidation reaction was accelerated with excess of oxygen or oxidant. The values determined from deposition curves are *2.9±0.2* nm/h (air bubbling), *10.4±0.6* nm/h (oxygen bubbling) and 32 nm/h (oxidant induction). A thin film of 8nm was formed within 15 minutes of deposition on surface in case of oxidant induction. However, this value later increased slowly with deposition time, reached to thickness of 13nm after 1 hour, and finally kept constant for many hours. Thicker films were obtained by multi-immersions of substrate into freshly prepared dopamine solution. The thickness increase linearly with number of immersion steps (8-9nm/layer), allowing a growth regime that is proportional to the reaction time.

Finally, *one-pot mussel inspired surface chemistry* with assistance of oxidant has been utilized for control of wetting of heterogeneous materials in nano- / micro- fluidic devices. The simple immersion of clean substrates into one-pot mix (including dopamine, AmPAM and oxidant) resulted in a thin coating of polymer brush on studied surfaces (DOPA-AmPAM). The modified surfaces were characterized by analytic surface techniques, including water contact angle, atomic force microscopy, cyclic voltammetry and protein adsorption.

Water contact angle measurement showed that the polyacrylamide coating adhere to all employed surfaces. And that all the materials become alike (theta of 31.5-36.6°) after the surface coating, except PDMS that is much more hydrophobic than other material, theta of 80.6° after and 124° before modification.

Redox peaks disappeared from cyclic voltammetry curve of gold electrode modified with DOPA-type thin films. This indicates that the surface coating hindered the eletroactive species to get onto gold surface and almost no electron exchange was established between the electrode and solution. We also calculated the specific capacitance of the DOPA and DOPA-AmPAM coatings by integrating the area under CV curves. The specific capacitance of DOPA film was 82 $\mu F / cm^2$ and slightly increased (109 $\mu F / cm^2$) for DOPA-AmPAM film that could reflect high porosity of these coatings. This is an important finding as it shows that these organic films on metals could potentially find an application as supercapacitors or actuators.

The analysis of images obtained from fluorescence microscopy showed the anti-fouling property of surface modified with DOPA-AmPAM. This comes from the entropic barrier effect of polymer brushes.

In summary, a universal technology has been developed to functionalize various surfaces. This new technology is based on mussel inspired surface chemistry. The use of oxidant in one-pot approach enables us to apply this method for the modification of heterogeneous surfaces in nano- and micro-fluidic systems. Herein, we utilized this approach to exploit the anti-fouling properties of surfaces prepared from hydrophilic polymer brushes, allowing minimization of protein/cell/bacteria adhesion.

Future outlook

The ultralow-fouling behavior of DOPA-AmPAM thin film towards bovine serum albumin is important evidence that proved its ability in achieving surface coatings without non-specific protein adsorption for nano- / micro-fluidics. However, the anti-fouling properties of these films towards *different proteins* (e.g., bovine gamma globulin, serum amyloid P component) and other biomolecules (e.g., antibodies, cells) need to be studied in future works. Besides, hydrophilic modification of surfaces can be achieved by one-pot mussel inspired surface chemistry using *different water soluble polymers* (e.g., PEG, HEC, PVA, Poly(tertiary amide)s, PDMA, PHEA, PMMA, pSBMA, etc). The new polymer surfaces will be exploited as novel coatings for separation of biomolecules by capillary electrophoresis.

We have currently started to develop *stimuli-responsive surfaces* based on DOPA-AmPNIPAM films using one-pot MiSC. The functional polymer has been synthesized at our laboratory using CTRP and thoroughly characterized (see chapter 3, synthesis of amine terminated polymer). The cell adhesion is one of the first observations that indicated the presence of PNIPAM on modified surfaces. These stimuli-responsive polymer brushes have many potential applications for tissue engineering and biosensors.

We expect that in the near future, this surface chemistry can be transferred onto other materials, such as different plastics, Teflon, paper…. It is clear that we have the possibility to apply one-pot MiSC that has been demonstrated here to be universal for any virtually materials.

Résumé

1. Introduction

L'objectif de cette thèse était de développer une nouvelle technologie de fonctionnalisation des surfaces dans les dispositifs nano- / micro- fluidiques. Ceci est réalisé par *l'utilisation de la chimie de surface inspirée des moules* pour fonctionnaliser des surfaces. Cette nouvelle technologie nous a permis d'homogénéiser l'énergie de surface des matériaux étudiés.

Laboratoire sur puce (lab-on-a-chip en anglais, LOC), également appelé « Micro-système d'analyse total (μTAS), est une nouvelle discipline qui représente une percée dans l'analyse ainsi que le diagnostic biomédical. Cette discipline consiste à la miniaturisation et l'intégration des dispositifs fluidiques pour l'autonomie. Du point de vue historique, LOC a émergé des efforts pour contrôler l'écoulement liquide à l'échelle sub-nanolitre au début des années 90. Au cours des vingt-cinq dernières années, de nombreux groupes de recherche et des dizaines d'entreprises relatives à la microfluidique ont été établies. A l'heure actuelle, nous pouvons facilement trouver quelques produits commerciaux basés sur LOC, tels que l'analyseur de sang iSTAT (Abbott, USA), le glucomètre (Bayer, Allemand) et l'analyseur de peptide et d'ADN (Agilent, USA).

Il y a plusieurs matériaux (par exemple, silicium, verre et plastiques) qui peuvent être utilisés pour fabriquer les dispositifs microfluidiques complexes. Le matériel de choix est régi par l'application ciblée tandis que le prix du dispositif peut jouer un rôle essentiel. On a démontré que le coût d'un dispositif microfluidique peut être réduit considérablement en appliquant la technologie hybride dans laquelle des actionneurs basés sur silicium sont incorporés aux matériaux polymères non coûteux [1]. D'autre part, nous savons que la diminution de la taille de n'importe quel dispositif entraîne une augmentation du rapport surface / volume [2]. Ceci impose la nécessité de la modification (chimique et / ou physique) des surfaces, particulièrement dans les dispositifs microfluidiques et nanofluidiques consacrés aux applications biologiques. Les modifications de surface sont généralement développées au cas par cas. Elles dépendent des propriétés des matériaux modifiés et des molécules attachées. Les méthodes les plus généralement utilisées pour la modification des surfaces solides incluent la formation des mono-couches auto-assemblées (self assembled monolayers en anglais, SAMs) sur des métaux, la chimie basée sur le silane pour les substrats de silicium et en verre, et l'assemblage couche-par-couche de polyélectrolytes sur des surfaces chargées. Cet état de l'art de la modification de surfaces

nous montre l'impossibilité d'homogénéiser les propriétés des surfaces dans les dispositifs fluidiques hybrides (l'intégration de l'ensemble de silicium, verres, métaux, résines photosensibles, i.e. SU8, élastomères, i.e. PDMS).

La moule est un mollusque talent qui peut s'attacher sur toutes les surfaces solides à haute force d'attachement dans les conditions humides de l'océan [3]. Pour résister aux forces de cisaillement créées par des vagues à haute marée, la moule doit s'ancrer à quelque chose fixé dans l'océan. A cet effet, cet invertébré construit une plaque de mousse sur ces objets fixés, puis il adhère en permanence. L'adhérence de la moule est exceptionnelle car elle est forte, durable, résistante à l'eau, et surtout, elle est universelle.

L'adhérence de la moule sur n'importe quelle surface solide est devenue l'inspiration pour une technologie universelle de fonctionnalisation des surfaces : *La chimie de surface inspirée des moules (mussel inspired surface chemistry en anglais, MiSC)*. Cette nouvelle technologie est basée sur l'utilisation des adhésifs (les familles de catécholamines) qui imitent les protéines de moules dont la dopamine est la plus utilisée. Dans une solution alcaline (pH marin), la dopamine est oxydée et forme des réactifs (nommé DOPA) qui peuvent facilement adhérer aux surfaces solides [4]. De plus, les molécules qui sont fonctionnalisées avec le groupement amine, thiol ou carboxyle peuvent également être collées sur des couches de DOPA. La découverte de *la chimie de surface inspirée des moules* est une percée technologique visant à surmonter les difficultés des chimies spécifiques de surface. En général, la couche de DOPA agit comme un scotch double-face : une face est adhérée à une surface solide et l'autre permet d'ancrer certaines molécules désirées.

Dans cette étude, nous présentons un protocole basé sur *la chimie de surface inspirée des moules* afin de greffer des chaines de polyacrylamide sur différentes surfaces solides. Dans une solution alcaline, la dopamine s'oxyde spontanément, formant des produits réactifs (DOPA), par conséquent, ces produits oxydés s'assemblent sur n'importe quelle surface solide. Ceci forme une couche mince de DOPA qui peut probablement être modifiée avec les molécules désirées. Selon la littérature, les amines, les thiols et les groupes carboxyles réagissent avec le DOPA. Nous avons synthétisé une variété de polyacrylamide et ses dérivés avec une fonction amine, à différents poids moléculaires. Les polymères ont été fixés sur différents matériaux par *la chimie de surface inspirée des*

moules par une voie « **one-pot »** et les surfaces modifiées ont été étudiées par différents techniques de caractérisation.

2. Expériences

2.1. Synthèse de polymères à terminaison amine

La polymérisation radicalaire de transfert de chaine est utilisée pour synthétiser les polymères à terminaison amine. Cela est une méthode efficace qui nous permet de synthétiser des polymères avec une terminaison fonctionnelle et un poids moléculaire désiré [5]. Dans notre étude, la cystéamine ($HS\text{-}CH_2\text{-}CH_2\text{-}NH_2$) et le persulfate de potassium ($K_2S_2O_8$) sont utilisés comme étant l'atome de transfert et l'initiateur, respectivement.

Deux séries de polymères, i.e. polyacrylamide (abrégé *AmPAM, amine terminated polyacrylamide*) et poly-N-Isopropylacrylamide (abrégé *AmPNIPAM, amine terminated poly(N-isopropylacrylamide)*) ont été synthétisées par la procédure suivante: Le monomère a été dissous dans l'eau et la solution a été bullée avec un courant d'argon pendant 1-2 heures. Les initiateurs (la cystéamine et le persulfate de potassium) ont été ajoutés séparément et rapidement dans la solution dégazée du monomère. La température a été gardé constante (ajustée à 26±2°C avec un bain d'eau). La réaction a été procédée pendant 18-24 heures. Les polymères synthétisés ont été purifiés par dialyse dans l'eau distillée, utilisant une cassette de dialyse avec une valeur de coupure de poids moléculaire (molecular weight cut-off en anglais, MWCO) de 3500 Daltons. Finalement, les polymères synthétisés sont séchés par lyophilisation.

Les polymères synthétisés ont été caractérisés par différentes techniques : spectroscopie infrarouge à transformée de Fourier (FTIR), résonance magnétique nucléaire (RMN), spectroscopie de masse à désorption-ionisation laser assistée par matrice (MALDI-TOF), et chromatographie d'exclusion stérique (SEC).

2.2. Optimisation d'oxydation de la dopamine

Dans une solution alcaline, la dopamine s'oxyde spontanément, formant des produits réactifs (DOPA), par conséquent, ces produits oxydés s'assemblent sur n'importe quelle

surface solide. Ceci forme une couche mince de DOPA (schéma 1) qui peut probablement être modifiée avec les molécules désirées.

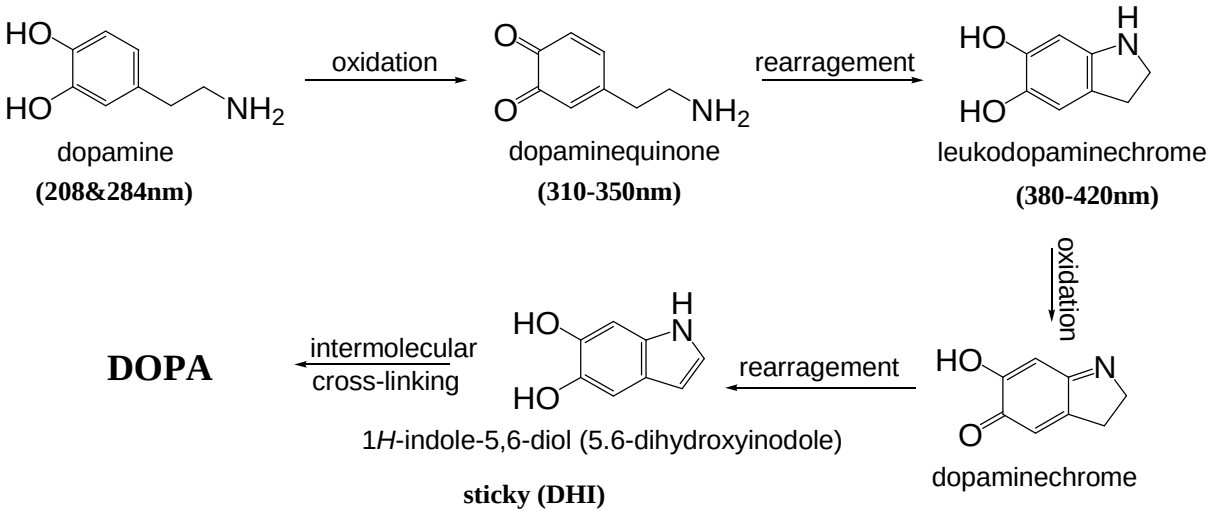

Schéma 1. Oxydation de la dopamine : L'oxydation de la dopamine mène à la formation de plusieurs produits intermédiaire (quinones, chromes, indoles) et le produit final est nommé DOPA. La structure de DOPA n'est pas encore défini mais il est bien connu que le DOPA est une colle multifonctionnel.

La cinétique d'oxydation de la dopamine est le paramètre critique pour améliorer l'efficacité de la modification de surfaces avec *la chimie de surface inspirée des moules*. L'effet de la cinétique d'oxydation sur la cinétique de dépôt des couches minces de DOPA (dopamine oxydée) est étudié sous trois conditions d'oxydation: (i) bullage d'air ; (ii) bullage d'oxygène en excès; (iii) utilisation d'un oxydant. L'oxyde de silicium est employé comme le premier substrat en raison de sa caractérisation facile.

(i) Bullage d'air: Des substrats ont été plongés dans une solution diluée de dopamine, dans le tampon Tris.HCl 50 mM, titré à pH 8.5 (pH marin), à concentration de 2 mg / ml. Le dépôt a été effectué dans un bécher ouvert à grand col sous une agitation permanente pour assurer un écoulement continu de l'oxygène.

(ii) Bullage d'oxygène en excès : Des substrats ont été plongés dans une solution diluée de dopamine, dans le tampon Tris.HCl 50 mM, titré à pH 8.5, à concentration de 2 mg / ml. Le dépôt a été effectué sous oxygène en excès. Le courant d'oxygène est toujours mis le plus fort possible.

(iii) Utilisation d'un oxydant: des substrats ont été plongés dans une solution diluée de dopamine, dans le tampon Tris.HCl 50 mM, titré à pH 9.0, à concentration de 2 mg / ml. Le persulfate d'ammonium à la concentration de 1 mg/ml a été ajouté dans la solution de dopamine afin d'oxyder celle-ci.

Tous les substrats ont été nettoyés par sonication dans l'isopropanol et l'eau déionisée pendant deux minutes, puis rincés avec l'eau, et finalement séchés avant la modification. Les surfaces propres ont été rapidement plongées dans la solution de dopamine durant son oxydation (bullage d'air, bullage d'oxygène ou utilisation d'un oxydant). Les substrats étaient maintenus verticaux pour éviter la formation de microparticules sur les surfaces. Puis, celles-ci ont été rincées avec l'eau Millipore et séchées avec un courant d'azote avant stockage ou utilisation. Toutes les expériences ont été exécutées à température ambiante (20-22°C). Les procédures de dépôt pourraient être répétées pour augmenter l'épaisseur de la couche de DOPA.

Les propriétés des surfaces (par exemple, topographie et mouillabilité) seront étudiées pour mettre au point des conditions d'oxydation de la dopamine, afin d'obtenir des couches de DOPA de haute qualité (moins d'agrégation avec une rugosité réduite). La condition optimale sera plus tard appliquée dans la modification des surfaces avec les chaines de polymère utilisant *la chimie de surface inspirée des moules* par une voie « **one-pot »**.

2.3. Modification de surface avec polyacrylamide par la chimie de surface inspirée des moules par une voie « one-pot »

Nous avons développé un protocole universel pour greffer des chaines de polymère hydrophile sur des surfaces solides. Ceci est accompli par *la chimie de surface inspirée des moules* par une voie « **one-pot »**. Les surfaces étudiées sont modifiées après immersion dans une solution alcaline **one-pot**, contenant le tampon Tris.HCl 50 mM à pH 9.0, la dopamine à la concentration de 2 mg / ml, le polyacrylamide à terminaison amine (AmPAM) à la concentration de 1 mg/ml, et le persulfate de ammonium (oxydant) à la concentration de 1 mg/ml. Généralement, une solution nouvellement préparée est injectée dans un canal microfluidique et / ou des substrats plats sont plongés dans cette solution pendant quelques heures (habituellement trois heures), et par conséquent, les canaux et / ou les substrats sont rincés et ultérieurement séchés avec un courant d'azote avant utilisation ou caractérisation. Toutes les expériences ont été exécutées à température ambiante (20-

22°C). Les procédures de dépôt pourraient être répétées pour augmenter l'épaisseur de la couche de DOPA.

Les propriétés de surfaces, i.e. la mouillabilité et la topographie, seront étudiées par deux techniques de caractérisation : l'angle de contact avec l'eau et la microscopie à force atomique. La voltampérométrie cyclique est également utilisée pour évaluer la couverture des couches organiques sur la surface. L'adsorption de protéine est employée pour étudier les propriétés de non-encrassement des surfaces modifiées avec AmPAM.

3. Résultats et discussions

3.1. Polymères à terminaison amine

3.1.1. Spectroscopie infrarouge à transformée de Fourier (FTIR)

Les spectres infrarouges des polymères synthétisés ont été mesurés utilisant le spectromètre dans la région de nombre d'onde de 4000 à 500cm^{-1}.

Les spectres FTIR ont montré des bandes caractéristiques de polyacrylamide et ses dérivés à 2932 cm^{-1} ($-CH_2-$), 1673 cm^{-1} (C=O) et 1415 cm^{-1} (C-N). La disparition de la bande d'absorption correspondant au groupe vinyle (1641 cm^{-1} et 989 cm^{-1}) a indiqué que les polymères synthétisés sont bien purifiés. Cependant, aucun signal significatif de la fonction amine terminale n'a été obtenu sur les spectres, probablement en raison de la basse concentration du groupe amine (un groupe par chaine).

3.1.2. Résonance magnétique nucléaire (RMN)

Les polymères synthétisés ont été également caractérisés par RMN avec un spectromètre de Bruker Avance 300 (Bruker, Allemagne) à 300MHz.

Les spectres RMN ont montré que les polymères synthétisés sont bien organisés, avec des chaînes linéaires de polymères et une terminaison amine. La présence d'un multiplet correspondant au groupement $(-CH_2-CH-)_n$, dans la région 2.50-0.50 ppm pour AmPNIPAM et 2.60 – 0.50 ppm pour AmPAM, indique les chaines linéaires de polymères. Les signaux consécutifs dans la région 3.60-2.50 ppm relatifs au groupement éthylène montrent la présence de la terminaison éthylamine.

La même technique analytique montre également que les polymères sont synthétisés avec une forte conversion de polymérisation (80-98%) et sont récupérés à un haut degré de pureté.

3.1.3. Spectrométrie de masse à désorption-ionisation laser assistée par matrice (MALDI-TOF)

La spectrométrie de masse à désorption-ionisation laser assistée par matrice (MALDI-TOF) est utilisée pour étudier la structure d'AmPNIPAM. Les fragments de polymère ont montré l'unité de répétition correspondant aux multiples du monomère NIPAM (Mw 113) et le groupe terminal amine (Mw 71). Le poids moléculaire mesuré par MALDI-TOF est plus petit que celui obtenu par les mesures de chromatographie d'exclusion stérique (vers 3 kDa pour la matrice de DHB, 5 kDa pour la matrice d'acide sinapinique). Ceci provient des difficultés dans l'ionisation des fragments.

3.1.4. Chromatographie d'exclusion stérique (SEC)

Le poids moléculaire obtenu par la chromatographie d'exclusion stérique est plus fiable que celui obtenu de la spectrométrie de masse à désorption-ionisation laser assistée par matrice. La masse moléculaire des polymères, mesurée par chromatographie d'exclusion stérique (SEC), augmente avec la concentration de monomères et diminue avec la concentration en cystéamine (le tableau 1). Cependant, elle est indépendante de la concentration en initiateur (KPS). Le contrôle de la masse des polymères nous permettra de contrôler la taille des brosses polymères.

De plus, la valeur de masse moléculaire (entre 5000 et 15000 Daltons) est idéale pour les applications biomédicales. Cette distribution en masse est relativement large. Cette large distribution de taille pourrait être utile pour élaborer des brosses de polymères denses en greffant les chaines courtes et longues les unes à coté des autres en réduisant au minimum le problème d'**effet de volume exclu**[3].

[3] La répulsion entre les chaines de polymère qui sont entrain d'approcher la surface et celles-ci qui sont déjà greffées sur la surface peuvent empêcher ses ancrages à la surface.

Tableau 1. Le poids moléculaire des polymères synthétisés (obtenu par SEC).

	Initial conditions			SEC	
Telomer	$[Monomer]_0$ (M)	$[AET]_0$ (M)	$[KPS]_0$ (M)	MW (Da)	I_p
PAM5	0,85	0,042	0,017	4577	1,297
PAMd	0,64	0,026	0,013	6435	1,185
PAM10	1,28	0,026	0,013	8620	1,344
PAMc	2,56	0,026	0,013	15080	1,433
PNId	0,64	0,026	0,013	5150	1,23
PNI5	0,85	0,042	0,017	5227	1,16
PNI10	1,28	0,026	0,013	8561	1,14
PNIi	1,28	0,021	0,013	8950	1,10
PNIa	1,28	0,013	0,013	12970	1,06

3.1.5. L'étiquetage de fluorescence

Le groupe amine terminal des chaines de polyacrylamide est évalué par son étiquetage avec l'isothiocyanate (-N=C=S) du fluorophore FITC. L'étiquetage a été effectué par la méthode d'Oppermann : le polyacrylamide est dissous dans 0.01M Na_2CO_3 (pH 11.0) à une concentration finale de 50 mg / ml et nous avons ajouté à cette solution un excès molaire quintuple, par rapport à la quantité d'amine dans le mélange de la réaction, de FITC dans DMF anhydre (20 mg/200µl). Le polymère a été conjugué avec le FITC dans la chambre noire pendant 24 heures sous une agitation permanente. Le polymère étiqueté a été caractérisé par chromatographie sur couche mince (CCM) et résonance magnétique nucléaire (RMN^1H).

Sur la plaque CCM du polymère modifié après sa purification, on observe une tache placée à la ligne base qui indique que le polymère est bien étiqueté (la figure 1.b).

De plus, le spectre RMN^1H du polyacrylamide réagissant avec le FITC fluorescent (la figure 1.c) a montré le déplacement chimique des groupes aromatiques (6.0 ppm - 8.0 ppm), indiquant la conjugaison entre le groupe amine terminal et le cyanate.

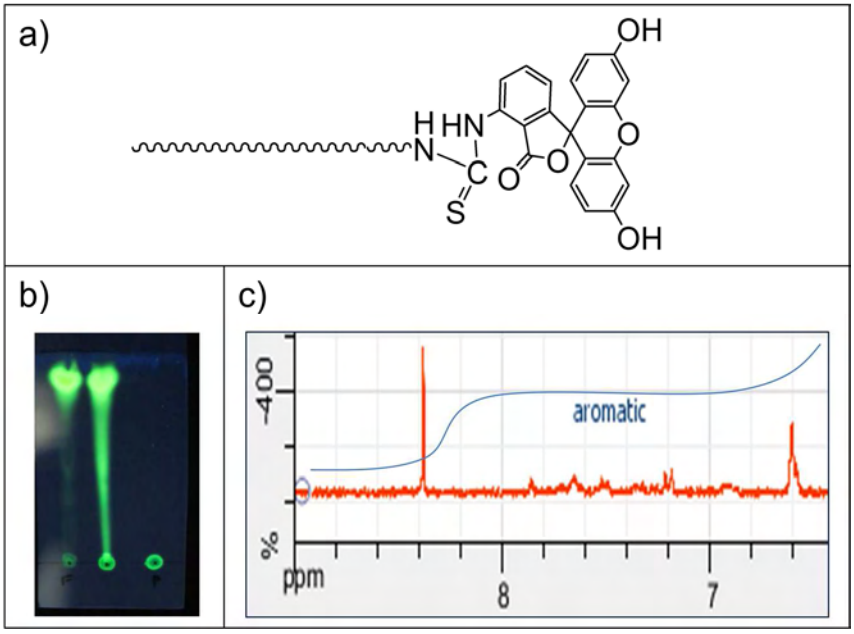

Figure 1. *FITC conjugated polyacrylamide:* a) Structural formula; b) TLC with eluent $CHCl_3$/MeOH=7/3 and UV stain of 365nm; c) ^1H NMR in D_2O (δ: 6.61-7.86ppm).

A partir des résultats de CCM et de RMN^{1}H, on peut conclure que notre polymère a bien été modifié avec la sonde FITC.

3.1.6. Amidation

La présence de l'amine terminale des chaines de poly(N-Isopropylacrylamide) a été mise en évidence par sa réaction avec l'acide acrylique.

En premier lieu, l'acide acrylique a été activé à l'aide du DCC: le HOBT (689 mg, 5.1 MM) a été suspendu dans le DCM anhydre (10ml) et ajouté à une solution de (i) DCC (5.3 ml, 5.3 mM) et (ii) d'acide acrylique (341µl, 4.98mM) dans le DCM (15ml). La réaction a été agitée pendant 1.5h à température ambiante. La dicyclohexylurée (DCU) a été enlevée par filtration. La CCM a été employée pour surveiller la réaction en utilisant le mélange Cyc/AcOEt (5/5) comme éluant.

Puis, 1g de polymère a été dissous dans le DCM anhydride (5ml) et ajouté goutte-à-goutte à la solution filtrée d'acide activé. La réaction a été réalisée pendant 15h et le produit final a été obtenu par précipitation dans Et_2O et évaporation.

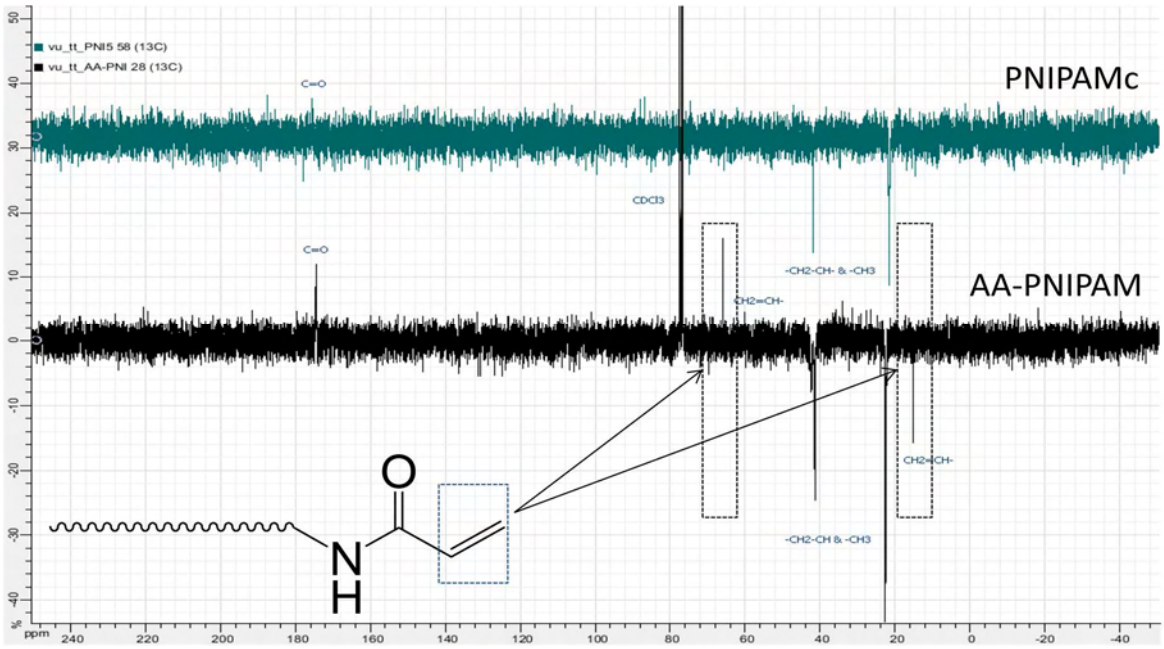

Figure 2. RMN^{13}C (dans $CDCl_3$) d'AmPAM avant et près réaction avec l'acide acrylique.

Le spectre RMN^{13}C du poly(N-Isopropylacrylamide) réagissant avec l'acide acrylique (la figure 2) montre les signaux correspondant au groupement vinyle, indiquant que l'estérification a été effectuée.

3.2. Optimisation de d'état d'oxydation de la dopamine

3.2.1. Effet des états d'oxydation sur la cinétique d'oxydation

La cinétique d'oxydation des solutions de dopamine a été étudiée par des mesures d'absorption UV-vis.

La consommation de la dopamine, évaluée à partir des spectres d'absorption, est de 98% après 1 heure d'oxydation, en présence de persulfate d'ammonium (l'oxydation est complète). Cependent, elle est de seulement 38% avec le bullage d'air et de 60% avec le bullage d'oxygène en excès.

3.2.2. Effet des états d'oxydation sur la cinétique de dépôt

La cinétique de dépôt de la DOPA sur le substrat d'oxyde de silicium a été étudiée par AFM. L'oxyde de silicium a été choisi comme substrat modèle dans cette étude en raison de sa topologie plate.

Lorsque l'oxygène est utilisé pour induire l'oxydation de la dopamine (bullage d'air ou bullage d'oxygène en excès), la constante cinétique et la vitesse initiale du dépôt sont calculées à partir de la courbe d'évolution des couches de DOPA:

- Bullage d'air: α =14.9 (h) et v_0=2.9±0.2 (nm/h)
- Bullage d'oxygène excès : α =4.09 (h) et v_0=10.4±0.6 (nm/h).

Lorsque le persulfate d'ammonium est utilisé en tant qu'oxydant pour induire l'oxydation de la dopamine, une couche de 8 nanomètres de DOPA se forme sur la surface après 15 minutes de dépôt (correspondant à une vitesse de dépôt de 32 nm/h). Après les 15 minutes, l'épaisseur de la couche de DOPA augmente légèrement. Elle reste constante à 13±1nm après 1h de dépôt. Le fait que les films de DOPA arrêtent de développer est encore inexplicable.

Alternativement, des couches plus épaisses pourraient être obtenues par **multi-immersions** de substrat modifiées dans la solution de dopamine nouvellement préparée, jusqu'à ce que l'épaisseur désirée soit obtenue. Nous avons examiné le dépôt des multicouches de dopamine induites par l'oxydant sur le substrat d'oxyde de silicium, et avons constaté que l'épaisseur augmente de 8-9 nm/immersion.

3.2.3. Effet des états d'oxydation sur la morphologie de surface

A partir des images AFM, on a trouvé que l'augmentation de la vitesse d'oxydation de la dopamine, en utilisant le persulfate de potassium, donne des couches de DOPA de haute qualité. Par rapport au bullage d'air ou bullage d'oxygène en excès, l'utilisation d'un 'oxydant donne beaucoup moins d'agrégation. De plus, la rugosité de la couche de DOPA en utilisant l'oxydant (1.05nm) est réduite considérablement, comparé aux autres cas (1.63 nm pour bullage d'air, 2.44 nm pour bullage d'oxygène excès).

Nous pensons que l'effet du persulfate d'ammonium sur la morphologie des couches de DOPA est double : (i) il agit en tant qu'oxydant pour accélérer l'oxydation de la dopamine et (ii) il agit en tant qu'acide de Lewis qui peut favoriser des réactions d'addition de Michael entre les produits oxydés de dopamine (par exemple, DHI et ses déritives). Dans le cas où ces produits sont formés à haute vitesse et conjugués rapidement ensemble, ils s'ancreront à la surface à forte densité, et par conséquent, une couche de DOPA sera formée sur la surface avec une faible rugosité.

3.3. Contrôle de mouillabilité des surfaces hétérogènes dans les dispositifs fluidiques

3.3.1. Angle de contact de l'eau

La fonctionnalisation des surfaces solides est essentielle en chimie de surface. Nous avons montré ici la modification des surfaces telles que SiO_2, verre, Cu, Au, SU8, Si et PDMS avec des chaines de polyacrylamide à terminaison amine, utilisant un protocole optimisé pour *la chimie de surface inspirée des moules* en une voie **one-pot**. Les résultats d'angle de contact avec l'eau sont présentés dans la figure 3.

Les mesures d'angle de contact avec l'eau prouvent que la couche DOPA adhère à toutes les surfaces étudiées. Après modification avec DOPA, l'angle de contact avec l'eau de toutes les surfaces devient le même (entre 50.5 et 53.9°), sauf pour le PDMS (92.8°) qui est plus hydrophobe que les autres surfaces.

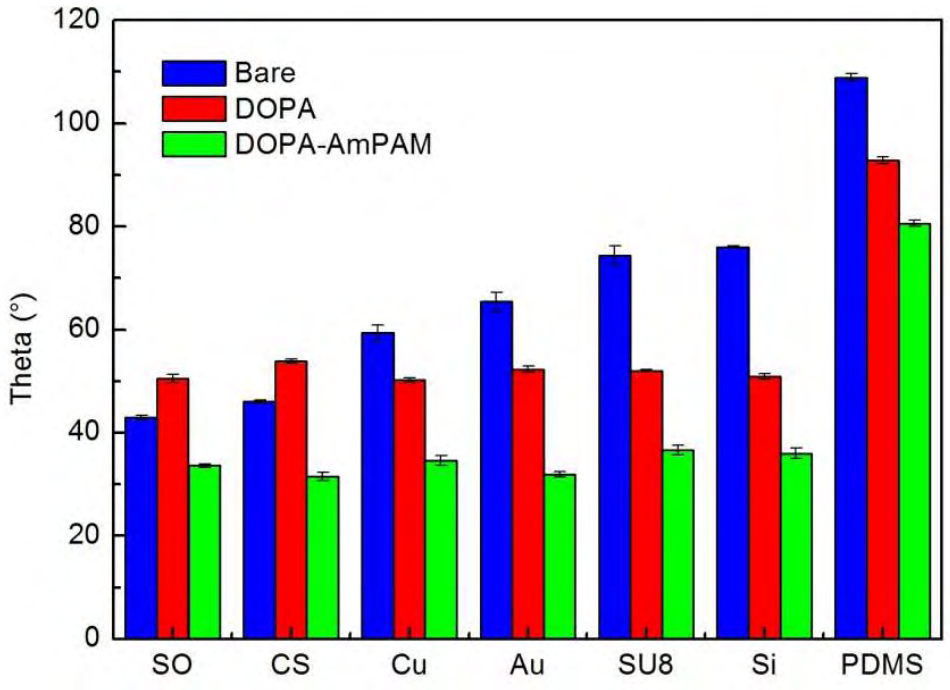

Figure 3. L'angle de contact avec l'eau des different substrats avant modification (bleu), après modification avec DOPA (rouge) et après modification avec DOPA-AmPAM (vert).

Lorsque le polymère (polyacrylamide à terminaison amine) est ajouté à la solution de DOPA, l'angle de contact diminue pour toutes les surfaces, indiquant que les terminaisons des chaines de polyacrylamide sont attachées sur les surfaces. L'angle de contact pour les

surfaces de DOPA-AmPAM est entre 31.5° et 36.6° pour tous les matériaux, sauf pour le PDMS (80.6°). A l'heure actuelle, nous ne savons pas encore expliquer la grande hydrophobicité de la surface de PDMS après la modification.

3.3.2. Microscopie à force atomique

Des mesures d'AFM ont été effectuées pour étudier la morphologie des surfaces modifiées et pour déterminer l'épaisseur des films formés après 3 heures de dépôt en utilisant d'un oxydant (le persulfate d'ammonium). L'épaisseur du film de DOPA et d'AmPAM-DOPA sont similaires, environ 10-12 nanomètres. Nous avons voulu étudier l'effet de l'oxygène, du persulfate d'ammonium et de l'AmPAM sur la rugosité et l'uniformité des films formés. La figure 4 représente la morphologie de la surface non-modifiée, modifiée avec DOPA et modifié avec DOPA-AmPAM. La morphologie de la surface modifié dans les autre cas (bullage d'air ou d'oxygène en excès) sont également comparé avec ce la de la surface modifié en absence d'oxydant.

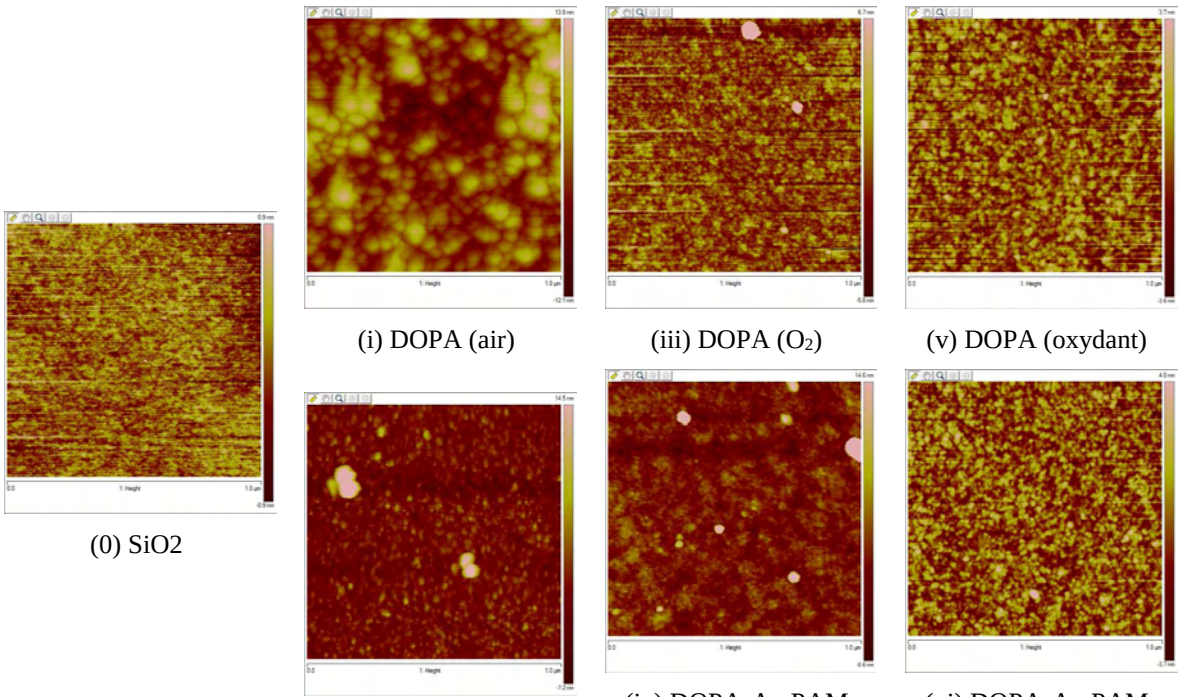

Figure 4. Les images AFM du substrat d'oxyde de silicium avant modification (0), après modification en absence d'oxydant (i→iv) et en présence d'oxydant (v, vi).

A partir des images AFM (la figure 4), on observe que les surfaces deviennent plus lisses quand le persulfate d'ammonium est utilisé comme oxydant, comparé au bullage d'air ou d'oxygène en excès. La rugosité des couches de DOPA et DOPA-AmPAM est respectivement de 1.05 et 0.96 nm. Cependant, elles sont de 2.44 et 1.92 nm avec le bouillonnement d'air, puis de 1.63 et 1.17 nm avec le bullage d'oxygène en excès.

Par ailleurs, la densité d'agrégats sur les surfaces a diminué considérablement en utilisant le persulfate d'ammonium. Selon la littérature, le dépôt des films contenant la DOPA est initié par adsorption des radicaux oxydés (DHI et ses dérivés) sur les surfaces ; et il continue avec un processus de traitement dans lequel ces molécules réticulent par liaison covalente ou non-covalente [6]. Nous pensons que l'utilisation du persulfate d'ammonium entraine l'augmentation du nombre de radicaux initiaux, par conséquent, la couche contenant la DOPA est plus uniforme, lisse et moins rugueuse.

3.3.3. Voltampérométrie cyclique

La couverture des films de DOPA et de DOPA-AmPAM sur les substrats d'or a été évaluée par voltampérométrie cyclique, utilisant le ferrocyanure ($K_4[Fe(CN)_6]$) comme sonde électro-actif.

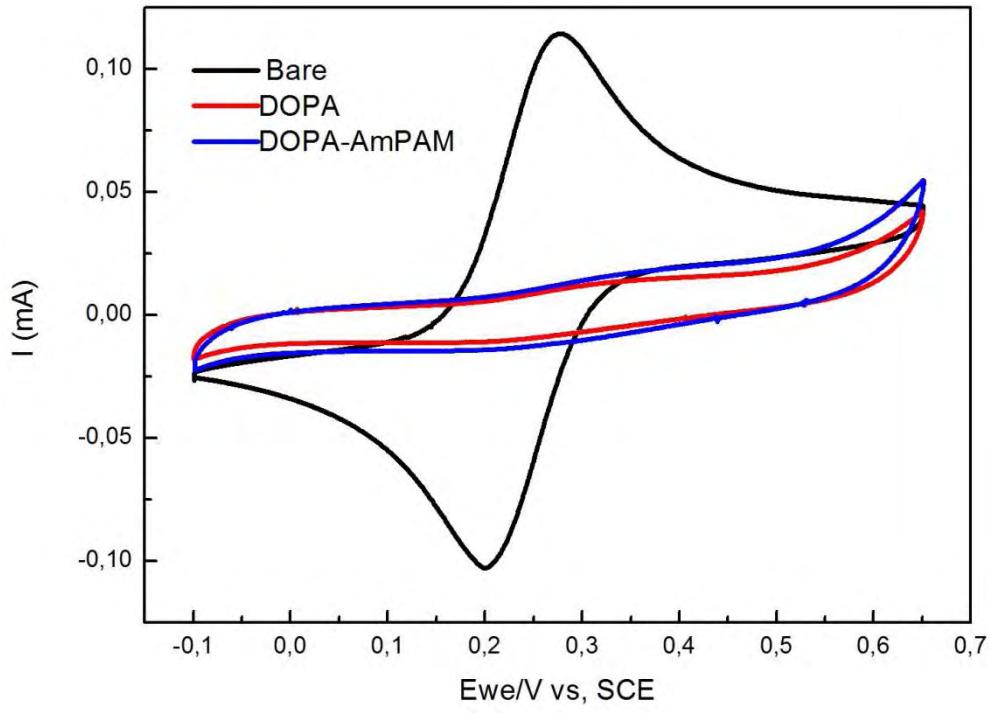

Figure 5. Voltampérogramme de ferrocyanure, utilisant électrode de travail d'or qui est non-modifiée (noir), modifiée avec le DOPA (rouge) et modifiée avec le DOPA-AmPAM (bleu).

Les pics typiques d'oxydation et de réduction du ferrocyanure sont observés sur le voltampérogramme d'électrode avant modification (la figure 5, la courbe noir). Le pic d'oxydation est situé à +274mV et celui de la réduction à +200mV (ΔE=74mV), *v.s.* d'Ag / AgCl / KCl saturé.

Le voltampérogramme des électrodes après modification avec DOPA ou DOPA-AmPAM montre une diminution dramatique de l'intensité des pics redox (la figure 5, la courbe rouge et la courbe bleu). Cela indique que les couches organiques empêchent la pénétration des espèces électro-actives à la surface de l'électrode, et donc aucun échange d'électrons n'a été établi entre l'électrode et la solution.

Nous avons également calculé la capacité spécifique des couches de la DOPA et de la DOPA-AmPAM par l'aire sous la courbe du voltampérogramme. Les capacités spécifiques des films de DOPA et de DOPA-AMmPAM sont de 82 et 109 $\mu F/cm^2$, respectivement. Cela pourrait refléter la structure poreuse de ces couches organiques. Cela prouve qu'on peut modifier des surfaces métaux avec ces couches organiques pour des applications dans les super-condensateurs ou les actionneurs.

3.3.4. L'adsorption de protéine

Pour prouver la résistance à l'encrassement des surfaces par la protéine, on a testé l'absorption de l'albumine conjuguée avec la fluorescéine (FITC-BSA). L'encrassement de l'albumine sur les surfaces est observé par microscopie de fluorescence. La protéine a été dissoute dans le tampon PBS de pH 7.4 à concentration de 1 mg/ml. Les surfaces non-modifiées et modifiées ont été plongées dans la solution d'albumine et incubées à température ambiante pendant 18 heures. Après incubation, les surfaces ont été lavées avec de l'eau déionisée, puis séchées avec un courant d'azote.

Nous avons observé le signal restant de fluorescence sur le microscope, utilisant les objectifs 5X et 20X. Les surfaces non modifiée et modifiée avec DOPA sont fluorescentes après incubation avec l'albumine conjuguée avec la fluorescéine, cependant, l'intensité de fluorescence a été nettement diminuée pour la surface modifiée avec DOPA-AmPAM (la figure 6). Ceci indique que l'absorption de la protéine est réduite grâce à la brosse hydrophile de PAM. Selon la littérature, la brosse polymère hydrophile sur la surface forme une barrière entropique qui ne permet pas aux protéines ou d'autres molécules d'adsorber à la surface [7]. Nous avons également examiné les substrats SU8 et avons

obtenu des résultats très similaires, montrant que toutes les surfaces solides peuvent être modifiées avec notre approche optimisée.

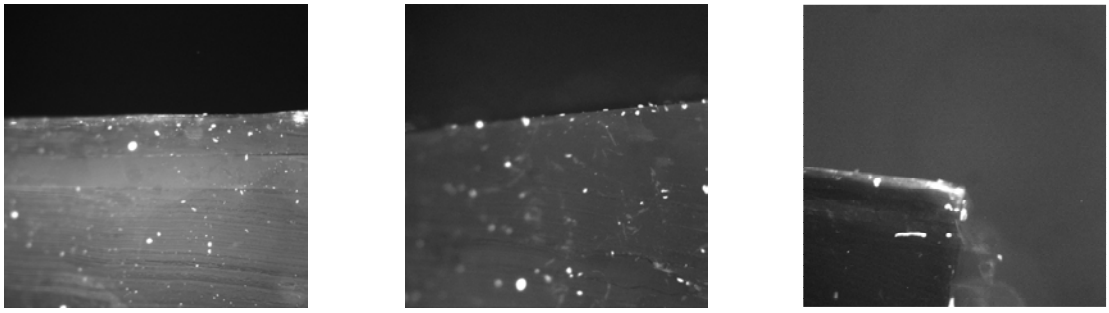

(a) (b) (c)

Figure 6. L'absorption de l'albumine-FITC sur la surface PDMS non-modifiée (a), modifiée avec DOPA (b) et modifiée avec DOPA-AmPAM (c).

Nous avons également modifié les surfaces intérieures des canaux microfluidiques hétérogènes. La profondeur, la largeur et la longueur de canal est de 10 µm, 300 µm et 3 cm. Les canaux ont été fabriqués avec du PDMS et recouverts avec une lamelle en verre. Les canaux ont été remplis de solution de dopamine (contenant la dopamine 2 mg/ml, l'AmPAM 1 mg/ml, le persulfate de l'ammonium 1 mg/ml dans le tampon Tris.HCl pH 9.0) ou de solution de dopamine-AmPAM (contenant la dopamine 2 mg/ml, le persulfate de l'ammonium 1 mg/ml dans le tampon Tris.HCl pH 9.0). Après 12 heures, les canaux ont été lavés avec le tampon Tris.HCl.

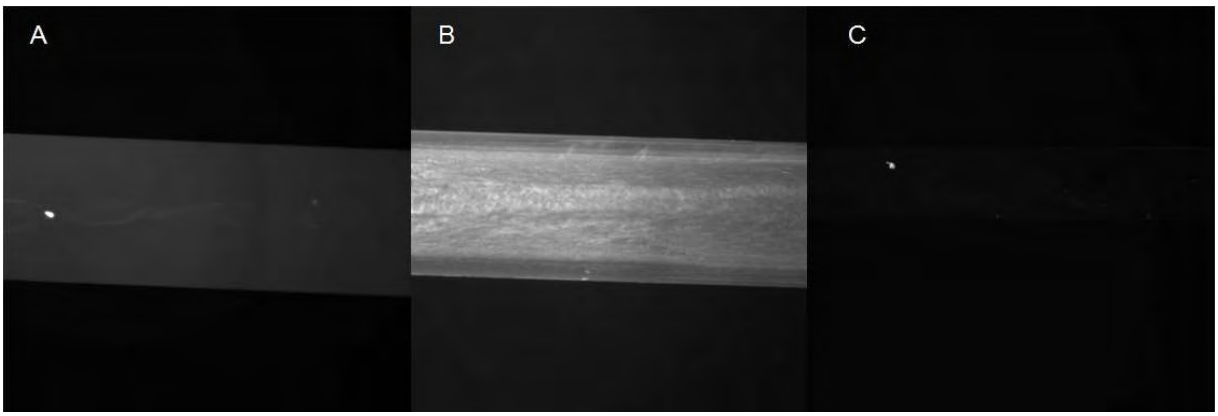

Figure 7. L'absorption de l'albumine-FITC sur le canal PDMS non-modifiée (a), modifiée avec DOPA (b) et modifiée avec DOPA-AmPAM (c).

Pour l'adsorption des protéines, les canaux non-modifiés, ceux modifiés avec DOPA ou avec DOPA-AmPAM ont été rincés pendant deux heures (débit 10µl/s) avec la solution de FITC-BSA dissoute dans le tampon PBS (pH 7.4) à une concentration de 0.3 mg/ml. La solution de FITC-BSA a été laissée dans les canaux pendant 12 heures et, par conséquent, les canaux ont été rincés par la solution de PBS pendant 30 minutes (débit 10µl/s). Une fluorescence résiduelle a été observée sur la surface non-modifiée et la surface modifiée avec DOPA, alors qu'elle est beaucoup plus faible sur les surfaces de DOPA-AmPAM (la figure 7). Ces résultats sont en adéquation avec ceux de l'étude précédente effectuée sur les surfaces plates de PDMS et de SU8.

4. Conclusion

Dans ce mémoire, une technologie simple et nouvelle a été développée pour contrôler les propriétés des surfaces dans les dispositifs micro- / nano- fluidiques. Cette technologie utilise la chimie de surface inspirée des moules qui permettra le greffage des brosses de polymères hydrophiles sur toutes les surfaces dans un régime à faible viscosité. L'utilisation d'un oxydant par une voie one-pot a nous permis à appliquer notre protocole à modifier des surfaces dans les systèmes hétérogène micro- / nano- fluidiques. Les quatre avantages de notre approche sont exposés : *(i)* l'indépendance aux substrats ; *(ii)* la compatibilité avec des molécules biologiques telles que les enzymes, *(iii)* la facilité de régénération et *(iv)* la capacité à fonctionner dans un régime à faible viscosité (paramètre important pour l'utilisation des canaux à l'échelle sous-micromètre).

Nous avons synthétisé plusieurs chaînes de polymères (AmPAM et AmPNIPAM) en utilisant le système redox cystéamine / persulfate de potassium. La structure des polymères synthétisés a été caractérisée par FTIR, RMN et MALDI-TOF. La présence de l'amine terminale des polymères (AmPAM et AmPNIPAM) a été évaluée par la conjugaison des chaînes polymères avec l'analyse FITC et par la réaction avec l'acide acrylique, respectivement. Le poids moléculaire des polymères a été déterminé par MALDI-TOF et SEC. Les résultats de la SEC ont été jugés plus fiables que ceux des analyses MALDI-TOF, en raison de la difficulté d'ionisation des fragments de polymères avec le MALDI-TOF. Le protocole de polymérisation choisi a permis de synthétiser des polymères bien structurés, possédant un groupement amine terminal et de poids moléculaire contrôlé. Par conséquent, ces polymères ont pu être utilisés pour la fonctionnalisation de surfaces avec des brosses de polymères.

Les conditions d'oxydation de la dopamine sont mises aux points afin de améliorer la qualité de la couche contenant DOPA. Les propriétés des films de DOPA ont été étudiées en fonction des différentes conditions d'oxydation. Les surfaces modifiées ont été étudiées par des mesures d'angle de contact avec l'eau et par microscopie à force atomique. L'augmentation de la vitesse de dépôt, dépendant de la vitesse d'oxydation, a permis d'améliorer la qualité des surfaces. En effet, on a observé une rugosité réduite et beaucoup moins d'agrégations en utilisant un oxydant. Des études approfondies de la cinétique de dépôt pourraient être menées afin de comprendre la différence des mécanismes de dépôt en présence et en absence d'oxydant. Dans cette étude, nous avons choisi l'oxydation induite par l'oxydant (ammonium persulfate) pour optimiser la formation des films de DOPA. Dans les systèmes microfluidiques pour lesquels le contrôle de l'écoulement de l'oxygène est extrêmement difficile, l'utilisation de l'oxydant au lieu de l'oxygène facilite les manipulations.

Nous avons greffe des brosses de polymère hydrophile (AmPAM) sur la surface dans les conditions optimisé d'oxydation de la dopamine. Les substrats sont simplement plongés dans une solution one-pot (contenant la dopamine, l'AmPAM et l'oxydant) pour former une couche de polymère sur eux. Les substrats modifiés ont étudiés par des techniques d'analyse de surface : l'angle de contact avec l'eau, microscopie à force atomique, voltampérométrie cyclique et l'adsorption de protéines. Les résultats d'angle de contact nous montrent que le polymère adhère à toutes les surfaces étudiées. Les voltampérogrammes nous indique que les couches organiques (DOPA et / ou DOPA-AmPAM) ont bien couvert les électrodes et empêchent la pénétration des espèces électro-actives à la surface de l'électrode. L'étude de l'adsorption de protéines a confirmé la propriété de non-encrassement (*anti-fouling* en anglais) de la surface modifiée avec le DOPA-AmPAM. Ceci provient de la formation d'une barrière entropique par les brosses de polymère.

Références

[1] S. Charlot, A.M. Gué, J. Tasselli, A. Marty, P. Abgrall, D. Estève, J. Micromech. Microeng., 2008, 18(1), pp 1–8.

[2] Patrick Tabeling, *Introduction to Microfluidics*, Oxford University Press, UK (2005).

[3] H. Lee, S.M. Pellatore, P.B. Messersmith, Science, 2007, 318, pp 426–430.

[4] G.S Heather, F.R. Francisco, Mar. Biotechnol., 2007, 9(6), pp 661–681.

[5] Alain Durand, Dominique Hourdet, Polymer, 1999, 40 (17), pp 4941–4951.

[6] F. Bernsmann, A. Ponche, C. Ringwald, J. Hemmerlé, J. Raya, B. Bechinger, J.C. Voegel, P. Schaaf, V. Ball, J. Phys. Chem. C, 2009, 113(19), pp 8234–8242.

[7] *(a)* P.G. De Gennes, J. Physic Paris, 1976, 37, pp 1445–1452 ; *(b)* S. Alexander, Physic Paris, 1977, 38(8), pp 977–981.